POLITECNICO
MILANO 1863

SCUOLA DI INGEGNERIA INDUSTRIALE
E DELL'INFORMAZIONE

Executive Summary of the Thesis

Donor Acceptor Stenhouse Adducts: novel photochromic nanoactuators for biooptics

Laurea Magistrale in Materials Engineering and Nanotechnology - Ingegneria dei materiali e delle nanotecnologie

Author: Maéna Marlène Galeron

Advisor: Prof.ssa Chiara Bertarelli

Co-advisor: Dott.ssa Paola Moretti

Academic year: 2021-2022

1. Introduction

Smart materials interact with external stimuli by reversibly changing chemical or physical properties. Light-activated systems (called photoresponsive materials) constitute the building block of photoswitches and light driven molecular motors and machines. Thanks to an extended aromatic system, photoswitches interconvert between isomeric states upon suitable light irradiation, a phenomenon known as photochromism. In the past decades photochromic azobenzenes have been used to modulate neuronal cell membranes potential. By undergoing a photoinduced change in geometry and polarity, they act as ion conduction blockers or ion conduction enhancers when targeting the cell membrane. The ion flux crossing the membrane through the ion channels is responsible for the interaction between the cell and its environment. Henceforth, by modulating the membrane polarity and ion flux, namely by stimulating the cell, biological events such as cell differentiation or proliferation, could be better understood and controlled [1].

In this work, we will focus on a recent class of photochromic compounds: the Donor-Acceptor Stenhouse Adducts (DASAs). Thanks to their planar structure and conjugated backbone, they absorb visible light and show negative photochromism by switching from a coloured to uncoloured isomer. This is worth-noting as red light provides high light penetration efficiency through living tissues [2]. DASAs also switch from apolar to polar upon irradiation, and they change their conformation from a linear structure to a cyclic one. By partitioning inside the membrane and changing conformation and geometry upon irradiation, the DASAs would be able to modulate the membrane potential. Some specific features closely linked to both the strength and steric hindrance of the donor and acceptor moieties, such as the thermal equilibrium between the open and closed isomer and the photoswitching kinetics, still need to be investigated. Moreover, for biological applications, these compounds will need a fine tuning of their properties in order to achieve a faster photoswitching with respect to the previously published results.

2. Photochromism and DASAs

Photochromism is defined by the IUPAC as: "*a reversible transformation of a chemical species induced in one or both directions by absorption of electromagnetic radiation between two forms having different absorption spectra*" [3]. According to the stability of the photoproduct, the photochromic process can be of P-type (the back reaction is induced by absorption of photons at a different wavelength) or of T-type (the back reaction spontaneously occurs through a thermal mechanism).

The DASAs are constituted of a nucleophilic moiety (an amine) and an electrophilic moiety, linked by a triene backbone spacer (see Figure 1). Under visible light irradiation, the strongly coloured hydrophobic linear form of DASAs is reversibly turned into a colourless hydrophilic cyclic photoproduct. The linear isomer, compared to the cyclic one, has a noticeably different geometry (about twice the size), lower polarity, and exhibits a molar extinction coefficient around 10^5 M^{-1} cm^{-1}, which allows for good responsiveness. The reverse reaction is thermally activated and occurs spontaneously in the dark.

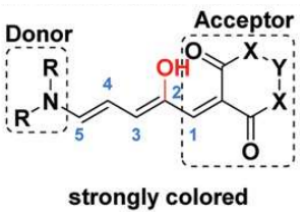

Figure 1: DASAs chemical structure

The mechanistic pathway of photoswitching has been determined through quantum chemical calculations and kinetic modelling, as well as experimental analysis (time-resolved infrared absorption spectroscopy). Several isomers are formed by photoisomerization and rotation steps, followed by a reversible Nazarov-type 4π-electrocyclization and by a final proton transfer leading to the cyclized form of the compound [4].

3. Molecular design and synthesis of DASAs

Over the years, the development of DASAs with variable donors, acceptors, and spacer linkers, has allowed a considerable reduction of the photoswitching response time [2]. For cell stimulation, the DASAs kinetics need to match biological events timescale, close to the millisecond. That is why, the main goal of this work is to find adequate designs of DASAs allowing for their partitioning inside the cell membrane and featuring a rapid photoswitching.

To increase the photoswitching rate, the focus has been onto the acidic part of DASAs, which has a strong influence on the absorption properties of the compounds. Moreover, the anchoring property has been conferred through a polar head attached to the donor part. An alkyl halide has been linked to the amine, and the halide has been eventually replaced with a pyridinium. The alkyl chain has been made 4 to 6 carbons long for steric optimization. Among the halides, bromine has been chosen as the best option for two reasons: its reactivity (better than chlorine but worse than iodine) and the low cytotoxicity towards cells, iodine being hazardous.

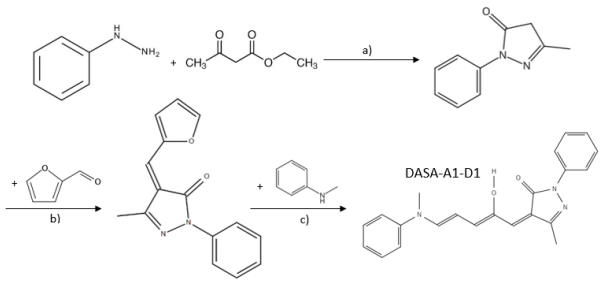

Figure 2: General reaction pathway applied to the formation of the DASA-A1-D1[1]: (a) 3h, acetic acid, 118°C, (b): 2h, DCM, RT°C, (c): 2h, DCM/HFiP (20%), RT°C

The synthetic route to obtain the DASAs has been inspired from the literature [2], and uses as a building block the furfural, a bio-based molecule derived from various agricultural by-products. Figure 2 shows the general scheme applied to the synthesis of the first DASA here synthesized. The reaction scheme starts with a cyclo-condensation to yield the chosen acidic part (Figure 2a). Then, a Knoevenagel condensation of the acidic group with the furfural is carried out (Figure 2b). This condensation reaction

[1]The DASA-A1-D1 has been synthesized without polar head, as a first trial. It has been useful to elaborate a systemic photophysical characterization procedure.

activates the furan ring that can be successfully opened thanks to a donor moiety to form the triene backbone featuring a hydroxy group on the carbon "2" (see Figure 1)(Figure 2c). In this work, different donors and acceptors have been synthesized and combined to yield new DASAs (Figure 3). On two of them, the polar head has been effectively attached (Figure 4). The activation of the furan ring and its successive combination with the amine are fast reactions occurring at room temperature. Moreover, starting from few chemicals (donors and acceptors), a large number of final products can be yielded. However, to make this reaction route even more eco-friendly, the use of a greener solvent compared to dichloromethane is to be thought of.

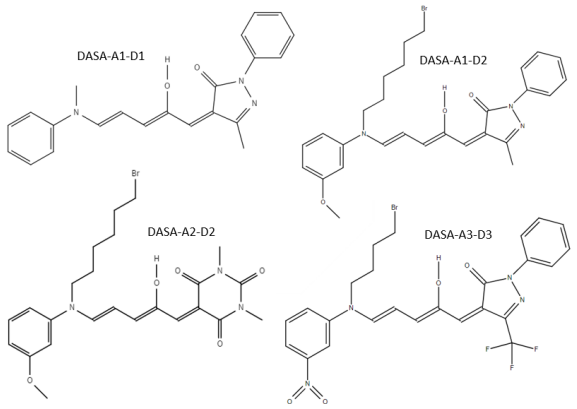

Figure 3: Chemical structure of the synthesized DASAs

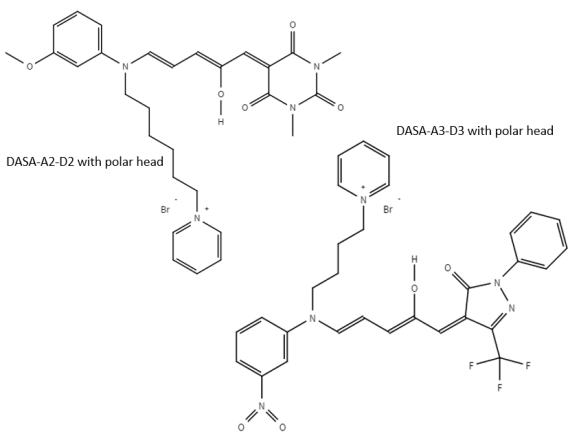

Figure 4: Chemical structure of the 2 DASAs with the polar head fully attached

The reactions were monitored through thin layer chromatography (TLC) on aluminum backed silica gel plates. The chemical characterization of the final products was conducted with hydrogen nuclear magnetic resonance (^{1}H-NMR) and mass spectroscopy.

4. Photophysical characterization of DASAs

To study the optical properties of the synthesized materials absorption spectra of the dark and the photostationary states were recorded in various solvent. The thermal back relaxation was investigated by monitoring the variation of the absorbance at the maximum for the open form in time. For the most promising derivate a more in depth study was performed, namely a preliminary fatigue resistance test, and emission spectra were collected in time after and during irradiation.

4.1. Red shift study with absorption spectra

The UV/vis absorption spectrum of the open form isomer is an interesting feature to be studied as bio-optics ideally require systems to be addressed with red and near-infrared light to maximize light penetration through living tissues. UV-visible spectra were recorded between 350 nm and 700 nm. Figure 5 shows the absorption spectrum of the synthesized DASAs. The value of the absorption maxima are listed in Table 2.

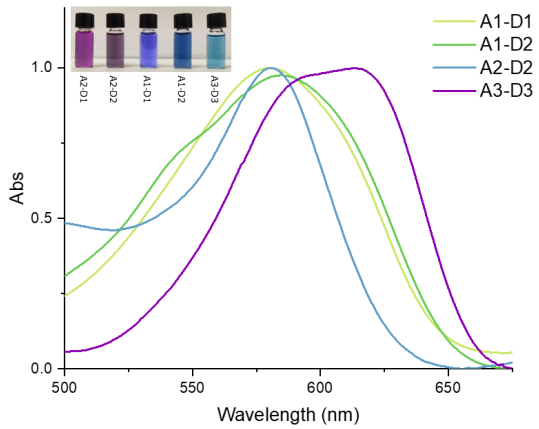

Figure 5: Absorption spectrum of the DASAs derivates in chloroform 10^{-5} M in the dark. Inset: picture of the compounds before irradiation

The absorption profile of the open isomer is quite redshifted for all compounds, with the position of the maximum only slightly affected by their

molecular structure. The different donors do not affect much the absorbance maxima, as expected since the substitution is in meta position of the phenyl ring, which leads to a milder effect on the electronic properties of the amine. The only significant effect going from the derivates with the acid A2, more studied in literature, to those with A1, is a broadening of the absorption band which might be due to a more dense population of the vibrational levels of the states involved in the transition. The bathochromic shift for A3-D3 might be due to the stronger acid used. The presence of two bands instead of one for the open isomer might be due to the presence of fluorine. For the compounds bearing a polar head the absence of a peak at wavelengths similar to the other derivatives might suggest that the presence of pyridine promotes the zwitterionic closed form or the degradation of the material.

4.2. Photoswitching study

4.2.1. Kinetics of photoswitching

Another interesting feature to study is the kinetics of photoswitching of the DASAs. Two experiments have been set up with the UV-Vis spectrophotometer. The spectra collected in time for one compound are reported in Figures 6 and 7 as an example. The first experiment consists in irradiating the DASAs before recording several absorbance curves in time in the dark, following the back isomerization, from the closed to open form (see Figure 6). The acquisition is made in the range 300 to 700 nm. Several cycles of measures have been recorded, without time delay between each cycle.

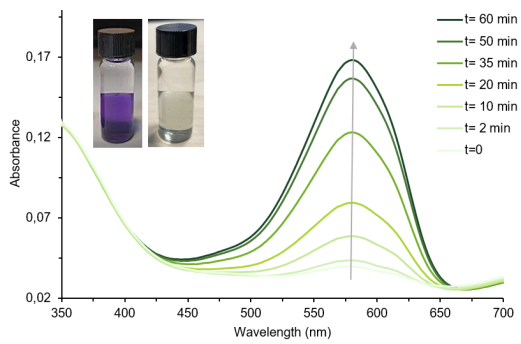

Figure 6: Absorption spectra of DASA-A1-D1 in time in chloroform at 10^{-4} M after 30 min of irradiation. Inset: switching from coloured to uncoloured isomer

Figure 6 evidences the photochromic behaviour of the DASA-A1-D1. Under visible light irradiation a fading in color is observed, from dark purple to transparent. Starting from the irradiated compound at t= 0, the figure shows that the initial absorbance at 580 nm is weak, and it is increasing in time. The Table 1 shows the in-time absorbance recovery (δ) that can be computed with the equation (1):

$$\delta(t) = \frac{A(\lambda_{max}, t0 + t) - A(\lambda_{max}, T0)}{A_0(\lambda_{max})} * 100 \quad (1)$$

with A(λ_{max}, t0 + t) and A(λ_{max}, t0) the value of the absorbance at a specific time t and at the start of the experiment, respectively, and $A_0(\lambda_{max})$ the value of the absorbance before the irradiation of the compounds. The latter has been graphically read on the absorption spectra.

	10 min	20 min	35 min	60 min
δ (%)	2.2	4.4	10	18.9

Table 1: % of absorbance recovery of the DASA-A1-D1 in chloroform at 10^{-4} M at different times

The second experiment consists in monitoring the absorbance intensity at a specific wavelength (here the absorption wavelength of the open isomers) over time. The back reaction rate can be monitored if the recording of the absorbance at the λ_{max} over time is made after having irradiated the compound.

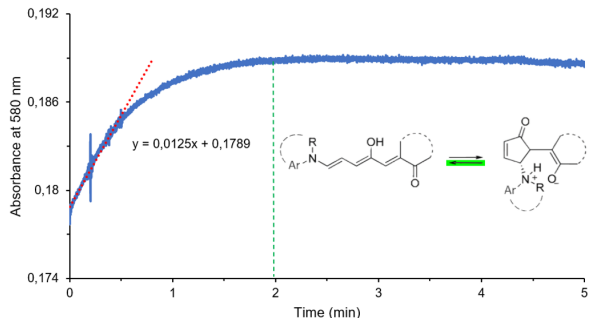

Figure 7: Absorbance at 580 nm in time after 15 min of irradiation of DASA-A1-D1 in chloroform at 10^{-4} M and molecular scheme of the switching from the open to closed isomer

For each obtained curve, the initial slope on the linear part has been computed (μ) giving hints

on the speed at which the molecules in solution switch back from the closed to the open form right after turning the light off. The time at which the plateau (maximum recovery) is reached (τ) and the percentage of absorbance recovered when the plateau is reached ($\delta(\tau)$) have been determined too (see Figure 7). While the first two parameters are determined graphically on the kinetic curves, the percentage of recovered absorbance is computed as in the equation (1), taking t equal to τ. All the data collected and elaborated are presented in Table 2.

4.2.2. Emission/excitation spectra

Finally, for the DASA-A1-D1 the photoisomerization was studied also through photoluminescence. The spectrofluorimeter can provide emission spectra. Basically the compound is irradiated at a selected wavelength (excitation wavelength) and the emitted light is possibly recorded at a higher wavelength. The absorption maximum is kept as the excitation wavelength, being 580 nm for the DASA-A1-D1. A measure of the intensity of emission has been realized every 1 nm from 600 to 800 nm. In the Figure 8, the change in emission properties during the reverse reaction occurring after irradiation is monitored, from the closed (T0) to the open isomer (T0 + delay time).

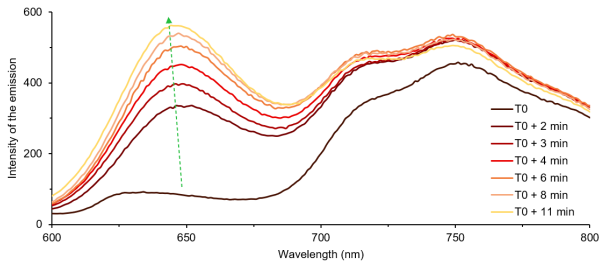

Figure 8: Emission spectra after irradiation of the DASA-A1-D1 at 10^{-4} M in chloroform and excitation at 580 nm

Figure 8 shows that the starting compound exhibits an intense emission band around 650 nm (signal that can be attributed to the formation of aggregates) while upon light irradiation this peak becomes very weak (T0). The closed form of the DASA-A1-D1 is just weakly emissive in the visible range. The presence of an emission band at wavelength different from that of cell autofluorescence, which is between 350 and 550 nm, is quite useful. In fact this might allow for a better visualization of the localization of the actuator in the cell, without the need for a fluorescent marker that might modify the properties of the compound.

5. Results discussion

In the Table 2 are gathered all the results obtained with the previously described experiments, for each synthesized DASA.

Considering their absorption maxima, all the prepared compounds absorb light in or close to the therapeutic window. However, the introduction of the pyridinium-terminated alkyl chain results in a loss of that signal, possibly after the isomerization to the photo-inactive zwitterionic form. The alkyl chain with the polar head might increase the distortions, or stabilize the closed form through interactions between the various ions. Therefore, the absorption bands observed for the DASAs with polar head would be related to their cyclic isomers. The DASA-A1-D1 at a very dilute concentration ($5x10^{-6}$M) appears to be the fastest one to photoswitch among those tested. However, it shows a poor absorbance recovery at higher concentration (10^{-4}M), which could be explained by the formation of aggregates impeding the complete recovery of the signal. All of the synthesized DASAs show a photoswitching kinetics faster than the ones published in the literature, albeit not yet quick enough for some biological applications, such as cell stimulation.

Moreover, it seems that when attaching the polar head, the photochromic behaviour is hindered. This behaviour might be explained by the presence of a counterion in the salts, which might stabilize the zwitterionic isomer of the closed DASA, effectively preventing the thermal back-relaxation. However, this might be avoided by using a polar head with an inner salt, such as phosphocholine. Besides, the bromine counterion should not be able to penetrate inside the cellular membrane, so even if adequate experiments would have to be performed to confirm this hypothesis, the photoswitching of those compounds might still be effective for bio-optics purposes. Lastly the presence of an emission

			Absorption spectra			Kinetic experiments		
DASA	Solvent	Molar concentration (g/mol)	λ_{max} (nm)	δ(t) (%) at 10' and 20'		μ (min^{-1})	τ (min)	$\delta(\tau)$ (%)
DASA-A1-D1	CHCl3	10^{-4} and $5x10^{-6}$	580	2.2	4.4	0.0125	2	2.4
DASA-A1-D2	TOL	10^{-3}	585	92	117[2]	0.0042		
DASA-A2-D2	TOL	10^{-4}	580	16.4	24.2	0.0023	88	24
DASA-A3-D3	CHCl3	10^{-4}	614	31	51	0.0053	87	115[2]
DASA-A2-D2 w/ polar head	DMSO	10^{-4}	487	0	0	0.0004		
DASA-A3-D3 w/ polar head	CHCl3	10^{-4}	397	0	0			

Table 2: Summary of the optical properties of the synthesized DASAs

profile different from that of the cell autofluorescence proves useful for biological studies, as no further labelling would be required.

6. Conclusions

In this project, the synthesis of new DASAs was tested, and proven to be efficient, following some green chemistry principles. A photophysical characterization has been conducted on each synthesized DASA to study the optical and photochromic properties. The results of the photophysical experiments have shown that the majority of the synthesized DASAs presented well red-shifted absorption spectra. Moreover, the recorded photoswitching kinetics are still slow in comparison to biological events timescale, nonetheless the results are better than those reported in literature, and already acceptable for some bio-applications. It should be noted that the data recorded are for the bulk materials, in order to determine the isomerization rates of the single photoswitch pump probe experiments will be performed in the future on the most promising candidates. Moreover, the study has shown that the DASAs in which the polar head had been fully attached to the skeleton showed a poor, or nonexistent, photochromism. Nevertheless, this might not be the case inside the cellular membrane, in which the counterions do not partition, and hence cannot stabilize the zwitterionic form. Appropriate experiments should be conducted to draw deeper conclusions. Besides, this issue might be overcome through the use of a different polar moiety. Because of their many advantages, the synthesized DASAs in this work are very attractive for biological applications, and even if fast enough rates cannot be achieved for cell stimulation, several other uses might be developed, such as photocages for drug delivery, platforms for controlled photorelease, or even as orthogonal wavelength selective systems when paired with other photoswitches.

[2] The value of the recovered absorbance exceeds 100%. This might be due to the fact that some molecules of this DASA had already switched into the closed form due to the natural light entering the room when the absorption spectrum has been realized "in the dark".

7. Acknowledgements

I would like to acknowledge here my co-advisor, the dott.ssa Paola Moretti for the considerable help she provided me during this work.

References

[1] A. M. et al., "Light at the end of the channel: optical manipulation of intrinsic neuronal excitability with chemical photoswitches," **2013**.

[2] J. R. H. et al., "Controlling dark equilibria and enhancing donoracceptor stenhouse adduct photoswitching properties through carbon acid design," **2018**.

[3] H. B.-L. et al., "Organic photochromism (iupac technical report)," **2001**.

[4] H. Z. et al., "Taming the complexity of donoracceptor stenhouse adducts: Infrared motion pictures of the complete switching pathway," **2019**.

POLITECNICO
MILANO 1863

SCUOLA DI INGEGNERIA INDUSTRIALE
E DELL'INFORMAZIONE

Donor Acceptor Stenhouse Adducts: novel photochromic nanoactuators for bio-optics

Tesi di Laurea Magistrale in
Materials engineering and nanotechnology -
Ingegneria dei materiali e delle nanotecnologie

Author: **Maéna Marlène Galeron**

Student ID: 963796
Advisor: Prof.ssa Chiara Bertarelli
Co-advisors: Dott.ssa Paola Moretti
Academic Year: 2021-22

Acknowledgements

I would first like to express my gratitude towards my co-advisor, the dott.ssa Paola Moretti for her considerable help, shared experience and always relevant advices she provided me during this work. Thank you for your constant availability.

Secondly I wish to acknowledge my advisor, the prof.ssa Chiara Bertarelli for her trust and benevolence. Thank you for having given me the opportunity to accomplish this project.

I wish to say a warm thank you to the chemistry, materials and chemical engineering department's PhD team for their friendly welcome, and for making this laboratory a place of mutual support and conviviality.

Finally, I wish to thank the Ecole Centrale de Nantes and the school Politecnico di Milano for giving me the chance to do this double degree, without which I would never have been able to conduct this master thesis project, and never have learned so much about research and teamwork.

Abstract

Photochromic materials interact with light converting into a different isomeric state when irradiated with a suitable wavelength. They constitute the building block of light driven molecular switches and machines, and their use in biological environment is currently being developed. The donor-acceptor Stenhouse adducts (DASAs) are an emerging family of photochromic compounds, able to switch from an open isomer to a closed one upon visible light irradiation. It is thought that, with some optimization, they could be well suited to act as all-optical probes to monitor and/or control the interaction of cells with their environment through their membrane. By properly designing the molecular structure of the DASAs, their photochromic properties, as their red-shift in absorption or their photoswitching kinetics, can be finely tuned. In this work, several new DASAs have been synthesized with different donor and acceptor moieties, in order to elaborate a proper structure able to be anchored in a cell membrane and featuring a rapid photoswitching rate. The attachment of a polar head onto the DASAs is one of the requirement for the desired application. Each new DASA synthesis has been followed by a photo-physical characterization realized by UV-vis spectroscopy, and emission excitation spectroscopy. The results of the performed spectral experiments show that the actuators prepared possess a well red-shifted absorption, up to 614 nm for one compound. Moreover, the kinetics study determined photoswitching rates faster than those previously reported in literature for bulk materials. Even though the photochromic switch still requires illumination times longer than biological events, possibly preventing cell membrane stimulation, some features have been uncovered that might allow for even further fastening of the switching rates. Still, many applications in the biological field are already attainable, such as photocages for drug delivery or platforms for controlled photorelease.

Keywords: Donor-Acceptor Stenhouse Adducts, photochromism, molecular design, photoswitching kinetics, spectrophotometry, molecular photoswitch

Abstract in lingua italiana

I materiali fotocromici interagiscono con la luce convertendosi in uno stato isomerico diverso sotto irradiazione con una lunghezza d'onda adeguata. Costituiscono l'elemento di base di interruttori e macchine molecolari azionati dalla luce ed il loro uso in ambiente biologico è in corso di sviluppo. I donor-acceptor Stenhouse adducts (DASAs) sono una famiglia emergente di composti fotocromici, in grado di passare da un isomero aperto a uno chiuso con l'irradiazione di luce visibile. Con una certa ottimizzazione, potrebbero essere adatti a fungere da sonde ottiche per monitorare e/o controllare l'interazione delle cellule con l'ambiente attraverso la loro membrana. Progettando adeguatamente la struttura molecolare dei DASAs, è possibile regolare finemente le loro proprietà fotocromatiche, come il red-shift dell'assorbimento o la cinetica di fotoswitching. In questo lavoro, sono stati sintetizzati nuovi DASAs con diversi gruppi donatori e accettori, al fine di elaborare una struttura molecolare in grado di essere ancorata alla membrana cellulare e caratterizzata da una rapida velocità di fotoswitching. Il fissaggio di una testa polare sui DASAs è uno dei requisiti per l'applicazione desiderata. La sintesi di ogni nuovo DASA è stata seguita da una caratterizzazione fotofisica realizzata mediante spettroscopia UV-vis e spettroscopia di eccitazione ed emissione. I risultati degli esperimenti spettrali effettuati mostrano che gli attuatori preparati possiedono un assorbimento ben spostato verso il rosso, fino a 614 nm per un composto. Inoltre, lo studio della cinetica ha determinato tassi di fotoswitching più rapidi di quelli precedentemente riportati in letteratura per le soluzioni. Anche se lo switch fotocromatico richiede ancora tempi di illuminazione più lunghi degli eventi biologici, impedendo forse la stimolazione della membrana cellulare, alcune caratteristiche non sono state studiate, che potrebbero consentire di accelerare ulteriormente i tassi di fotoswitching. Tuttavia, molte applicazioni in campo biologico sono già realizzabili, come le fotocage per la somministrazione di farmaci o le piattaforme per il fotorilascio controllato.

Parole chiave: Donor-Acceptor Stenhouse Adducts, design molecolare, cinetica di fotoswitching, spettrofotometria, fotoswitch molecolare

Contents

Introduction

Smart materials (also known as responsive materials) are defined as materials able to interact with an external stimulus such as light, temperature, electrical or magnetic field, mechanical action, ... and, resulting from this interaction, a reversible change in some chemical or physical properties occurs. They are at the basis of several applications in various fields, for example, sensors, actuators, artificial muscles, optical devices, security documents, self-healing materials, ... Light activated systems (called photoresponsive materials) present numerous advantages over the other types of smart materials. They feature a controlled space resolution and a response intensity that can be easily tuned by the amount of light used as stimulus [1]. Recently, they have been widely used in optical data storage devices, cell detectors, ion sensors, nanomedicine, ... Those photoresponsive materials are the building block of light driven molecular motors and machines. A molecular photoswitch is usually an organic molecule containing an extended aromatic system making it responsive to light. Its interaction with light allows it to interconvert between two or more isomeric states, showing what is called photochromism [2]. Upon irradiation, the compound is excited towards a more energetic state, and several relaxation events can follow, back to the ground state of the compound itself, or of another isomer. This reversible isomerization features some structural and electronic changes, allowing the complete differentiation of the different states notably by their UV-vis absorption properties. Each photoswitch shows specific altered properties upon photoisomerization and can be then selected for different kind of application. For instance, cell stimulation with photoresponsive materials could be used as a novel type of tool in regenerative medicine.

Physiologically, the cellular membrane has several functions such as favouring cell adhesion on surfaces, regulating the permeability barrier, collecting and conserving nutrients, or even interacting with the central nervous system, or with other cells. This last function is made possible through small pores, called ion channels, present on its surface (see Figure 1). These channels allow the movement of electrically charged molecules (such as sodium or chloride ions [3]) from and to their inner part, resulting in an electrical current and in an action potential. This communication process is called quorum sensing, and the nearby cells are able to detect those released molecules thanks to specific receptors present

on their surface. The information thereby supplied is the building block of cell stimulation and is extremely important to activate many intracellular signaling pathway. Rapid information transfer within cells and towards their environment is complex and couples the membrane potential state and the opening-closing of the ion's channels gates. Therefore, the study of the electrical activity of cellular membrane is crucial to better understand biological processes such as cell migration, proliferation, and differentiation, and requires a method to measure and control their membrane potential. The traditional method used is the patchclamp technique, which consists in putting in contact the membrane with a glass micropipette filled with an electrolytic solution allowing the measurement of membrane voltage changes in real time. This technique is considered as the gold-standard to efficiently screen ion channels, thanks to its exceptional noise to signal ratio, and temporal resolution. However, the major drawback of this method, besides being delicate and requiring expensive devices, is its invasiveness, as electrodes are necessary. Such intrusion may also disrupt normal cell physiology [4]. That is why optical techniques making use of light started to gain interest among the scientific community. For biological systems, light is a favourable stimulus, as it is one of the most widely available energy sources, non-invasive, environmentally friendly and with high spatial and temporal resolution [5]. To be able to interact with biological systems, a tool responding to an external photon flux is needed. Molecular photoswitches making use of smart materials are interesting candidates for this purpose. Already in the late 1960s, they have been applied to study the electrical activity of neuronal cell membrane through photoregulation of ion channels using photochromic ligands [6].

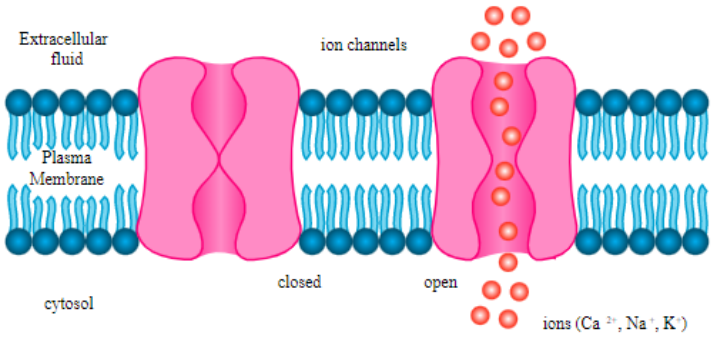

Figure 1: Ion channels inside a cellular membrane [7]

For biological purposes involving the interactive behaviour of cells through their membrane, photochromic compounds reveal themselves very interesting. As previously mentioned, the main issue is to control the function of ion channel in their natural environment. It is indeed their opening and closing that is responsible for the initiation and

propagation of the action potential (AP). Typically, when the cells are "excited", their membranes are depolarized above the initiation threshold AP, and the channels open to allow a flux of ions to enter or leave the cell, movement that will depolarize the membrane even more [6]. When the channels close, the opposite effect is observed, the membrane undergoes a repolarization, but as the closing process is slower, the membrane enters a hyperpolarization phase. By quickly photoregulating the flux of ions, one could success to modulate the AP firing. Such process could serve in many applications as the sight restoration by changing with light the electric potential of photoreceptors; the neuronal firing modulation, responsible for the communication between neurons through electrical impulses and neurotransmitters; or even bacteria stimulation. A molecular photoswitch can bring the membrane potential closer or further from the required potential threshold for initiating the action potential (AP firing). Upon light irradiation, the photochromic species involved in the molecular photoswitch undergo photoisomerization and some modifications on their spectral, chemical, physical and electronic properties occur. In the past decades azobenzenes have been largely used to modulate neuronal cell membranes potential. Those relatively small molecules are quite easily functionalized (necessary so that the molecule can anchor itself inside the membrane) and undergo a photoinduced change in geometry and polarity on a picosecond timescale, which is faster than most of the biological events. Depending on the conformation of the azobenzene moiety and on its in-time polarity, parameters controllable with light, the molecules will either act as ion conduction blockers either as ion conduction enhancer.

In this work, we will focus on another type of photochromic compounds that we believe present many advantages to be used for biological purposes: the Donor-Acceptor Stenhouse Adducts (DASAs). DASAs intrinsically contain a donor amine and an acid carbon acceptor linked by a triene (or triene-enol) backbone as shown in the figure 2 [8]. They are interesting for their characteristics that differentiate them from previous similar compounds. Thanks to their planar structure and conjugated backbone, they absorb visible light unlike most photochromic materials which absorb in the UV range. This is a great advantage of DASAs as in biological systems UV light can reveal itself hazardous for living cells and has a short penetration length is tissues. Consequently, smaller energy wavelength as visible light or NIR (near infrared) are better suited for in-vivo applications. DASAs show negative photochromism and go from a coloured to uncoloured isomer, therefore providing higher light penetration efficiency in the bulk of the compound during irradiation. Finally, they have an amphiphilic nature and switch from apolar to polar upon irradiation, changing their conformation from a linear structure to a cyclic one about half the size of the linear form. The polar nature of the isomer at the

photostationary state ideally allows for a spontaneous partitioning inside the cell membrane upon irradiation and changing their conformation and geometry, the DASAs would be able to modulate the thickness and the polarity of the membrane, generating a change in the membrane potential. To achieve this goal, they must be functionalized with a polar head to act as an anchor in the cell membrane. DASAs synthetic design enters the "green chemistry" and uses furfural, an industrial organic compound that is derived from various agricultural by-products such as corn, oat and wheat bran, and sawdust [9]. Despite the great advances made these last few years, some specific features closely linked to both the strength and steric occupation of the donor and acceptor moieties, such as the thermal equilibrium between the opened and the closed isomer and the photoswitching kinetics, still need to be investigated. Moreover, for biological applications, these compounds will need a fine tuning of their properties in order to achieve a faster photoswitching with respect to the previously published results.

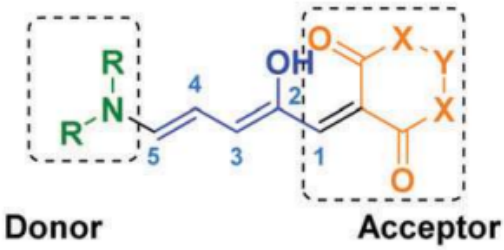

Figure 2: DASAs general structure [10]

1 | Introduction to photochromism

1.1. Historical context

During the second half of the 19th century, some scientists have witnessed photochromic phenomena. Fritzsche saw a coloured solution of tetracene bleaching when exposed to light, and getting back its color in the dark; Ter Meer reported a change in colour according to light exposure of the potassium salt of dinitroethane; Phipson noticed that a painted gate had not the same colour during the day and during the night. Some years later, Markwald studied this phenomenon on some molecules and decided to name it "phototropy". In 1911 Ciamician, who also worked on phototropy, said "The dress of a lady so prepared would change its colour according to the intensity of the light [...]: the last word of fashion for the future" [11]. At this time, he was far from imagining all the possible future applications of this type of photochromic substances. 50 years later, after some studies, Hirshberg proposed to change the name "phototropy" to "photochromism", coming from the Greek words: phos meaning light and chroma meaning colour (even if this phenomenon is not exclusive to coloured compound but includes also systems absorbing in the UV and in the IR). As chemical synthesis and photo-physical methods such as infrared spectroscopy or nuclear magnetic resonance were being developed, also studies on photochromism have expanded. Indeed, in 2003, according to the IUPAC, among the 9600 references on photochromism that existed at that time, almost 60% were published during the last decade (1990s) [12]. Today photochromic materials are found in various applications, mainly divided in two categories. The first one is exclusively using the change in absorption / emission spectra of photochromes. In this category, they are used as transmission optical materials, optical data storage devices, cosmetics, optical power limiting substances (used to preserve the human eye from powerful light flashes by suddenly becoming opaque when exposed to the flash and getting their transparency back right after). The second category enjoys the change in other physical and/or chemical properties under light irradiation such as the viscosity, the surface wettability, the polarity, the electric conductivity, solubility, etc... The most famous application of photochromic materials remains still today the so-called smart sunglasses which darken under

sunlight. In the biomedical field, the design of optobiolectronic devices benefits from the combination of photochromic compounds and biomaterials (mainly biopolymers), and a lot of new applications are nowadays emerging.

1.2. Theoretical concepts and mechanistic

The definition of photochromism adopted by the IUPAC is the following: "*a reversible transformation of a chemical species induced in one or both directions by absorption of electromagnetic radiation between two forms, A and B, having different absorption spectra*" [12]. A is called the thermodynamically stable form of the specie, and B is called photoproduct. According to the stability of the latter, the photochromic process can be of P-type (the back reaction is induced by absorption of photons at another wavelength) or of T-type (the back reaction spontaneously occurs by a thermal mechanism). Depending on the relative absorption wavelengths of the two isomers, the photochromism is classified as positive or negative. If A absorbs light at higher or lower wavelengths than B, the photochromic process is negative (or reverse), or positive, respectively. The first step of the photoreaction is the absorption of one (or more) photons by the molecule A at the ground state S0, to reach an excited level A* on S1 (or higher excited states), and several relaxation events can occur (vibrational relaxation, internal conversion, etc.), back to the ground state of the compound itself, or of another isomer. The figure 1.1 displays the energetic barriers to overcome in order to switch from one isomer to another, and shows the two stable and metastable equilibrium positions. For each deactivation process, a rate constant and a quantum yield can be defined, evaluating its relative relevance compared to the other deactivation processes. This reversible isomerization features some structural and electronic changes, allowing the complete differentiation of the states notably on their UV-vis absorption properties.

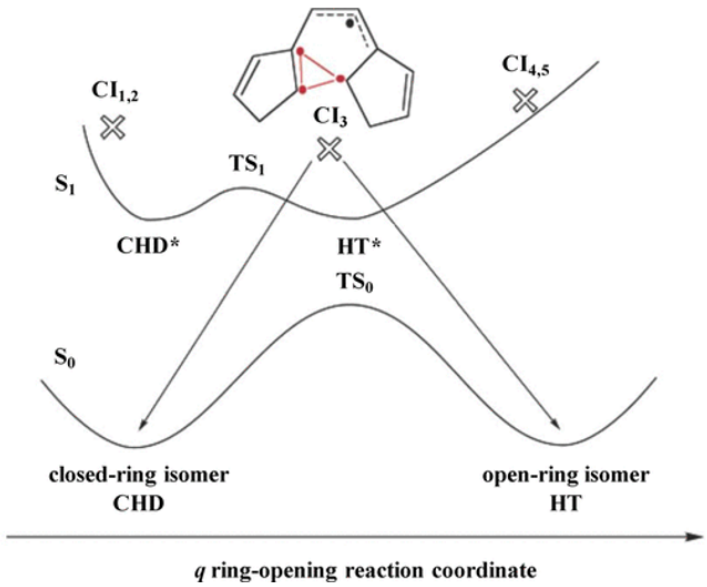

Figure 1.1: Conical intersection of potential energy associated with the ground and excited state of a molecule displaying two isomers [13]

To characterize the photoreaction from a mechanistic point of view, some relevant parameters must be introduced, mostly related to the efficiency of the reaction and to the performance of the photochrom.

As example the quantum yield of the photoreaction is defined as the molar ratio between the specie that is produced according to the deactivation process involved (photons for fluorescence and phosphorescence, or molecules for vibrational relaxation) and the absorbed photons. It has to be measured by specific experiments to access the immediate amount of the output species (emitted photons, thermodynamically stable form, photoproduct, eventual bi-product or degradation products, ...) and the incident flux of photon. The latter can be measured thanks to an actinometer. It consists in a chemical or physical tool able to determine the number of photons sent by a beam. As example, a solution of iron (III) oxalate can function as a chemical actinometer as it undergoes a photolysis when exposed to light and the production rate of Fe^{2+} can be measured and correlated with the number of photons absorbed by the solution [14].

Another important parameter is the response time. This feature can now be accessible thanks to the development of time resolved transient absorption spectroscopy that allows to detect transient chemical species, giving insights to the dynamics of the photochromic process.

As previously mentioned, photochromism is by essence a reversible process, this is what

distinguishes it from simple photochemical reactions. However, side reactions on organic photochromic materials (degradation, oxidation, isomerization into a non-photochromic product, ...) might occur leading to an irreversible process and inducing a loss of performance over time. Fatigue resistance is a measure of the number of photochromic cycles after which the initial absorbance at a certain wavelength has decreased by 20%. The fatigue resistance experiments consist first in irradiating the thermodynamically stable form A so that the absorption of the formed isomer B reaches 90% of the photostationary state. Then, B is irradiated with another suitable wavelength to induce its complete bleaching (reverse reaction into A, called photochemical relaxation) (an example is shown in Figure 1.2). Those two steps are repeated several times and at each step, the absorbance of the two isomers is measured and compared with the initial one.

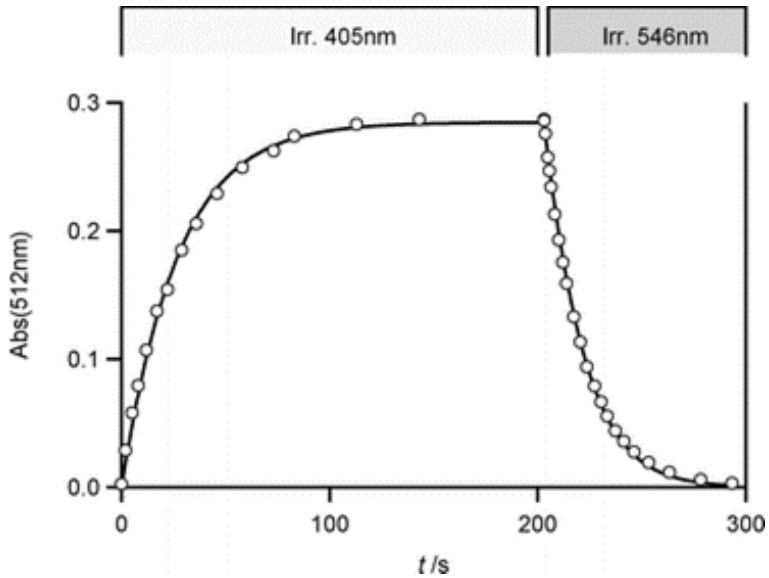

Figure 1.2: Example of evolution of the absorbance at 512 nm of a photochromic compound under continuous light irradiation [15]

Finally, another important parameter is the colorability, which gives the efficiency of a compound to color itself or to bleach immediately after a radiation pulse (measures the change in absorbance at the maximum absorption wavelength of the colored form).

1.3. Chemical processes involved in organic photochromism

Photochromic materials are usually divided in families depending on the chemical transformation that occurs through irradiation, the main processes are discussed in the following

sections.

Pericyclic reactions

Pericyclic reactions are organic reactions in which the excited molecule has a cyclic geometry and is opposed to linear reactions where the transition state is acyclic. They are usually electrocyclization reactions classified in 4n or 4n+2 depending on the number of electrons involved (see Figure 1.3), or cycloadditions / cycloelimination (commonly found in polycyclic aromatic hydrocarbons).

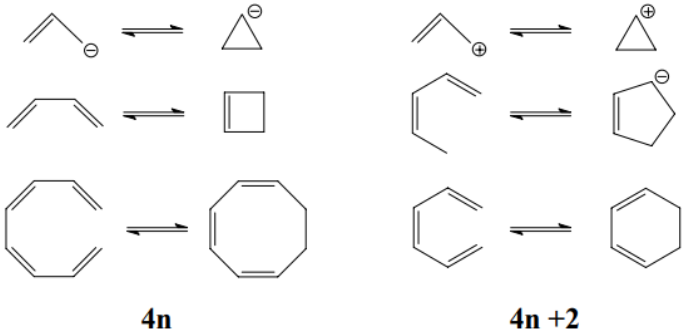

Figure 1.3: Examples of electrocyclic reactions [16]

Cis-trans (E/Z) isomerizations

Cis-trans isomerizations (also known as E/Z isomerization) are one of the main reactions involved in photochromism. As their name indicates it, the process is simply the interconversion between the cis and the trans isomer (or E and Z), featuring a 180° rotation around a double bond. The followed mechanism is characterized by two steps: firstly, the molecule absorbs a photon which promotes its excitation towards a more energetic state (as example from the trans isomer named t on the Figure 1.4, to one of its excited state, t*; or from the cis isomer, c, to c*). Then the relaxation into a perpendicular geometry state p* occurs and from here, through a non-radiative process, the molecule relaxes back towards the initial isomer or towards the other isomer. These cis-trans isomerizations are the processes involved in the photochromism of stilbenes, azo compounds, and also of some photochromic biological receptors which are part of living systems (retinal proteins like rhodopsin, or phytochromes which control the photomorphogenesis (light-induced development) of plants [16]).

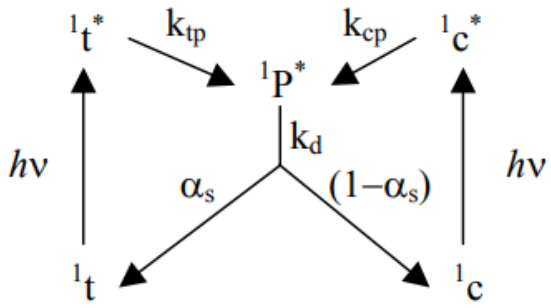

Figure 1.4: Cis to Trans isomerization mechanism [16]

Intramolecular hydrogen / group transfers (tautomerism)

The reaction involves the internal migration of a hydrogen atom, or respectively a group of atoms, to reach a more favourable energetic state [12].

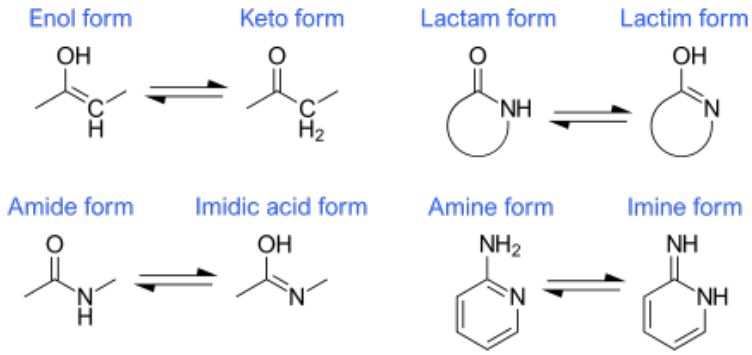

Figure 1.5: Examples of tautomerization reactions

Dissociation processes

Dissociation processes are either heterolytic (one atom gets the two shared electrons) or homolytic (the two electrons involved in the sigma bond are equally shared between the products) bond cleavages [12].

Electron transfers (oxido-reduction)

Photochromism can occur through oxido-reduction reaction by electron transfer. Usually in this case the compound can also undergo electrochromism (the properties of the material are changed when a voltage is applied). This is the case as example for viologen related systems [12].

1.4. Families of photochromes

Spiropyrans

Spiropyrans are possibly the predominant class of photochromic molecules. They are very much appreciated thanks to their sensitivity to many stimuli as light (UV, visible and near infrared), temperature, pH (acids or bases), mechanical forces, and thanks to their good color contrast. Their photochromic behaviour has been discovered in 1952 by Fischer and Hirshberg, and features a cleavage of one C-O bond upon irradiation to isomerize the molecule into the photoproduct (merocyanine form, see Figure 1.6). The latter can interact with biological systems, heavy metal ions, acids, and that makes it an interesting candidate to function as photoresponsive sensor to determine the presence of acid vapor, heavy metal cation (corrosive and highly toxic) in the human body which can cause serious health damages. However, they show a poor stability and photoreversibility, a possible toxicity towards some biological systems, a degradation into aqueous environment (and so into physiological environment), and photobleaching. Those drawbacks have limited their further application in optical field for example where the fatigue behaviour of photochromes is very important [1].

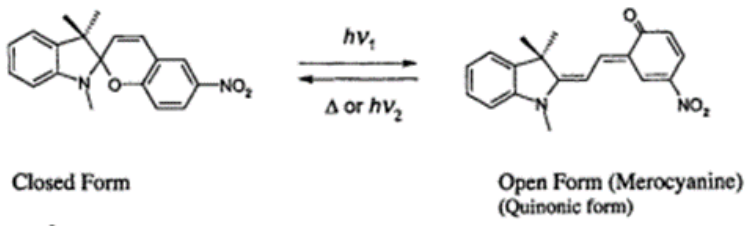

Figure 1.6: Chemical mechanism involved in the photochromism of spiropyrans [12]

Spirooxazines

Spirooxazine is a type of photochromic dye first synthesized in 1961 by Fox, showing positive photochromism: the colorless spirocyclic form (absorption band near the UV region) is changed into the intensely colored merocyanine form (strong absorption in the visible region) under irradiation with UV light (Figure 1.7). The mechanism involved is the heterolytic or homolytic cleavage of the C-O bond in the oxazine ring. This cleavage allows the extension of the conjugation system and is responsible for the strong colour of the open form. Those compounds are structurally very similar to the spiropyrans, the only difference lies in the replacement of one carbon atom involved in the heterocycle by a nitrogen atom. This small difference makes spirooxazines more stable than spiropyrans.

They show a better fatigue resistance and rapid response to light. Usually, the open form is quite unstable compared to the closed form, but they can coexist in equilibrium and a reversible shift towards the thermodinamically stable form can be reached with light irradiation or thermal treatment [17][18].

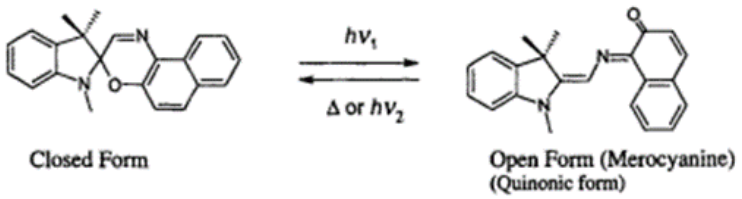

Figure 1.7: Chemical mechanism involved in the photochromism of spirooxazines [12]

Fulgides and fulgimides

Heterocyclic fulgides and fulgimides are also part of the most important photochromic compounds. Their names come from the latin word "fulgere" which means "to shine" due to their shiny colour as crystals in the solid state. Electromagnetic radiations promote structural rearrangements to reach a cyclohexadiene isomeric form of the compound (6π-electrocyclic rearrangement, see Figure 1.8). As the reverse reaction is photochemically induced, they are said to be P-type photochromes. Fulgimides are imide derivatives of fulgides. The colored cyclic isomers feature high thermal stability (attributed to the methyl groups on the triene in the open form), excellent switching reversibility without degradation and fatigue resistance. Moreover, fulgides and fulgimides are easily functionalized to acquire fluorescent properties (on one or both isomeric forms). These characteristics make them interesting as molecular switches, or optical data storage device using fluorescence as an efficient way of reading light-written data. Both fulgides and fulgimides haven't been greatly explored for biomedical purposes despite their highly interesting potential, fact that could be explained due to their challenging synthesis [19][20].

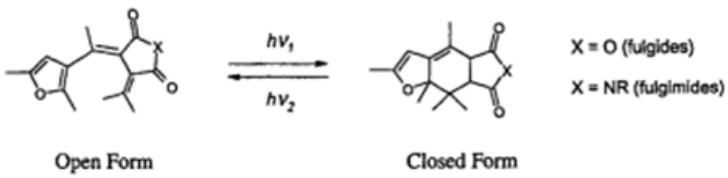

Figure 1.8: Chemical mechanism involved in the photochromism of fulgides and fulgimides [12]

Diarylethenes

Diarylethene is the common name of a family of chemical compounds having aromatic groups bonded together by a carbon-carbon double bond. They undergo an electrocyclization upon light irradiation (see Figure 1.9), showing positive photochromism. Diarylethene are maybe the most investigated photochromic compounds due to their fast response under electromagnetic irradiation. They also show high fatigue resistance and are thermally stable. The back reaction is usually photoinduced (P-type) but can also be thermally induced in some cases (T-type). Several applications use their photochromic properties such as photo-controlled fluorescent switching systems combined with nanoparticles or even with quantum dots. The open and closed form of diarylethene are differentiated through their absorption spectra but not only. Also their refractive indices, dielectric constants and oxido-reduction potential differ. As the closed form presents an extended conjugation through the entire molecule, and the open form does not, it allows the switching on and off of the electronic communication between functional groups linked to each side using UV and/or visible light [21].

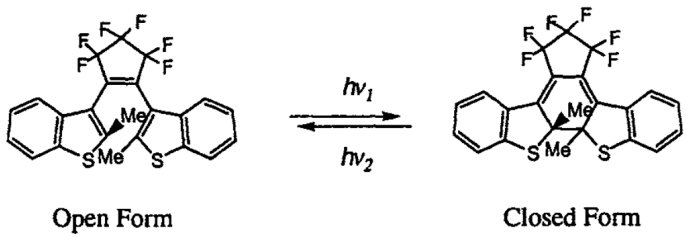

Figure 1.9: Chemical mechanism involved in the photochromism of diarylethenes [12]

Azo compounds

Azo compounds owe their names to the azo group (nitrogen-nitrogen double bond), responsible for the photochromism of the molecule. The organic family of azo compounds is large and divided in different categories according to the functional groups attached to the azo group. When this functional group is aromatic, the π system is expanded and the molecule can absorb visible light, while unsubstituted azobenzenes usually absorb in the UV range. Upon irradiation with light, azobenzenes undergo a reversible trans to cis photo-isomerization around the -N=N- bond, from the thermodynamically stable trans isomer to the metastable cis isomer. The reverse reaction can be triggered by light or by a suitable wavelength (Figure 1.10). The main advantages of this class of compounds are their facile synthesis and functionalization, rapid photoswitching (on the picosecond timescale) and high sensitivity. Their photochromic characteristics make them suitable

candidates for many applications: they are often incorporated in other materials, like in polymers to create optical memory devices, optical switch, in biopolymers (as cellulose) to create artificial muscles or to act as photo-regulated drug carriers [16][22][23].

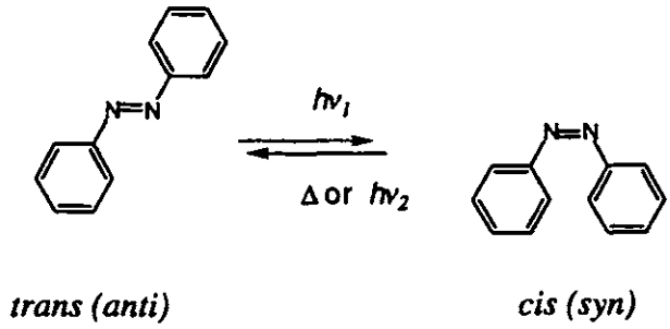

Figure 1.10: Chemical mechanism involved in the photochromism of azobenzenes [12]

Viologens

Viologens (also known as bipyridinium salts) are a family of compounds linking two pyridine rings functionalized at the nitrogen atom. They can undergo several reduction reactions: in the first one, one of the charged nitrogen gains one electron and becomes neutral (Figure 1.11), then other electrons can be transferred and the reduction reactions keep going. The first step produces a deep coloration of the molecule, and the intensity of the color is further controlled by the number of reductions involved. The color itself depends on the substituents linked to the nitrogen atoms [24].

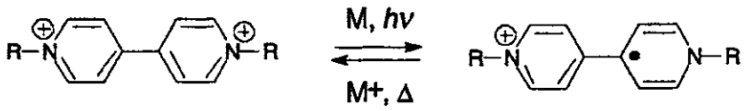

Figure 1.11: Chemical mechanism involved in the photochromism of viologens [12]

Chromenes

Chromenes are natural organic photochromic molecules undergoing an opening of a heterocycle upon UV light irradiation (Figure 1.12). The photoproducts that can be obtained are the two "opened" isomers, the transoid-cis and the transoid-trans (also called all trans). The open form is generally less stable than the closed one, and the reverse reaction (from the open to the closed form) can be achieved by thermal treatment or by a suitable irradiation. The open isomer is coloured and planar and has been for example used to form

complexes with DNA of cancer cells, showing a cytotoxic activity against them, while the closed form cannot interact with DNA [25].

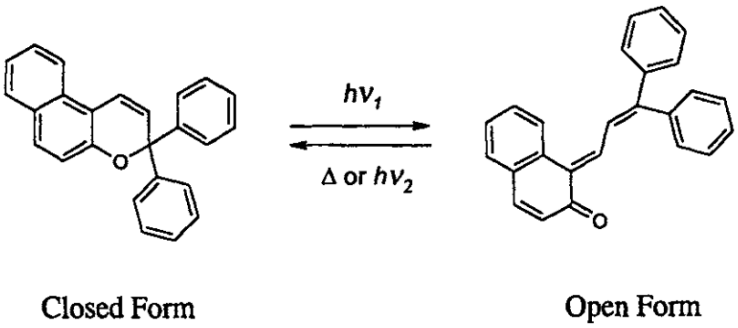

Figure 1.12: Chemical mechanism involved in the photochromism of chromenes [12]

Spirodihydroindolizines

Spirodihydroindolizines are an other example of photochromic compounds switching from a closed to an open form under light irradiation (Figure 1.13). The reverse reaction can be either thermally induced or photoinduced and shows a kinetics expanding from milliseconds to several weeks according to the nature of the substituents involved. The switching from the closed to open form involves three intermediates which can be detected thanks to time resolved spectroscopy [26].

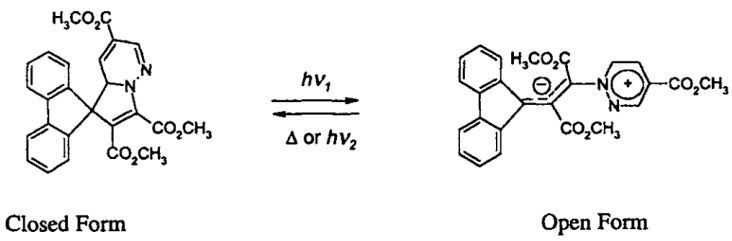

Figure 1.13: Chemical mechanism involved in the photochromism of spirodihydroindolizines [12]

Polycyclic aromatic compounds

Polycyclic aromatic compounds, and among them, polycyclic aromatic hydrocarbons, are a chemical family of compounds naturally found in coal, crude oil, and gasoline. In the last decade they have prompted great interest among the scientific community thanks to their large applications in optoelectronic devices (opto-transistors, organic field effect transistors, light emitting diodes, solar cells, ...) [27]. Under light irradiation or oxygen

atmosphere, they undergo a structural change conferring them a photochromic behaviour (Figure 1.14).

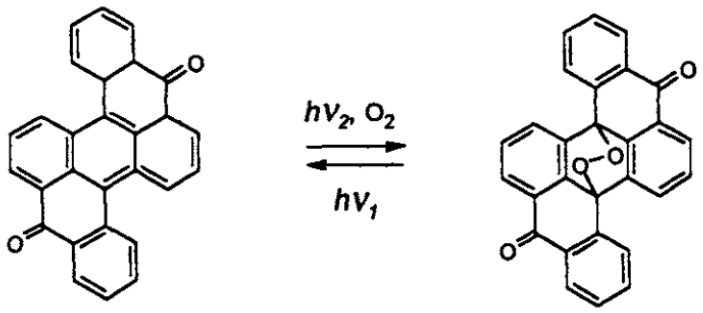

Figure 1.14: Chemical mechanism involved in the photochromism of polycyclic aromatic compounds [12]

Anils and related compounds (hydrogen transfer)

In organic chemistry, anils are any imine in which the nitrogen is linked to a phenyl group (thus also called N-phenyl imines). This family of compounds presents photochromic properties based on the transfer of a hydrogen atom upon irradiation, initially on a hydroxy group, to the imine nitrogen. A second photoinduced step occurs: a cis to trans isomerization (Figure 1.15). The reverse reaction is thermally activated, which makes this family of compounds T-type photochromes [28].

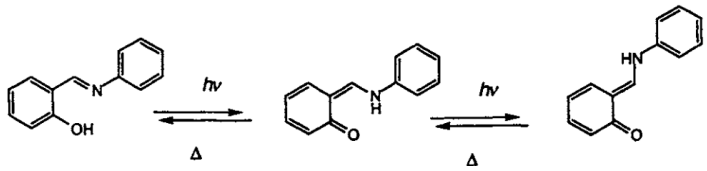

Figure 1.15: Chemical mechanism involved in the photochromism of anils [12]

Perimidinespirocyclohexadienones

This quite recent (beginning of the 20th century) family of photochromic compounds reveals photo and thermochromic properties. Upon light irradiation their undergo a reversible intramolecular hydrogen transfer that leads to a ring-opening reaction (Figure 1.16)[29].

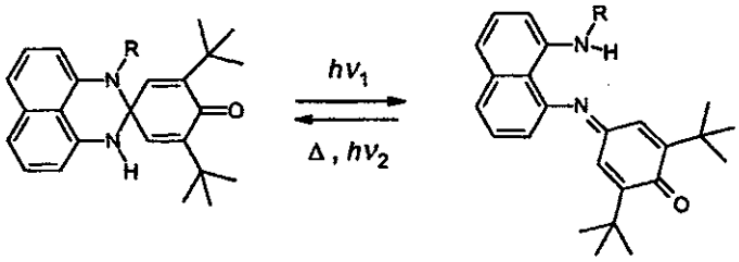

Figure 1.16: Chemical mechanism involved in the photochromism of perimidinespirocyclohexadienones [12]

Triarylmethanes

Triarylmethanes are organic compounds consisting of three aromatic rings linked by a central carbon atom with addition or not of substituent (generally added in the para position on the aromatic rings). They show intense and brilliant colour in the stable state, and are commercially used as colorants for foods or textiles. Under light irradiation they undergo photoinduced homolysis and heterolysis (Figure 1.17), processes being responsible for their photochromic behaviour [16][30].

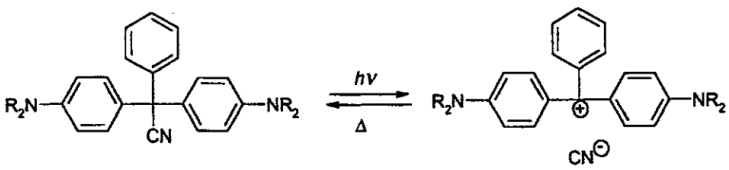

Figure 1.17: Chemical mechanism involved in the photochromism of triarylmethanes [12]

Donor Acceptor Stenhouse Adducts

Donor Acceptor Stenhouse Adducts, more simply referred to as DASAs, are an emerging class of photochromic compounds. Their chemical structure comprises a donor group and an acceptor moiety linked together by a conjugated triene backbone. Under visible light irradiation, the strongly colored open isomer undergoes an isomerization and a rotation step around a carbon-carbon double bond in the triene chain, followed by a reversible 4π-electrocyclization [2]. A colorless cyclic isomer is obtained as the photoproduct and the reverse reaction can be thermally activated, making the DASAs T-type photochromes.

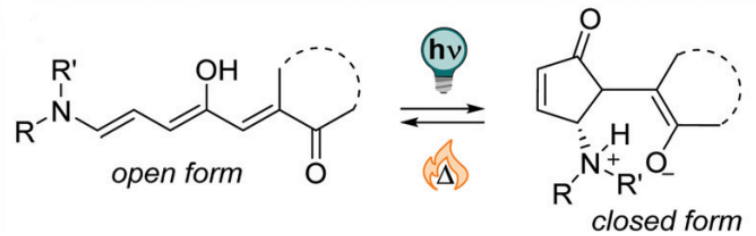

Figure 1.18: Chemical mechanism involved in the photochromism of DASAs [2]

In the next chapters, the chemistry of DASAs, as well as their photochromic properties will be explained in more details.

2 | Donor Acceptor Stenhouse adducts

2.1. History of DASAs

In the last few years a new class of photochromic compounds has been reported, possessing several promising structural features. They are known as Donor Acceptor Stenhouse Adducts (or DASA), and as suggested by the name possess a donor and an acceptor group, that is a push-pull compound. These materials are made of an electron donor group linked by a conjugated chain to an electron acceptor group. For this reason they allow for a fine tuning of their optical properties by modifying the strength of the groups or the length of the chain connecting them. This has attracted great interest in the study and research of such materials from the scientific community. DASAs in particular are highly coloured compounds (the molar extinction coefficient of the open form ranges around 10^5 M^{-1} cm^{-1} [31]), absorbing in the visible range of light (380 to 700 nanometers). Depending on their chemical structure, their absorption wavelength can vary from 450 nm to 750 nm [32]. Upon irradiation with light, they can be easily discolored, making them perfect candidates as negative molecular photoswitches.

The term DASA is very recent and appeared for the first time in 2014 in a work of Read de Alaniz and his co-workers, about a novel family of photochromic compounds. This name has been given as a recognition to John Stenhouse who described the Stenhouse salts in 1850 as the product formed by a condensation reaction of furfurals and amines leading to the opening of the furan ring (Figure 2.1).

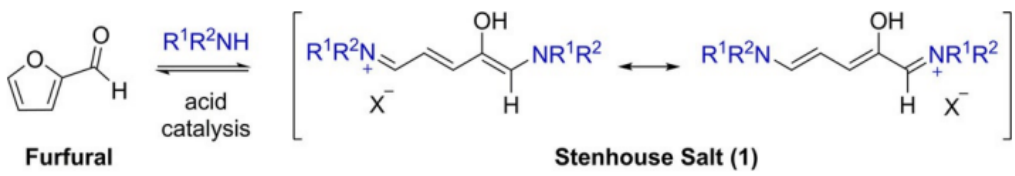

Figure 2.1: Stenhouse salts formation reaction [32]

2.2. Chemical structure and general synthesis

The chemical structure of DASAs is constituted of an electron donor moiety (an amine) and an electron acceptor moiety, linked by a triene backbone spacer (Figure 2.2). Originally the acidic part is composed of either Meldrum's acid or 1,3-dimethylbarbituric acid [32]. Nowadays we can classify the DASAs into three different generations: the first one employs as donor a dialkylamine, the second one, developed in 2016, uses a N-alkyl aniline as donor, and the third one, developed in 2018, comprises a strong electron-withdrawing carbon acid acceptor (Figure 2.3). The first generation of DASAs can't be isomerized in polar solvents, while the last generations feature a reversible photoswitching in polar and apolar solvents (better solvent compatibility) [33]. In the second and third generations, thanks to the introduction of aromatic rings into the donor part, a large bathochromic shift in the absorption wavelength is observed and the stability of the closed form is made modulable [34][35]. Finally, the last generation retains the advantages of the second one while providing a better control of the dark equilibrium (that is the relative ratio of the two isomers in the dark) [36]. These further developments made possible the use of DASAs for numerous new applications.

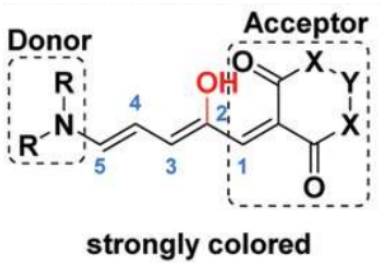

Figure 2.2: DASAs chemical structure [10]

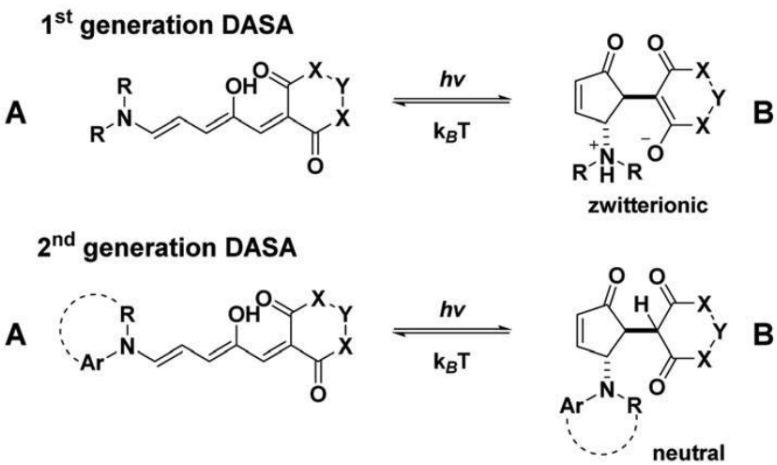

Figure 2.3: First and second generations of DASAs [10]

In the literature [8], an efficient synthetic pathway to obtain DASAs has been reported. This synthetic procedure starts with the combination of the chosen acid moiety with the furfural, which is, as previously mentioned, a bio-based molecule derived from various agricultural by-products. This first step is called a Knoevenagel condensation (Figure 2.4). It activates the furan ring that can be successfully opened thanks to a donor moiety to form the triene backbone featuring a hydroxy group on one of the carbons (C2-carbon on the Figure 2.2). The (aza)-Piancatelli reaction mechanism gives some clue to understand the ring-opening reaction leading to the formation of DASAs as well as Stenhouse salts. An example of such reaction is given in Figure 2.5. This ring opening reaction is strongly dependent on the sterics of the donor [10]. Moreover, if the donor moiety is not strong enough, its nucleophilicity might be too weak to promote the opening reaction. The activation of the furan ring and its successive combination with the amine are fast reactions occurring at room temperature. Finally, once the ring is fully opened, the final DASA is yielded by precipitating it in a proper solvent or by a trituration step, in order to get rid of the remaining aniline. The modulable chemical structure of DASAs is a key feature for understanding their photochemistry and for adjusting their photochromic properties depending on the desired application.

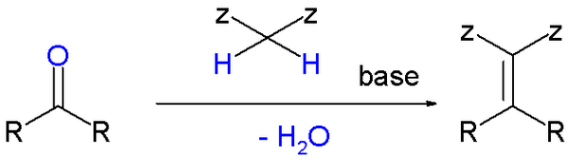

Figure 2.4: General mechanism of the Knoevenagel rearrangement

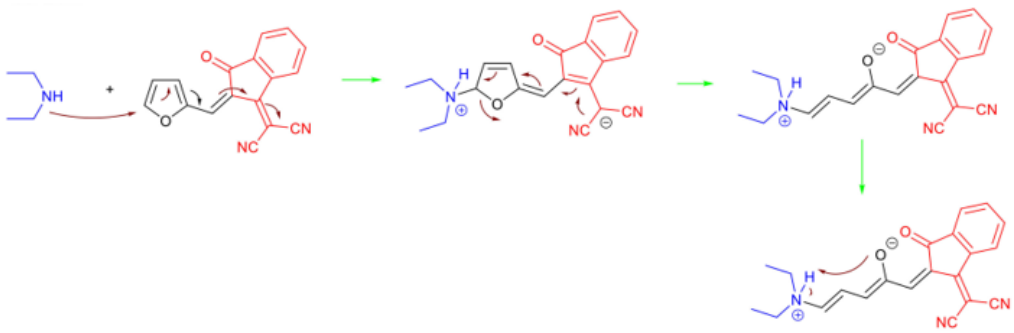

Figure 2.5: Example of (aza)-Piancatelli rearrangement [37]

In "Promoting the furan ring-opening reaction to access new donor–acceptor stenhouse adducts with hexafluoroiso-propanol" (2021), Michele Clerc et al. demonstrated that the use of 1,1,1,3,3,3-hexafluoro-2-propanol (HFiP) as a co-solvent was very efficient to promote the ring-opening reaction of furan adducts while decreasing the reaction time and stabilizing the open form isomer [36]. Moreover new DASA derivatives with donor parts which were previously not reactive enough to promote the ring-opening reaction, have been successfully synthesized in a mix of dichloromethane (DCM) and HFiP. DCM is a suitable co-solvent as it is nonreactive towards HFiP (no formation of hydrogen-bonded complexes) and it is inert in acidic environment.

2.3. Photochromism of DASAs

Under visible light irradiation, the strongly coloured hydrophobic linear form of DASAs is reversibly turned into a colourless cyclic hydrophilic photoproduct, therefore undergoing reverse photochromism. The linear triene form is the thermodynamically stable isomer and, compared to the cyclic colourless isomer, has a noticeably different geometry (about twice the size), and lower polarity. As the photoproduct does not absorb in the visible range, there is no inner filter effect, enhancing the photoconversion process, with light irradiation penetrating efficiently from the surface to the bulk of the material. The reverse reaction if thermally activated (T-type photochromism) and occurs naturally in the dark on a timescale depending on the chemical structure of the DASA and on the polarity of the solvent used [33].

To fully understand the mechanism of photoswitching of DASAs in solution and to identify the intermediate states, several studies comprising theoretical approaches (using for example quantum chemical calculations and kinetic modelling) as well as experimental ones (time-resolved infrared absorption spectroscopy) have been conducted. These studies have identified the formation of several isomers obtained by photoisomerization and rotation steps, followed by a reversible Nazarov-type 4π-electrocyclization and by a final proton transfer leading to the cyclized form of the compound. H. Zulfikri et al. in "Taming the complexity of donor acceptor stenhouse adducts: Infrared motion pictures of the complete switching pathway" (2019) proposed the following photoisomerization mechanism (Figure 2.6) [38]:

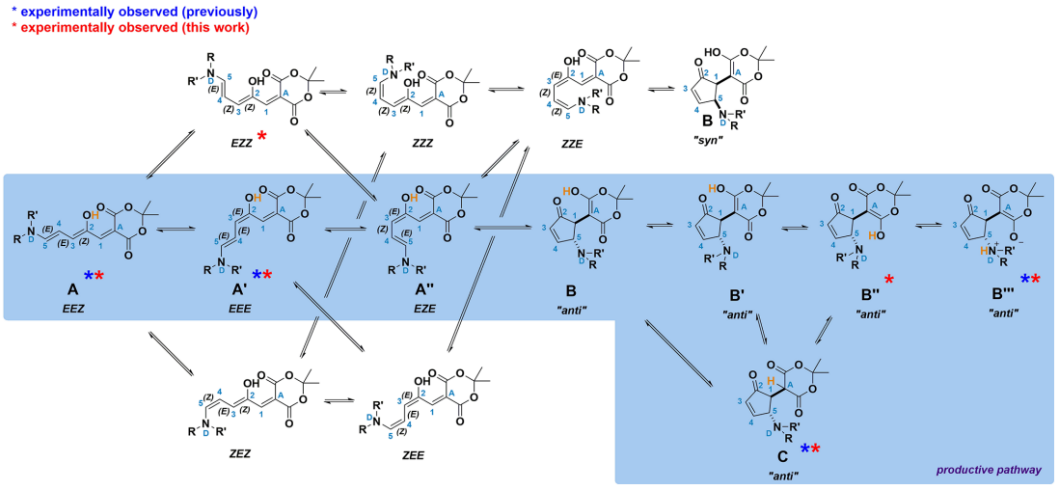

Figure 2.6: Mechanism of photoisomerization of DASAs [38]

The primary photochemical step (A → A') is the photoisomerization around the C2-C3 bond. This Z/E isomerization is extremely fast and occurs on a picosecond timescale. The hydroxy group on the C2 carbon seems to function as a pre-selector for the photoisomerization around the C2-C3 bond due to steric interactions and by modifying its bong length [2]. However, several other isomers can potentially be obtained by thermal rotation. Without this selective photoisomerization on the C2-C3 bond, the successive cyclization step is very difficult to be realized (it is for example the case for non-hydroxy DASAs).

The second step consists in a thermal isomerization of the previously obtained compound around the C3-C4 bond (A' → A") to form a spatially arranged specie ready for the electrocyclization step.

Finally, the ring-closure step occurs (4-π-electrocyclization) and three successive steps are needed to yield the final product (B"'): a nitrogen inversion (B'), a rotation of the acidic part (B") and finally a concomitant proton transfer from the hydroxy group to the nitrogen atom (B"'). The electrocyclization is thermally activated and is much slower than the photoisomerization (it happens on a 10s timescale), therefore this thermal step will be rate controlling for the whole process.

The reversibility of the photochromic reaction and the dark equilibrium of DASAs, and especially of amine-based DASAs, is highly solvent dependent. DASAs undergo what is called solvatochromism: thus their absorption properties, depend on the solvent in which they are dissolved. For instance, the photo isomerization from linear to cyclic form of first generation DASAs is quite limited in halogenated or protonated solvents [39], which

favour the linear form. Their solvatochromism can be seen as an advantage, using the same molecule in different solvents, different photochromic behaviours can be obtained, moreover the affinity of the different isomers for different solvents can be exploited for self delivery across interfaces. From another point of view, it can be limiting in some applications, and requires the study of the molecule in the environment of interest. To avoid this solvent dependence, one could think of using the DASAs directly in the solid state (when the application allows it). However, their photochromic behaviour as solids is limited due to the confinement of intermolecular agglomeration, reducing the molecules mobility and the space available for isomerization [39].

The chemical structure of DASAs, and especially the nucleophilic/electrophilic properties of the donor/acceptor moieties, reveals itself extremely important for the photoisomerization process. Therefore, by tuning the molecular structure, one can tune the photochromic behaviour until reaching the perfect result for a given application.

2.4. Main applications of DASAs

As previously mentioned, the specific features of the photochromic behaviour of DASAs and their tunable optical properties have made them optimal candidates for a wide range of applications. Their negative photochromism (which maximizes light penetration throughout the bulk of the material), inexpensive and green synthesis, visible light absorption, and good fatigue resistance are great advantages compared to the other known types of photoswitches [8]. Their use in chemistry and material science is facilitated by their easy combination with polymers, conferring them photochromic properties and increasing the range of their possible utilization [33]. Here, some of the main applications of DASAs are reported and described:

Artificial nanosystems in photopharmacology

Light-induced biochemical reactions are a key feature of photoreceptor cells. To mimic this behaviour, Omar Rifaie-Graham et al. (2018) created an artificial polymersome nanoreactor (artificial vesicle that encapsulates a solution) able to be switched on (increased permeability) by visible light and to be self reverted in the dark to its passive state. This nanoreactor is made by a block copolymer functionalized with a DASA, and is self-assembled into vesicles. Thanks to the isomerization and the switching of polarity of DASA under visible light, the overall permeability of the polymersone membrane can be modulated with light, and therefore also the release of the charged payload can be triggered by light and stopped as soon as the light is off (Figure 2.7). The negative

photochromism of DASA and its absorption in the visible range allows low scattering of light and a deep penetration inside the tissue, without damaging the cells as a UV light irradiation would do [40].

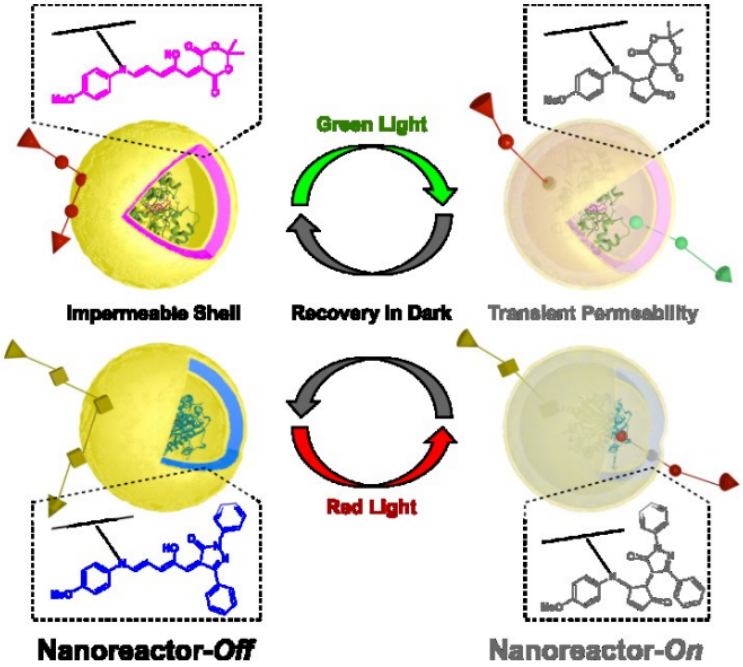

Figure 2.7: Scheme of the light-induced change in permeability of the artifical polymersome nanoreactor [40]

pH and temperature sensors

In "Polymer dots of dasa-functionalized polyethyleneimine: Synthesis, visible light/pH responsiveness, and their applications as chemosensors" (2017) a possible application of DASAs as pH sensor to detect Fe^{3+} and Cu^{2+} ions in aqueous solutions has been proposed [41]. Polymer dots of branched polyethyleneimine functionalized with DASAs have been synthesized and exhibited a typical photoresponsive behaviour as well as a pH sensitivity. Under irradiation of visible light, or under a change in the acidity of the environment, the DASA-PEI dots undergo a reversible transition between the open and closed isomers of the DASAs. Therefore, by following the isomerization of the DASA-PEI dots, the acidic or basic nature of the environment can be followed in time [42].

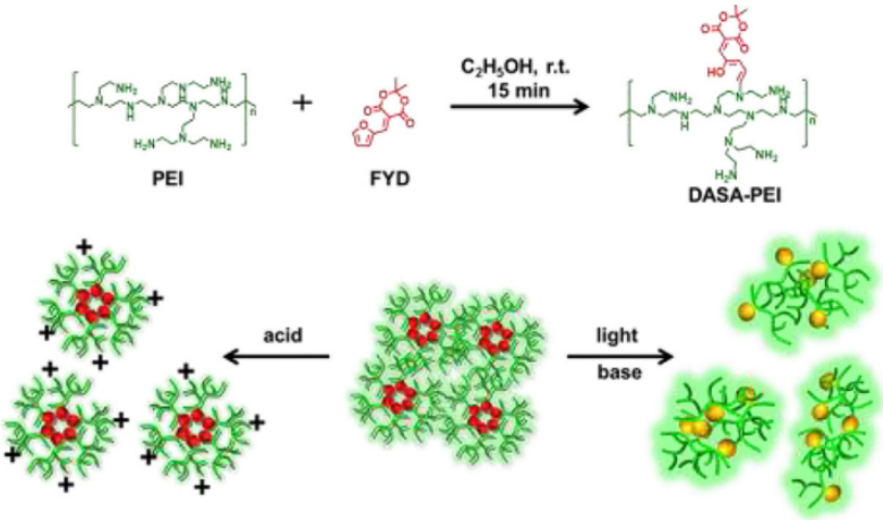

Figure 2.8: Influence of acid/base substances on the DASA-PEI dots structure [41]

DASAs can also be used as thermochromic molecular sensors for local temperature analysis [43]. By homogeneously dispersing a DASA inside a crosslinked polyurethane, B. P. Mason et al. (2016) managed to measure local temperature changes following an impact (bullet perforation) or a rapid heating (Figure 2.9). They used the suitable kinetics of the DASA activation with temperature (the activated form being the open coloured form) to determine peak temperatures, and to realize a precise temperature mapping on the materials as, inside the elastomer, a trace of the DASA activation remains visible even after the thermal event [43].

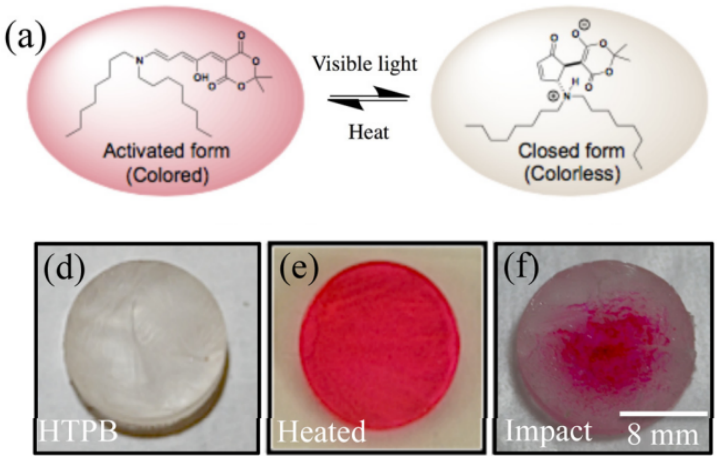

Figure 2.9: Thermal activation of DASAs (a) after heating (e) or mechanical impact (f) [43]

Colorimetric chemosensors

The amount of biogenic amine in food, and especially in meets, is an indicator of whether the food is spoiled or not. The common stains used to detect the presence of such amines, such as ninhydrin and chloranil, are rather unstable and involve toxic reagents. During their research, Y. J. Diaz et al. (2017) reported the use of DASAs as colorimetric detectors for the presence of amines in solution, on solid supports or in the vapour state [44]. The methodology has the advantage to be quite simple and benefits from the high molar extinction coefficient of DASAs, allowing for an easy analysis with the naked eye. An activated furan-based amine sensor reacts in the presence of an amine reagent to give a DASA of a specific colour according to the nature of the amine (Figure 2.10).

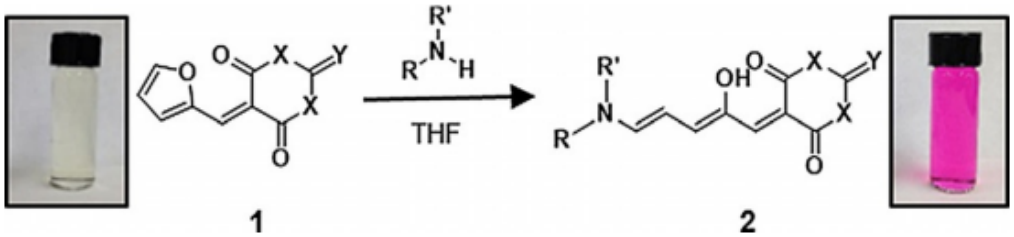

Figure 2.10: Reaction scheme for activated furan-based amine sensor [44]

For a quite different purpose, the DASAs can be incorporated in a polymeric backbone and used to detect the presence of nerve agent mimics which are extremely toxic to mankind. The introduction of a nucleophilic hydroxy group onto the N-alkyl position of the DASA forms a reactive site for the nerve agent that triggers its intramolecular cyclization and the formation of ammonium salts. As the cyclization of the DASA is accompanied by a bleaching, it can be use as a rapid and selective photoswitchable colorimeter for the in-time detection of nerve agents [45].

Spatiotemporal photopatterning

Photoresponsive molecules are an efficient tool for photopatterning polymer surfaces. For a long period, only UV light has been used as photoinduction source to create patterns on surfaces. However, the use of UV light is limited in biological applications, due to its damaging effect on cells; moreover photocleavage might release damaging species for the biological system. Therefore, for biological applications photoisomerization with visible light is one of the best suited technique. Thanks to the absorption in the visible range of DASAs and to their ability to change their conformation and polarity upon illumination, visible light can now be exploited for photopatterning. In their research, Sukhdeep

Singh et al. (2015) presented a method for grafting DASAs on an aminofunctionalized polycarbonate surface endowing the latter with photosensitive properties. Upon light irradiation, the isomerization of the DASAs from the coloured linear hydrophobic form to the colourless cyclic hydrophilic form induces a change in the wettability of the polymeric surface on which they are attached (Figure 2.11) [46].

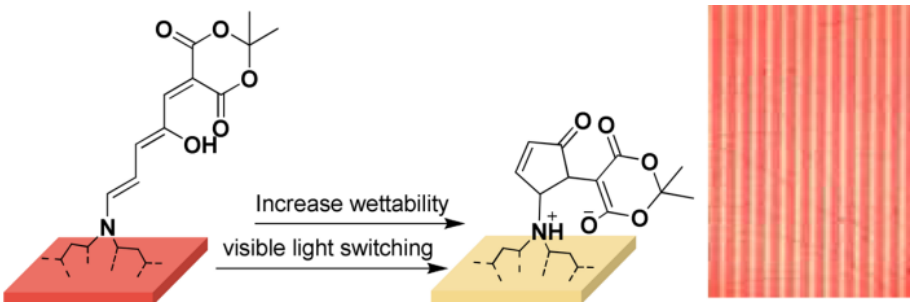

Figure 2.11: Patterns generated by photolithographic process on DASAs using visible light exposure [46]

Molecular mechanical movements onto a surface are responsible for the surface properties changes (wettability, friction, ...) and play an important role in the field of molecular motors, actuators and energy convertors. Surfaces with modulable wettability are of great interest in surface science, intelligent micro and nanodevices, biological engineering and in any applications related to adsorption or adhesion. Moreover, they are of revolutionary significance for microfluidic technology. By tuning the surface wettability, one can, for instance, dynamically manipulate the mobility of liquid droplets on surfaces. Therefore this type of photopatterned materials could be promising candidates for sensors and microfluidic devices [47].

Organic Field Effect Transistor and Solar cells

Here is reported the use, in a more general manner, of dyes with similar molecular structure as DASAs, meaning consisting in an electron donor group linked by a conjugated spacer to an electron acceptor group (push-pull system), to be used in organic field effect transistor (OFETs) or in solar cells [48]. This molecular structure presents the advantages to have a tunable energy band gap to improve the absorption of light (one of the main issue in solar cells), and allows to adjust the internal charge carrier mobility in OFETs. For this purpose, DASAs would need to be stabilized into their open isomer, showing a strong absorption in the visible range, without undergoing light-induced isomerization. Therefore DASAs salts, which are not photochromic anymore, could be used in such application.

3 | Molecular design and synthesis of DASAs

3.1. Molecular design

Over the years, the development of DASAs with variable donors, acceptors, and spacer linkers, allowed a considerable reduction of the photoswitching response time from hours to several seconds [8]. For cell stimulation, the DASAs kinetics, ideally, would match the characteristic time featured by biological entities, which is closer to the millisecond than to the second. In this framework, one of the main goals of this work is to find adequate structures of DASAs allowing them to partition inside the cellular membrane and to feature a photoswitching kinetics (in at least one of the two directions) comparable to biological events.

It has been shown that the donor part of DASAs has a considerable influence on the dark equilibrium between the two isomers, while the acceptor part is more influent on the absorption properties of the compound. The triene backbone seems to influence both the dark equilibrium and the kinetics of the photoswitching. Actually, as a concentration effect is observed on the kinetics of the photoswitching, the dark equilibrium (which relates to the relative concentration of each isomer) and the photoswitching kinetics are linked in a complex way [34]. It is indeed believed that some long-range electrostatic interactions between the DASAs molecules disturb the last steps of the isomerization (electrocyclization + proton transfer). J. A. Peterson et al. (2022) showed that while modifying the triene backbone a faster switching response was obtained, but a faster degradation was observed at the same time [49]. Considering all those different aspects, the focus for this project has been onto the acidic part of DASAs. In "Controlling dark equilibria and enhancing donor acceptor stenhouse adduct photoswitching properties through carbon acid design" (2018) several acid moieties have been synthesized and the photochromic properties of the corresponding DASAs have been tested [8]. This article acted as a guideline to synthesize different DASAs in this project. As for the desired application also the donor part is very important for the molecular design, different donor moieties have been tested

and a panel of new DASAs is obtained allowing a comparison between them.

Indeed, in order to obtain the desired features for the application as molecular photoswitch in the cell membrane, a specific molecular design is required. As previously mentioned, DASAs must be functionalized with a polar head (hydrophilic) to act as an anchor in the membrane (see Figure 3.1). This polar head can be attached either on the acid moiety or on the donor part.

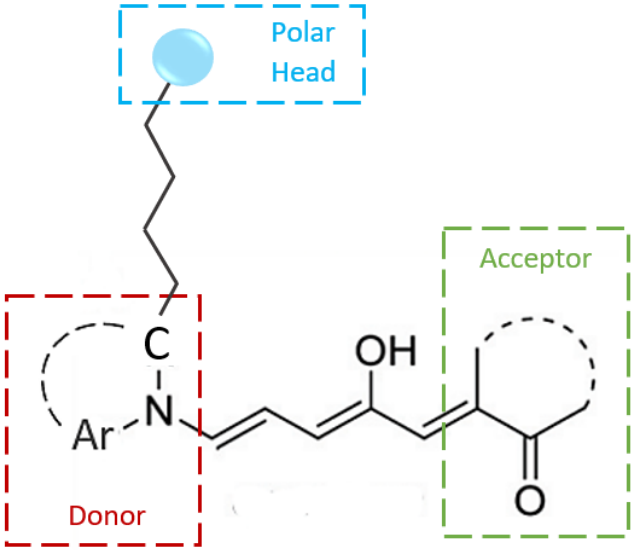

Figure 3.1: DASAs molecular design for cell stimulation applications

A simple way to do that is to start by attaching an alkyl halide which can be then be converted in a charged group via substitution with a ternary nitrogen. In this work, the polar head has been attached on the donor part, featuring an alkyl chain 4 or 6 carbon atoms long, for steric optimization, ending with a bromine atom. Among the halides, bromine has been chosen for two main reasons: the reactivity of halides increases from fluorine to iodine (RF $<$ RCl $<$ RBr $<$ RI) and the more reactive the halide, the higher the coupling yield. The second reason involves the cytotoxicity towards cells: iodine can sometimes be hazardous for cells, so bromine atoms are the preferred option for this purpose. Finally, once the alkyl bromide chain is attached, a suitable reaction with pyridine (see Figure 3.2) replaces the bromine atom by a pyridinium leading to the polar head.

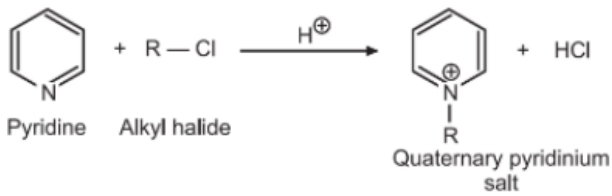

Figure 3.2: Scheme of the reaction between alkyl halides and pyridine [50]

Below are described all the steps performed in order to obtain the different DASAs synthesised during this project. The starting chemicals were all purchased from Sigma-Aldrich, TCI (Tokyo Chemical Industry), or Fluorochem. At each step, the evolution of the reaction was controlled through thin layer chromatography (TLC) on aluminum backed silica gel plates.

The chemical characterization of each final products has been conducted with nuclear magnetic resonance (NMR) using a Bruker Avance DRX-400 instrument. The ^{1}H-NMR spectra of the products have been acquired in deuterated solvents (chloroform $CDCl_3$-d6, dimethyl sulfoxide DMSO-d6 or acetonitrile CD_3CN). The reading of the ^{1}H-NMR spectra of DASAs was a bit delicate because of the dark equilibrium featuring both open and closed isomers in solution. This issue can be overcome by choosing a suitable solvent, which favours either the closed form, or the open one. For instance, acetonitrile is more polar than chloroform, so the polar closed form of DASAs is favoured in this solvent. Some peaks in the ^{1}H-NMR spectra are specific to the closed form, while others are specific to the open form. Hence, by comparing their relative intensity, the relative amount of each isomer in a specific solvent can be computed (see Appendix B). The chemical characterization was sometimes confirmed by mass spectroscopy using a Bruker Esquire 3000 PLUS (ESI Ion Trap LC/MSn System). The instrument was equipped with an ESI source (electrospray ionization source) and a quadrupole ion trap detector (QIT). The acquisition parameters were set to the following: needle: 4.5 kV, N2 flow rate: 10 L h^{-1} , cone voltage: 40 V, Scan resolution and range: 13 000 (m/z) s^{-1} over the mass range m/z 35–500, by direct infusion of methanol solution of compounds at rate: 4 microliter min^{-1}.

The reaction details, together with the ^{1}H-NMR resume of the products, and when necessary the mass spectra, are reported in Appendix A.

3.2. Synthesis of the acidic moieties

Acid moiety	Chemical name	Molecular structure
A1	4-(2-Furanylmethylene)-2,4-dihydro-5-methyl-2-phenyl-3H-pyrazol-3-one	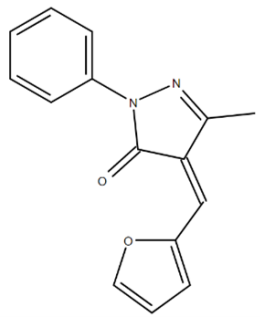
A2	5-(2-Furanylmethylene)-1,3-dimethyl-2,4,6(1H,3H,5H)-pyrimidinetrione	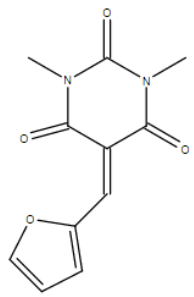
A3	3H-Pyrazol-3-one, 4-(2-furanylmethylene)-2,4-dihydro-2-phenyl-5-(trifluoromethyl)	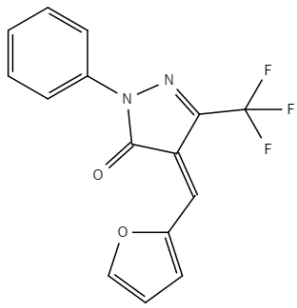
A4	4-(2-Furanylmethylene)-3-methyl-5(4H)-isoxazolone	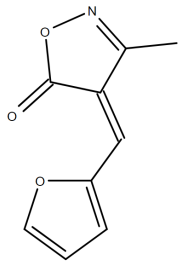

Table 3.1: Overview of the synthetized acid moieties

Since the acid moieties were all made as furfural derivatives, their synthetic strategies were quite similar. The preparation of each acid was performed following two subsequent reactions.

First step: cyclo-condensation

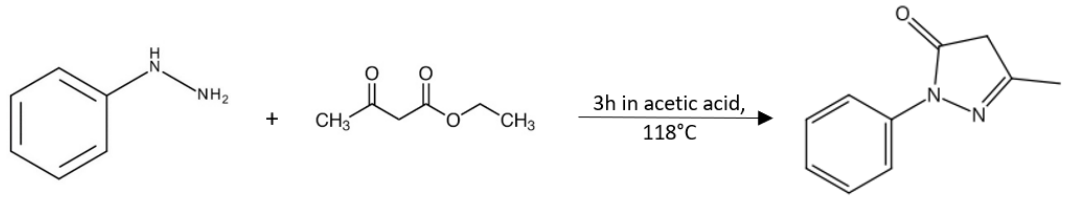

Figure 3.3: Reaction pathway for the precursor of A1

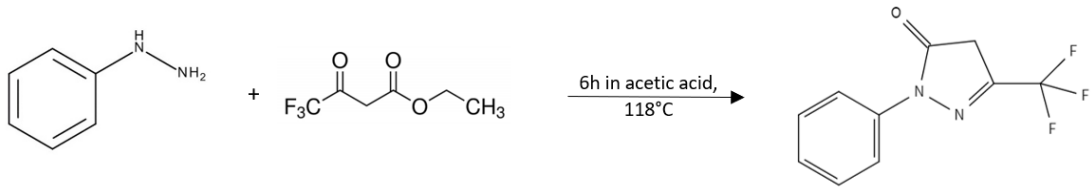

Figure 3.4: Reaction pathway for the precursor of A3

The first step of the synthetic pathway of the acids A1 and A3 consists in the formation of a pyrazolone derivative. The pyrazolone is a five-membered ring with two nitrogen atoms and one ketonic group in the ring. This step involves the cyclo-condensation of a β-ketoester (ethyl acetoacetate and 4,4,4-trifluoro-3-oxobutanoate for A1 and A3, respectively) with substituted or unsubstituted hydrazine [51]. Substituted hydrazine with a phenyl ring has been used. When mixed together, the nitrogen atom at the end of the hydrazine, being a nucleophilic site with its lone pair of electrons, attacks the carbon involved in the carbonyl group on the β-ketoester, and thanks to the acetic acid as solvent, a molecule of water is eliminated (condensation). Then, the second nitrogen atom attacks the carbon involved in the ester group and this time an alcohol is eliminated and the ring closes.

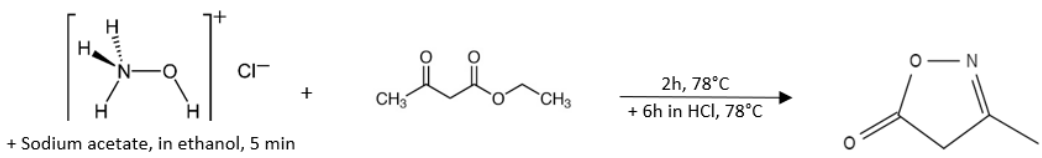

Figure 3.5: Reaction pathway for the precursor of A4

Concerning the acid moiety A4, this first step is quite similar as the one previously described, but the product to be obtained is an isoxazolone derivative. The reaction route consists in a cyclo-condensation of ethyl acetoacetate with hydroxylamine hydrochloride to yield the ring-closed product. In a similiar way, firstly the nitrogen atom of the hydroxylamine hydrochloride (made previously reactive thanks to sodium acetate) attacks the carbon involved in the carbonyl group on the β-ketoester and with hydrochloric acid (HCl) as solvent, a molecule of water is removed. Then the oxygen atom of the hydroxylamine hydrochloride attacks the carbon involved in the ester group and a hydroxy group is eliminated while the ring closes.

Second step: Knoevenagel condensation

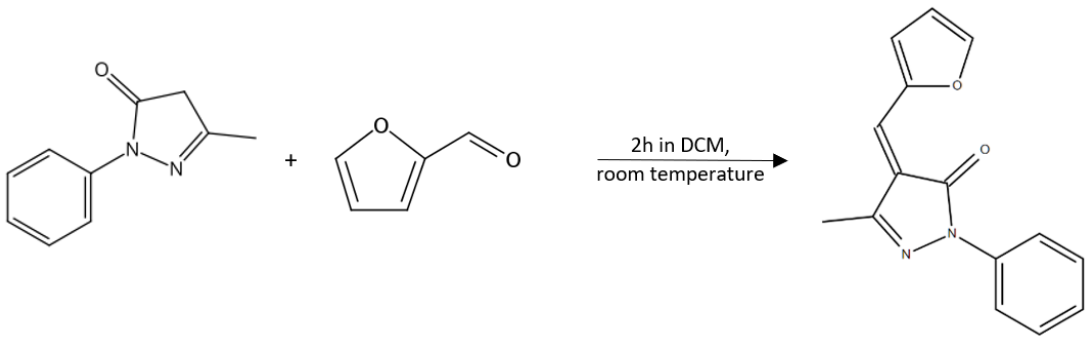

Figure 3.6: Reaction pathway of A1

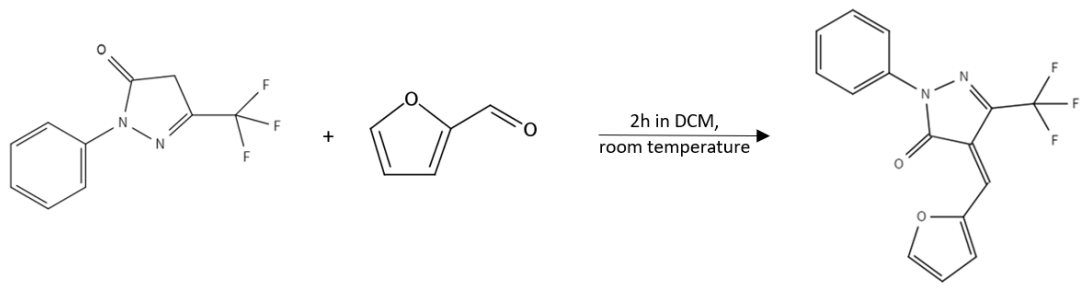

Figure 3.7: Reaction pathway of A3

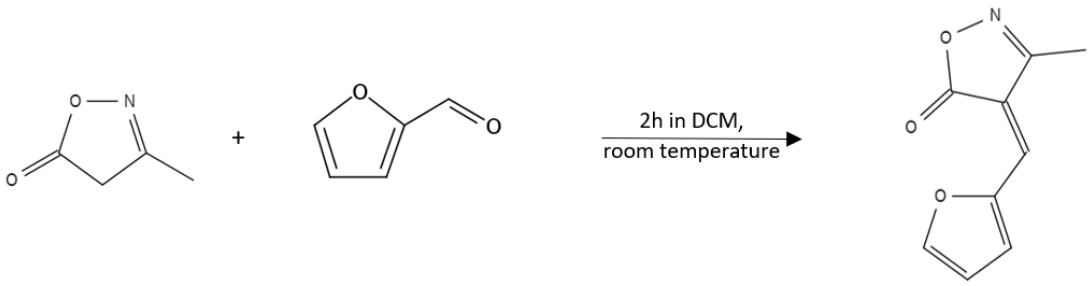

Figure 3.8: Reaction pathway of A4

For each previously obtained product, the second step is a Knoevenagel condensation to yield a furanyl derivative. It consists in a nucleophilic addition of an active hydrogen compound on a carbonyl group (aldehyde for the furfural), involving the formation of an alcohol. Then, in an acidic environment (dichloromethane) the hydroxy group and the neighbour hydrogen atom are removed as a molecule of water (dehydration step on an alcohol to form an alkene) and a carbon-carbon double bond is formed [52]. This reaction activates the furan ring thus enabling the following opening by a donor moiety.

3.3. Basic moieties utilized

Basic moiety	Chemical name	Molecular structure
D1	N-methyl aniline	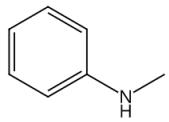
D2	N-(6-bromohexyl)-3-methoxybenzenamine	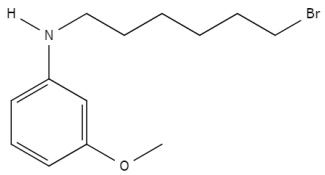
D3	N-(4-bromobutyl)-3-nitrobenzenamine	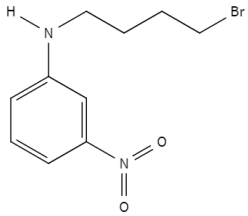

Table 3.2: Overview of the utilized basic moieties

D2

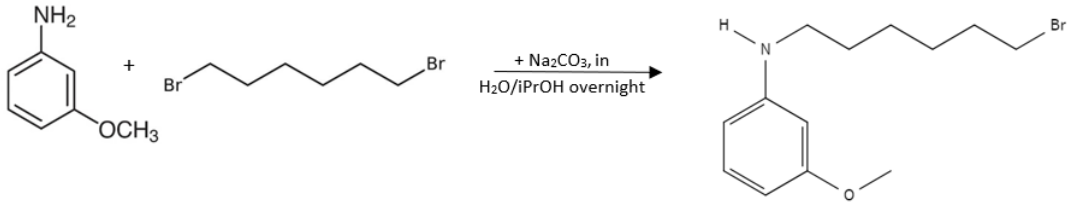

Figure 3.9: Reaction pathway of D2

The reaction to produce the desired donor moiety exploits the nucleophilic character of primary amines thanks to their active lone pair of electrons on the very electronegative nitrogen atom. Their reaction with halogenoalkanes consists in two steps: in the first one a nucleophilic substitution produces an ammonium salt and in the second step a basic specie removes one of the 2 hydrogen atoms on the positively charged nitrogen atom yielding a neutral secondary amine derivative. By increasing the reaction time a tertiary amine can be yielded. Here, m-anisidine has been reacted with dibromohexane in a sodium carbonate solution (alkaline salt). The monitoring of the obtained class of amine is a bit delicate, but as in the following reactions (see part 3.4) only the secondary amine derivative is able to react, having the two classes of amine derivatives (secondary and tertiary) is not a big issue in this reaction pathway. However, it decreases the yield of the following reactions.

3.4. Synthesis of DASAs

DASA	Chemical name	Molecular structure
DASA-A1-D1[1]	(Z)-4-((2Z,4E)-5-(N-methyl-benzeneamino)-2-hydroxypenta-2,4-dien-1-ylidene)-2-phenyl-5-(methyl)-pyrazol-3-one	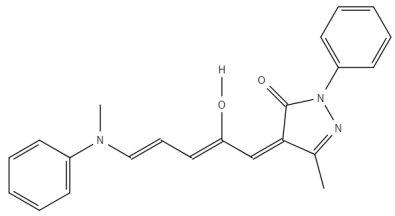
DASA-A1-D2	(Z)-4-((2Z,4E)-5-(N-(6-bromohexyl) -3-methoxybenzenamino)-2-hydroxypenta-2,4-dien-1-ylidene)-2-phenyl-5-(methyl)-pyrazol-3-one	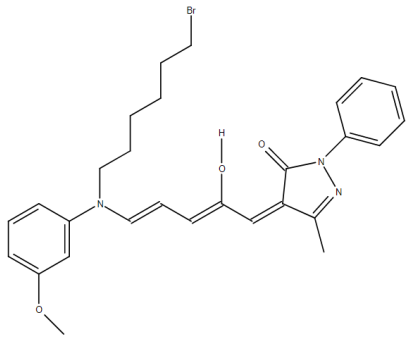
DASA-A2-D2	5-((2Z,4E)-5-(N-(6-bromohexyl) -3-methoxybenzenamino)-2-hydroxypenta-2,4-dien-1-ylidene)-1,3-dimethylpyrimidine-2,4,6-trione	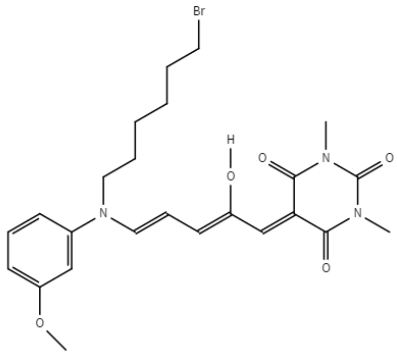
DASA-A3-D3	(Z)-4-((2Z,4E)-5-(N-(4-bromobutyl)-3-nitrobenzenamino)-2-hydroxypenta-2,4-dien-1-ylidene)-2-phenyl-5-(trifluoromethyl)-pyrazol-3-one	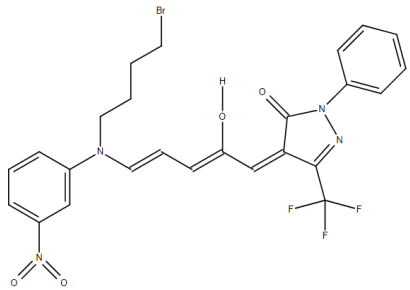
DASA-A4-D2	Not fully determined	Not fully determined

Table 3.3: Overview of the synthetized DASAs

[1]Note that the DASA-A1-D1 has been synthesized as a first attempt without the polar head and is therefore not suitably designed for the application described in this project. However, it has been useful to elaborate a systemic photophysical characterization procedure.

All DASAs schematized in the Table 3.3 are represented in the open form.

DASA-A1-D1

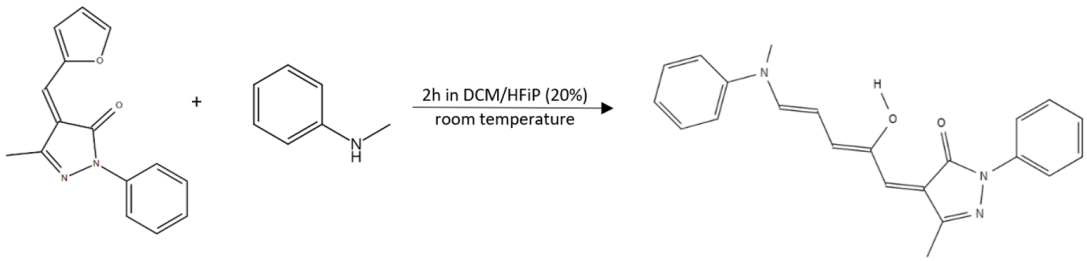

Figure 3.10: Synthesis of DASA-A1-D1

DASA-A1-D2

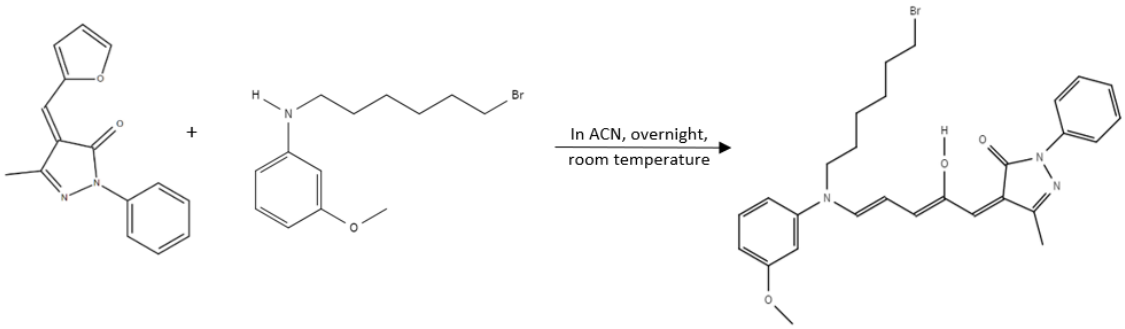

Figure 3.11: Synthesis of DASA-A1-D2

DASA-A2-D2

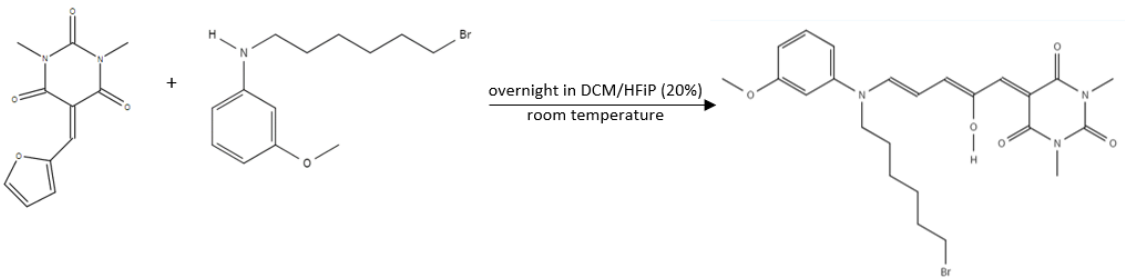

Figure 3.12: Synthesis of DASA-A2-D2

DASA-A3-D3

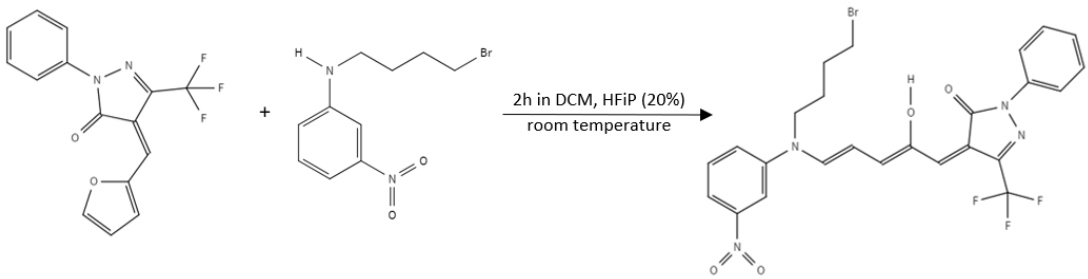

Figure 3.13: Synthesis of DASA-A3-D3

In order to form the DASAs starting from the furfural derivatives and from the donor parts, a simple step is needed, which is always the same for all DASAs with only some divergences in the solvent used or in the workup of the reactions. As the donor moiety possesses a nucleophilic site (the secondary amine), the furan ring of the furfural derivative is opened as a conjugated alkyl chain with a hydroxy group on one of the carbon atoms as a remaining trace of the furan ring.

DASA-A4-D2

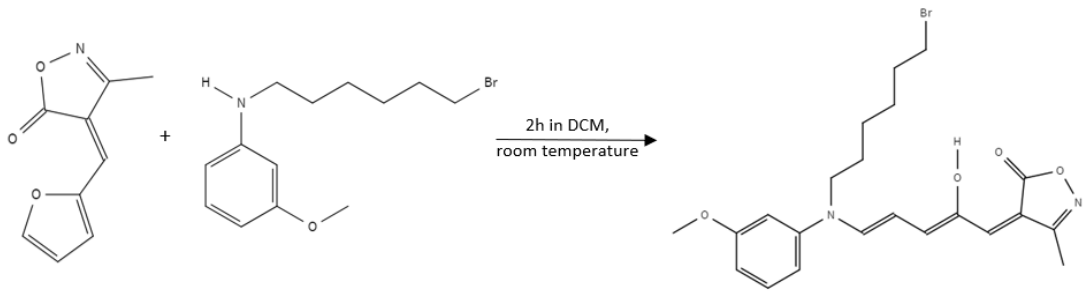

Figure 3.14: Synthesis of DASA-A4-D2

The DASA-A4-D2 has been prepared following the same reaction pathway as for the other DASAs. In the Figure 3.14 the expected molecular structure of the compound is shown. However, a mass spectrum of the obtained product was collected (see Appendix A, Figure A.5) and is not consistent with the previously described structure. Specifically, bromine has two abundant isotopes, ^{79}Br and ^{81}Br, which should be visible on the mass spectrum as two lines in the molecular ion region with a gap of 2 m/z units and with almost equal heights. This pattern was not present in the mass spectrum, leading to the

conclusion that the obtained product does not contain any bromine atom. More studies of the compound would have been necessary to determine the exact structure of the product, but for quantity issues they could not be done. However, a possible explanation can be the degradation of the aniline derivative during the reaction.

Attachment of the polar head

As explained in the section 3.1, the very final step to obtain the functional DASAs is to replace the bromine atom by a charged group: the pyridinium ion. This trial has been realized only on the DASAs A2-D2 and A3-D3, and the reaction pathway has been basically the same.

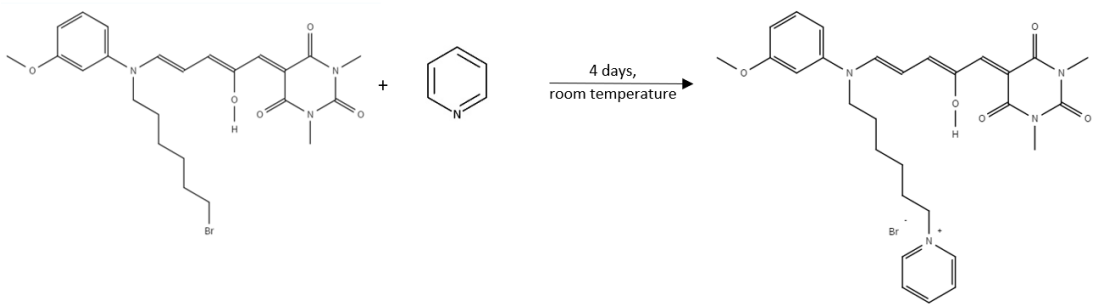

Figure 3.15: Attachment of the polar head on DASA-A2-D2

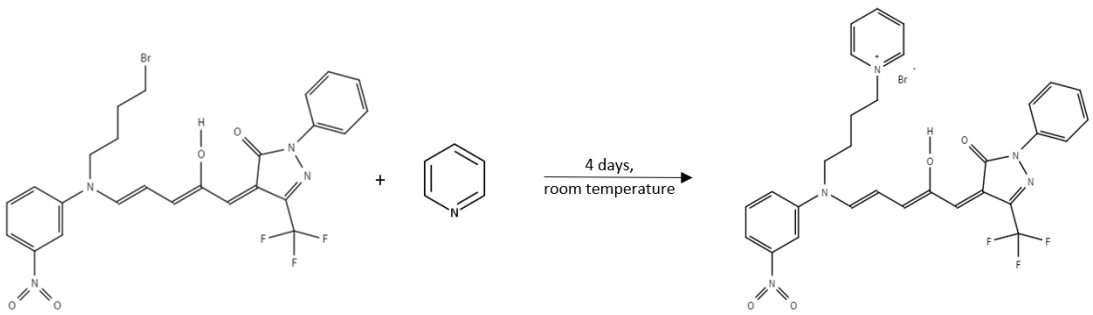

Figure 3.16: Attachment of the polar head on DASA-A3-D3

In both above reactions, the nitrogen atom in the pyridine ring, having a lone pair of electrons, attacks the carbon bearing the bromine atom: the resulting reaction is an alkylation of the nitrogen atom. A pyridinium salt is formed with a positive charge in the ring, supported by the nitrogen.

4 | Photophysical characterization of DASAs

UV-vis absorption spectroscopy and emission spectroscopy have been used to study the photophysical properties of the photochromic compounds synthesized. Instruments specifically were a double beam UV-visible spectrophotometer Cary 5000 version 1.12 and a spectrofluorometer JASCO FP-6600, and the fluorescence spectra have been read with the spectramanager software JCAMP-DX 4.24. To assess if the synthesized DASAs are well suited to serve as photoswitches to be put inside the cellular membrane, some optical properties are particularly relevant to be studied such as the red shift of the absorption (bathochromic shift) or the photoswitching rate of the DASAs in solution.

The experimental method to obtain all the UV-Vis and excitation/emission spectra was always the same: the DASAs were dissolved into a specific solvent at a concentration between 10^{-6} M and 10^{-3} M, and the obtained solution put into a parallelepipedic cuvette with an optical path of 1 cm. Several solvents have been used depending on their ability to dissolve the DASAs (linked with their polarity), their own absorption range, their ability to stabilize one of the two isomers, or their ability to preserve the DASAs from degradation. Moreover, as previously mentioned, since the DASAs display solvatochromism, the study of the same compound solubilized in different solvents might be interesting. Accordingly, solvents as acetonitrile, chloroform, dimethylsulfoxide, toluene, or dioxane, have been employed. Ideally the solvent employed should match the solvent actually used for biological applications.

In the hypothesis that every compound follows the Beer Lambert law recalled in the equation 4.1, where A is the absorbance, L the optical path length in cm, C the molar concentration in g/mol and ϵ the molar absorption coefficient in $mol.g^{-1}.cm^{-1}$, only the position of the absorption maxima can be compared for one compound at the same molar concentration in different solvents. The intensity of the absorbance (A) depends on the optical path length (which is always 1 cm in this project) but also on the molar absorption coefficient which is solvent dependent.

$$A = L.\epsilon.C \ ; \ valid \ for \ A \in [0.2; 0.5] \tag{4.1}$$

Therefore, if the absorbance intensities in different solvents need to be compared, the molar absorption coefficient has to be computed for each solvent, and then the absorbance must be normalized by the corresponding ϵ. However, for DASAs, it is a little bit trickier. Only one of the two isomers is responsible for the absorbance band in the visible and even if the global concentration of DASAs in different solvents is equal, the concentration of the coloured isomer may differ due to the different polarity of the solvents.

Another way to perform this comparison would be to keep as a reference a peak in absorbance that remains unchanged in different solvents, and to normalize the spectra by the intensity of this peak.

4.1. Photophysical characterization

The absorption wavelength (λ_{max}) of the open form isomer is an interesting feature to study as the goal application requires an absorption maxima as red-shifted as possible in the visible range so that the light used as stimulus for the photochromic reaction does not damage cells and it has a higher penetrance through living tissues. Absorption spectra were collected on the window 350 nm to 700 nm, the scan rate was set at 600 nm/min, with the absorbance measured every 1 nm and an average time between two measures of 0.1 second. The spectral band width of the instrument (SBW) was set to 2 nm. The figures presented hereunder show the red shift in absorption that is obtained with the molecular structures of the synthesized DASAs. A compound already reported in the literature (DASA-A2-D1, see Figure 4.1) was also studied and used as a reference to better interpret the data collected.

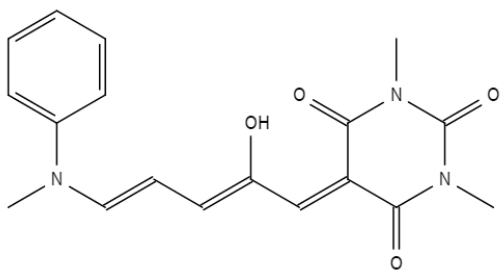

Figure 4.1: Structure of DASA-A2-D1

DASAs in chloroform

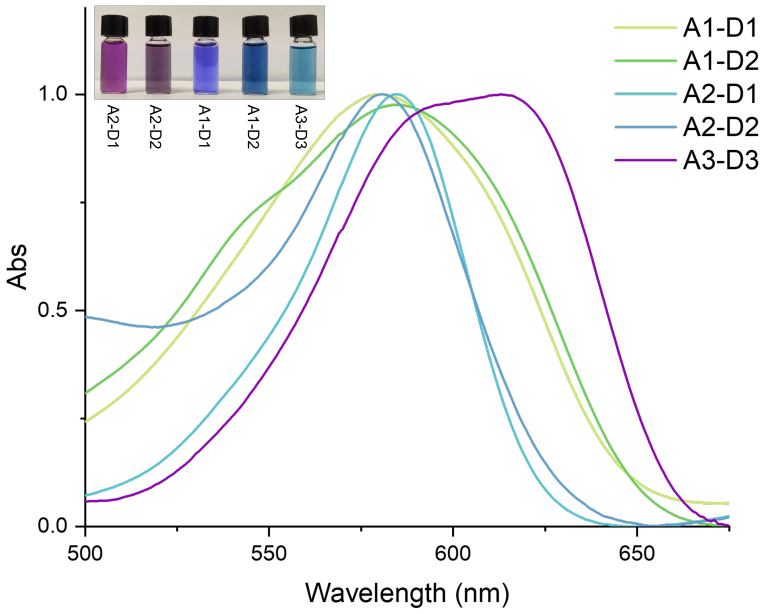

Figure 4.2: Absorption spectrum of the DASAs derivates in chloroform at 10^{-5} M in the dark. Inset: a picture of the compounds in chloroform before irradiation

DASAs in toluene

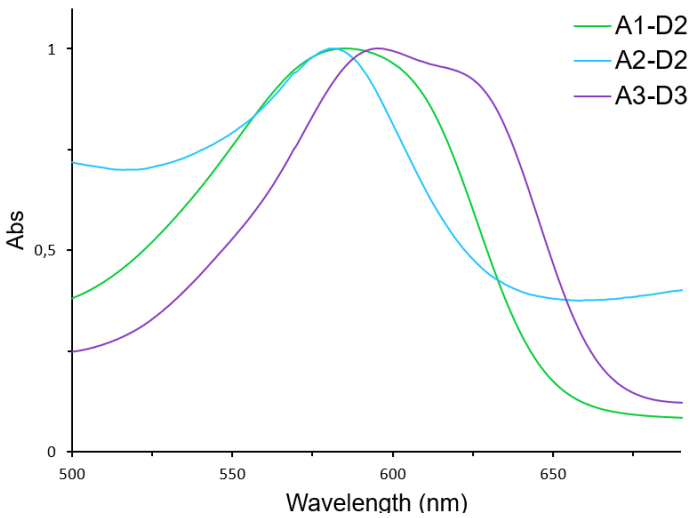

Figure 4.3: Absorption spectrum of the DASAs derivates in toluene at 10^{-4} M in the dark

Figures 4.2 and 4.3 show the absorption spectra of the compounds prepared in chloroform for solutions 10^{-5} M, and in toluene for solutions 10^{-4} M, respectively. The spectra are normalized to 1 so that the maximal absorption wavelength could be compared. The absorption profile of the open isomer is quite redshifted for all compounds, with the maximum for the absorption band being only slightly affected by their molecular structure. The different donors do not affect much the absorbance profile, as expected since the substitution is in meta position of the phenyl ring and has hence a milder effect on the electronic properties of the amine. For the acid A1 the only significant effect is a broadening of the absorption band. This might be due to a more dense population of the vibrational levels of the states involved in the transition, possibly related to the formation of aggregates. In the same way the presence of two bands close by for A3-D3 might suggest the presence of two states close in energy which can be populated through similar energies. In this case a stronger bathochromic shift is observed, of 36 nm, with the maximum of absorbance at 616 nm.

DASA-A4-D2

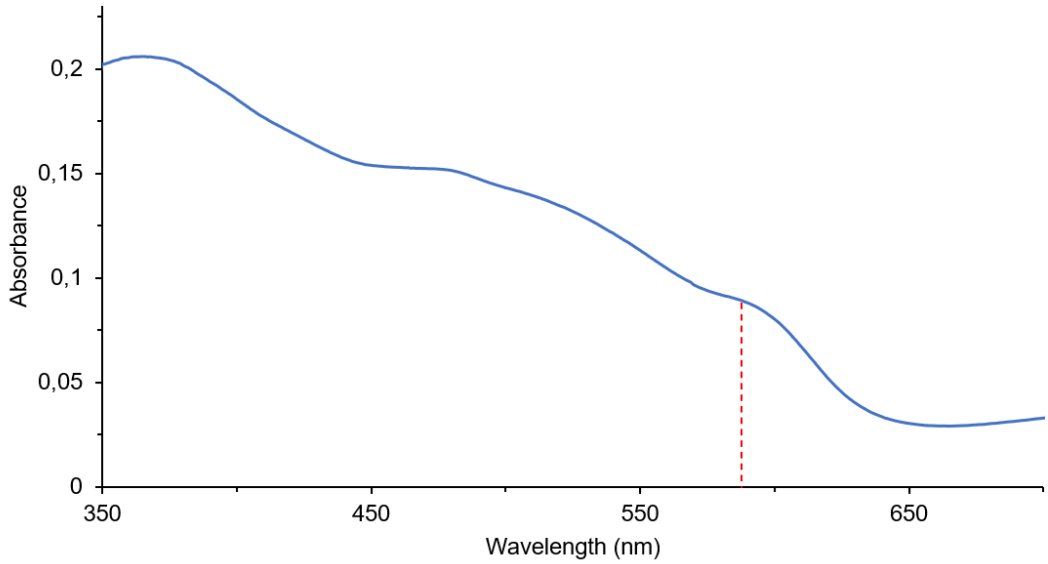

Figure 4.4: Absorption spectra of the DASA-A4-D2 at 10^{-4} M in acetonitrile

Despite the fact that the solution of DASA-A4-D2 in acetonitrile is not pure (known from the ^{1}H-NMR spectrum), the absorption wavelength of the compound in its open form can be assumed to be at 587 nm (Figure 4.4), where a band (half cut by the absorption range of the impurities) is observed.

DASA-A2-D2 with the polar head

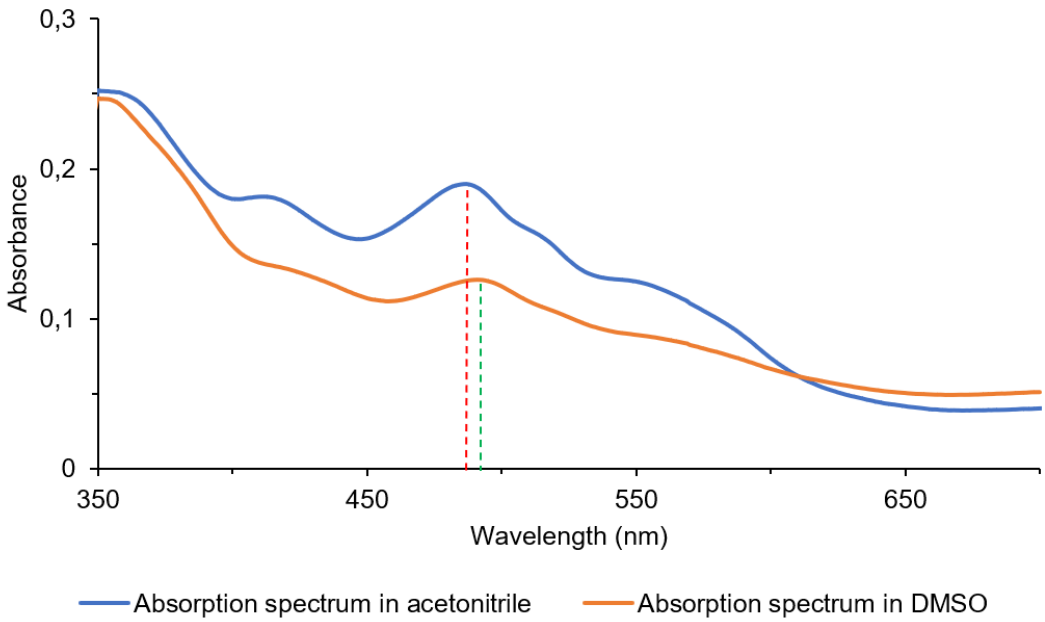

Figure 4.5: Absorption spectra of the DASA-A2-D2 with the polar head at 10^{-4} M in acetonitrile in blue and in DMSO in orange

DASA-A3-D3 with the polar head

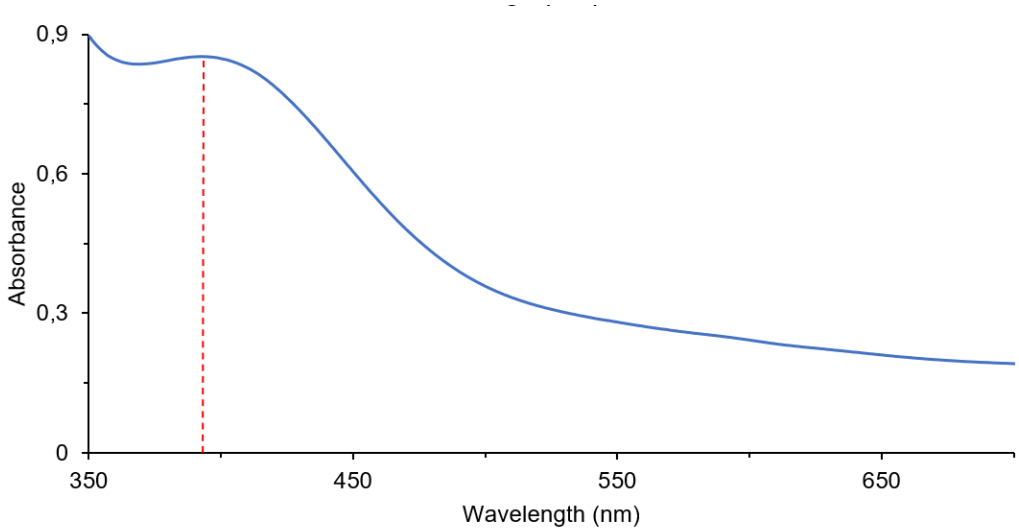

Figure 4.6: Absorption spectra of the DASA-A3-D3 with the polar head at 10^{-4} M in chloroform

Figures 4.5 and 4.6 show the absorption spectra of the two DASAs with polar head. The absorption maxima appears to be at 487 nm and 397 nm for the DASA-A2-D2 with polar head in acetonitrile and A3-D3 with polar head in chloroform, respectively. The strong blue-shift that is observed, if compared to the other derivatives, might suggest that the presence of pyridine promotes the closed form or a possible degradation of the material. This can be furtherly investigated through a photophysical study in time.

In the Table below the maxima of absorption for the different compounds are listed.

Compound	λ_{max} in chloroform (nm)	λ_{max} in toluene (nm)
DASA-A1-D1	580	
DASA-A1-D2	585	585
DASA-A2-D1	585	
DASA-A2-D2	581	580
DASA-A3-D3	614	595
DASA-A4-D2	587 (acetonitrile)	
DASA-A2-D2 w/ polar head	487 (acetonitrile)	
DASA-A3-D3 w/ polar head	397	

Table 4.1: Wavelength at the maximum absorption of the synthesized DASAs in solution

As the absorption spectra have been collected with very dilute solutions, the absorbance intensity rarely exceeded 0.2. Therefore, the conditions to maintain a linear relationship between the concentrations and the absorbance of the solutions stated by the Beer-Lambert law, allowing to compute the molar extinction coefficients, were not fulfilled. Consequently, the molar extinction coefficients of the synthesized DASAs have not been determined.

4.2. Photochromic study

4.2.1. Kinetics of photoswitching

One of the key point to study is the kinetics of the photoswitching of the DASAs in solution. To perform a preliminary study on the kinetics of photoswitching of the DASAs, the UV-Vis spectrophotometer allows for two experiments, as follows.

The first experiment consists in irradiating the DASAs dissolved in a specific solvent before recording several absorbance curves in time in the dark, following then the back isomerization, from the closed to the open form. The acquisition was made on the window 300 nm to 700 nm, the average time between two measures was 0.1 second and the SBW was set to 2 nm. In order to obtain the absorption spectra in time, several cycles of measures have been realized, without time delay between each cycle. It should be noted that generally the kinetics for the forward and the reverse reactions are not equal, therefore these experiments only provide the back reaction rate of the DASAs. It is also important to remind that in a strictly rigorous approach, only the spectra realized for solutions of the same molar concentration and in the same solvent can be compared.

As a second analysis, a specific wavelength can be followed in time, plotting then the absorbance at this wavelength over time. The measures have been realized every 0.1 second during 5 to 90 minutes. For these experiments, the spectral band width of the instrument has been set at 1 nm. Here is interesting to follow the intensity of the absorbance at the absorption wavelength of the open form of the DASAs in time, obtained thanks to the absorption spectra made beforehand. With this experiment, the reverse reaction rate can be monitored if the recording of the absorbance at the λ_{max} in time is made after having irradiated the compound. To be able to compare more quantitatively the kinetics of the DASAs, the initial slope on the linear part of the kinetic curves has been computed (μ). The value of the slope gives hints on the speed at which the molecules in solution switch from the closed to the open form right after turning off the light. Then, of course this is not the only relevant parameter, also the time at which the plateau (maximum recovery) is reached (τ) is to be taken in consideration, as well as the percentage of absorbance recovered when the plateau is reached ($\delta(\tau)$). While the first two parameters are determined graphically, the percentage of recovered absorbance is computed as:

$$\delta(\tau) = \frac{A(\lambda_{max}, \tau) - A(\lambda_{max}, 0)}{A_0(\lambda_{max})} * 100 \tag{4.2}$$

Being A(λ_{max}, τ) and A(λ_{max}, 0) the value of the absorbance at τ and at the start of

the recovery experiments, respectively, and $A_0(\lambda_{max})$ the value of the absorbance before the irradiation of the compounds. The latter has been graphically read on the absorption spectra (in the same solvents, and at the same concentrations) realized in the part 4.1.

DASA-A1-D1

By irradiating the DASA-A1-D1 dissolved in chloroform at 580 nm, the photoswitching from the open to the closed form is observed (Figure 4.7).

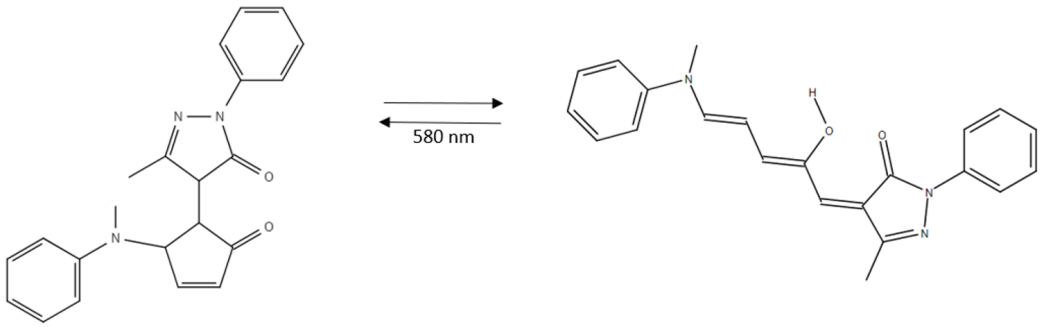

Figure 4.7: Photoisomerization from the close to open form of the DASA-A1-D1

On the Figure 4.8 the changes in optical properties of the DASA-A1-D1 under visible light irradiation (therefore comprising the absorption wavelength at 580 nm) are shown. With the naked eye, a clear loss in color was observed, from purple to transparent. The same behaviour can be followed in a more quantitative way, with the absorption spectra recorded in time, following the reverse reaction. Starting from the irradiated compound at t= 0, Figure 4.8 shows that the initial absorbance at 580 nm is weak (around 0.04), and it is increasing in time until reaching almost 0.22 60 minutes after illumination. Those results are consistent with the fact that the DASA-A1-D1 switches from the open to the closed and transparent form upon irradiation at 580 nm showing little or no absorption in the visible. In time, the open form recovers, and therefore the solution gets colored back and the absorbance at 580 nm increases. This figure confirms the photochromic behaviour of the compound.

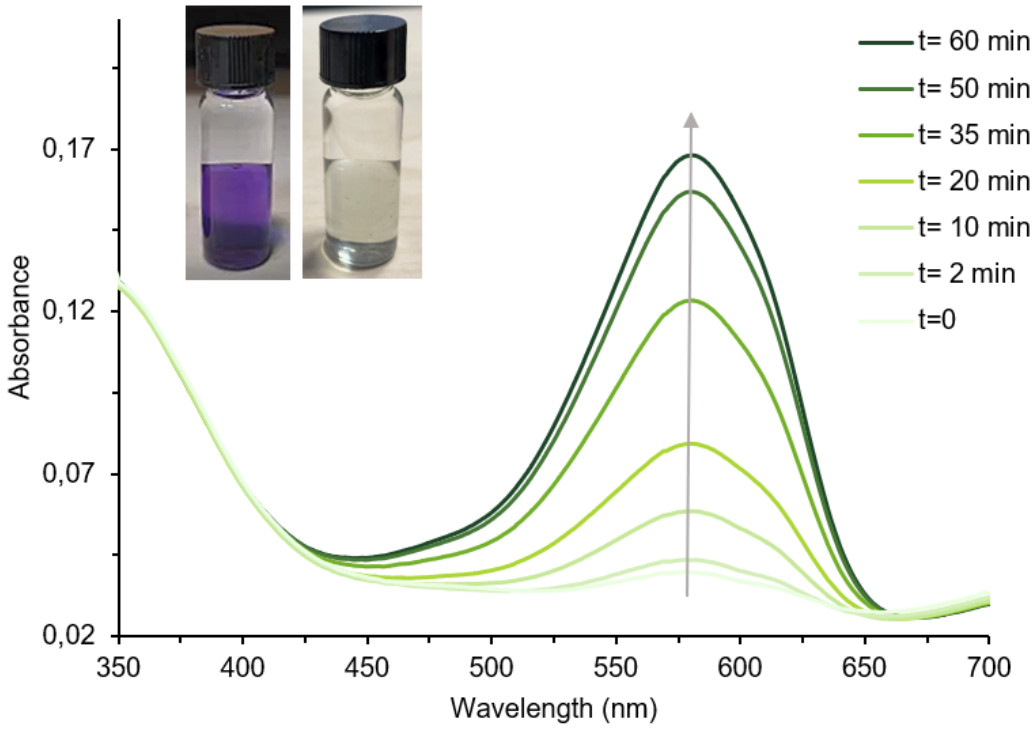

Figure 4.8: Absorption spectra of the DASA-A1-D1 in time in chloroform at 10^{-4} M after 30 min of irradiation. Inset: DASA-A1-D1 in chloroform before irradiation on the left and after irradiation on the right

From the Figure 4.8 can be computed the percentages of recovery of the absorbance at different times. This percentage is computed as:

$$\%\ of\ recovery\ (t) = \frac{A(\lambda_{max}, T0 + t) - A(\lambda_{max}, T0)}{A_0(\lambda_{max})} * 100 \tag{4.3}$$

being A(λ_{max}, t0 + t) and A(λ_{max}, t0) the value of the absorbance at a specific time t and at the start of the experiment, respectively, and $A_0(\lambda_{max})$ the value of the absorbance before the irradiation of the compounds. The latter can be graphically read on the absorption spectra (in the same solvents, and at the same concentrations) discussed in the part 4.1. The value of the absorbance at the start of the experiment accounts for the fact that usually 30 minutes of irradiation were not enough to bring the absorbance to zero. Therefore, to get rid of the differences in the minimum absorbance value between the DASAs, the percentage of recovery has to be computed between the minimum and the maximum absorbance reached. This consideration leads to question the term "recovery" which is maybe not the best suited here, as this parameter also takes into account the ability to switch in the forward reaction, and not only in the reverse one.

	after 10 min	after 20 min	after 35 min	after 60 min
% of recovery	2.2	4.4	10	18.9

Table 4.2: % of absorbance recovery of the DASA-A1-D1 in chloroform at 10^{-4} M at different times

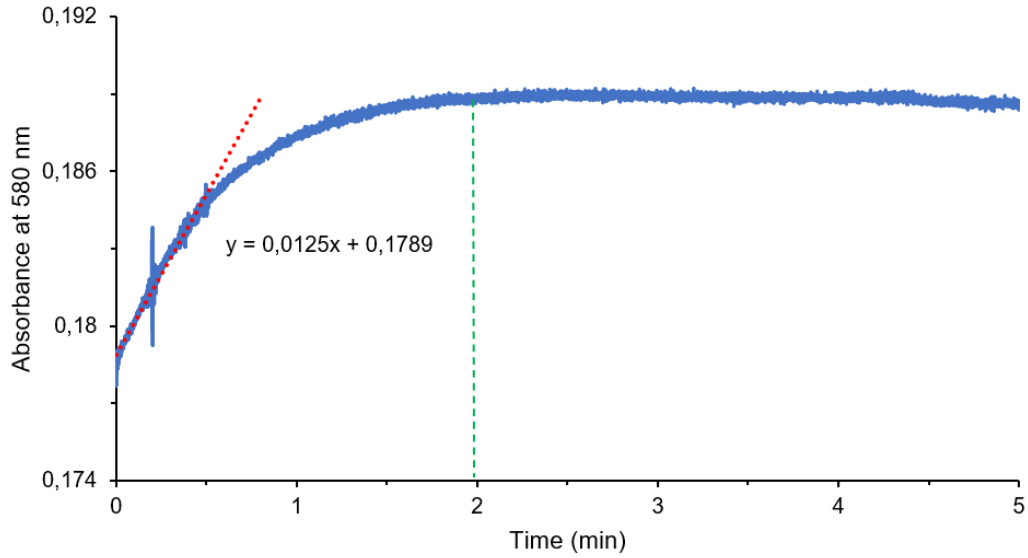

Figure 4.9: Evolution of the absorbance at 580 nm in time after 15 min of irradiation of the DASA-A1-D1 in chloroform at $5x10^{-6}$ M

After irradiation of the DASA-A1-D1 for 15 minutes in chloroform, and collection of the absorbance intensity at 580 nm in time, the Figure 4.9 has been plotted. The initial slope fitting the linear part of the curve (μ), the time to reach the plateau (τ) and the percentage of absorbance recovered when the plateau is reached ($\delta(\tau)$) can be estimated as:

$$\begin{cases} \mu = 0.0125\ min^{-1} \\ \tau = 2\ min \\ \delta(\tau) = 2.4\% \end{cases} \tag{4.4}$$

To compute $\delta(\tau)$, the required data have been taken from Figure 4.9 and from the absorption spectrum of the DASA-A1-D1 in chloroform at a concentration of $5x10^{-6}$ M recorded in the section 4.1.

DASA-A1-D2

By irradiating the DASA-A1-D2 dissolved in toluene at 585 nm, the photoswitching from the open to the closed form is observed (Figure 4.10).

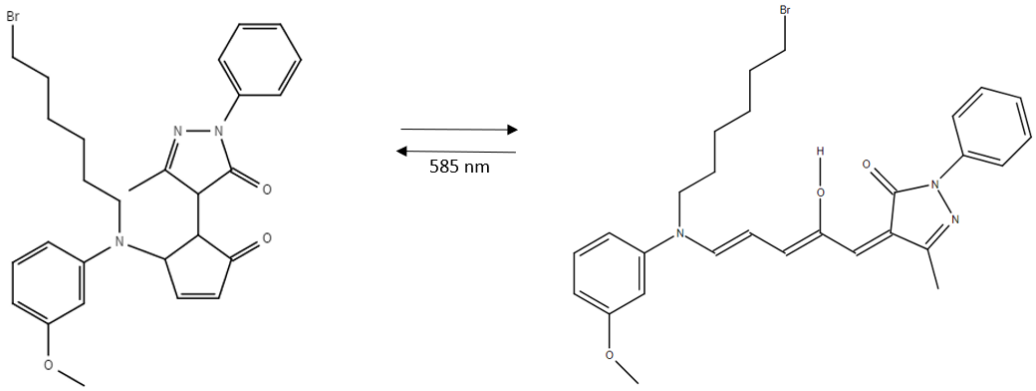

Figure 4.10: Photoisomerization from the close to open form of the DASA-A1-D2

Similarly to the previous analysis on the DASA-A1-D1, on the Figure 4.11 the changes in optical properties of the DASA-A1-D2 under visible light irradiation are shown. With the naked eye, a clear change in color was observed, from purple to light brown. The absorption spectra collected in time, following the reverse reaction show the same behaviour. Starting from the irradiated compound at t= 0, Figure 4.11 shows that the initial absorbance at 585 nm is weak (around 0.5), and it is increasing in time. The solution being probably too concentrated, the absorbance curves are reaching a saturated level around 3 so the true absorbance value cannot be read beyond 20 minutes. However, this figure confirms the photochromic behaviour of the compound.

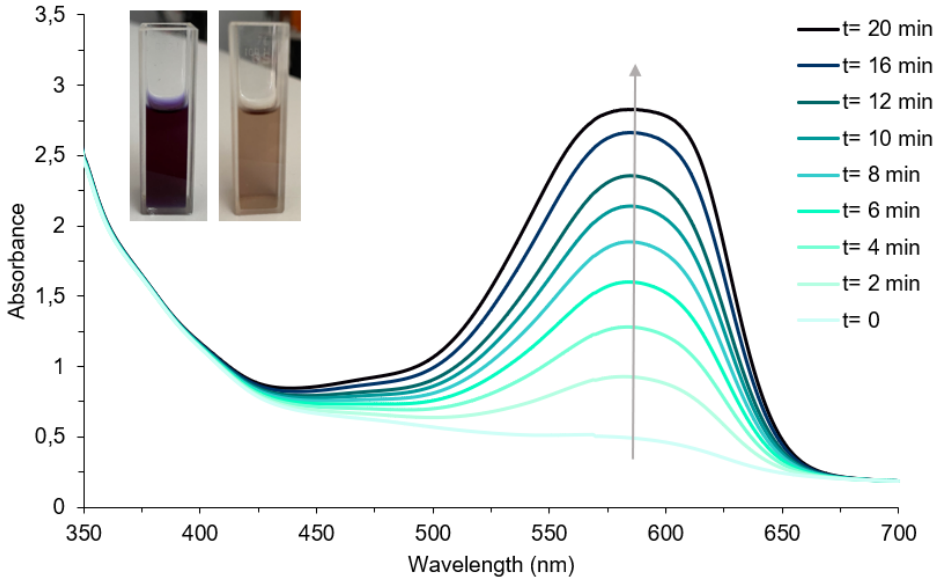

Figure 4.11: Absorption spectra of the DASA-A1-D2 in time in toluene at 10^{-3} M after 30 min of irradiation. Inset: DASA-A1-D2 in toluene before irradiation on the left and after irradiation on the right

Similarly to the previous compound, the percentages of recovery of the absorbance at different times have been computed:

	after 6 min	after 10 min	after 16 min	after 20 min
% of recovery	42	92	109	117

Table 4.3: % of absorbance recovery of the DASA-A1-D2 in toluene at 10^{-3} M at different times

Table 4.3 shows that the recovery exceeds 100% after 15 minutes, which probably means that when the initial absorption spectrum has been recorded, some external light had already induced some photoswitching inside the solution, that is a non-complete dark equilibrium when the first measurement was performed.

In a similar way, after irradiation of the DASA-A1-D2 for 15 minutes in toluene, and collection of the absorbance intensity at 585 nm in time, the Figure 4.12 has been plotted. Here, only the initial slope of the curve can be estimated. Indeed, after 60 min of recovery in the dark, the plateau was still not reached. The experiment has been stopped as the kinetics seemed way too slow to match with the biological events timescale for cell stimulation.

$$\left\{\mu = 0.0042\ min^{-1}\right. \tag{4.5}$$

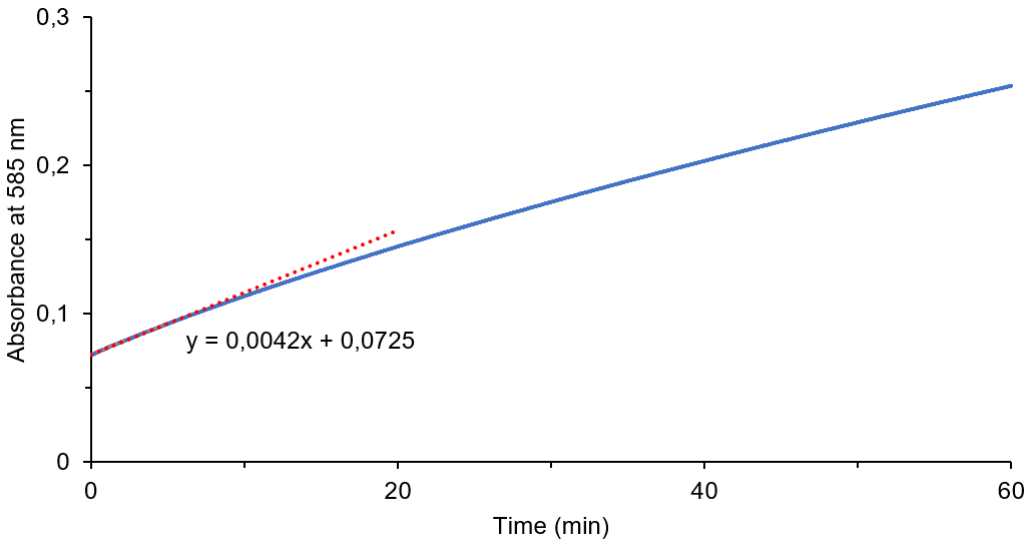

Figure 4.12: Evolution of the absorbance at 585 nm in time after 15 min of irradiation of the DASA-A1-D2 in toluene at 10^{-3} M

DASA-A2-D2

By irradiating the DASA-A2-D2 dissolved in toluene at 580 nm, the photoswitching from the open to the closed form is observed (Figure 4.13).

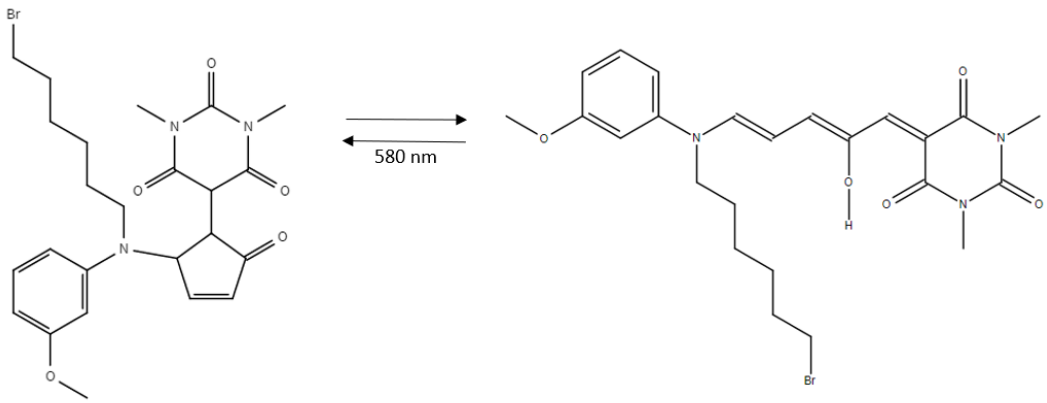

Figure 4.13: Photoisomerization from the close to open form of the DASA-A2-D2

Again Figure 4.14 shows the changes in optical properties of the DASA-A2-D2 under visible light irradiation. With the naked eye, a fading of the color was observed, from dark

purple to clear purple. The absorption spectra collected over time, following the reverse reaction confirm the photochromic behaviour. Starting from the irradiated compound at t= 0, Figure 4.14 shows that the initial absorbance at 580 nm is weak (around 0.08), and it is increasing in time until reaching almost 0.13 40 minutes after illumination. This figure confirms the photochromic behaviour of the compound.

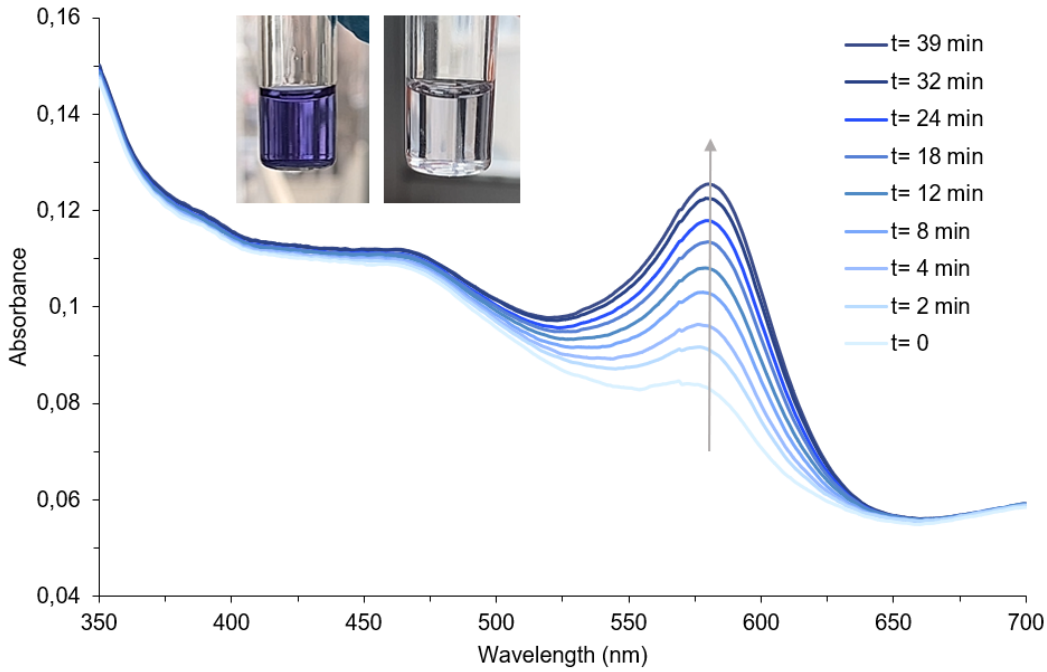

Figure 4.14: Absorption spectra of the DASA-A2-D2 in time in toluene at 10^{-4} M after 30 min of irradiation. Inset: DASA-A2-D2 in toluene before irradiation on the left and after irradiation on the right

Table 4.4 shows the in-time absorbance recovery.

	after 4 min	after 12 min	after 24 min	after 39 min
% of recovery	10.9	18	27.3	33.6

Table 4.4: % of absorbance recovery of the DASA-A2-D2 in toluene at 10^{-4} M at different times

After 90 min irradiation of the DASA-A2-D2 in toluene, and monitoring of the absorbance intensity at 580 nm in time, the Figure 4.15 has been plotted. The initial slope, the time to reach the plateau and the percentage of absorbance recovered can be estimated as:

$$\begin{cases} \mu = 0.0023\ min^{-1} \\ \tau = 88\ min \\ \delta(\tau) = 26\% \end{cases} \tag{4.6}$$

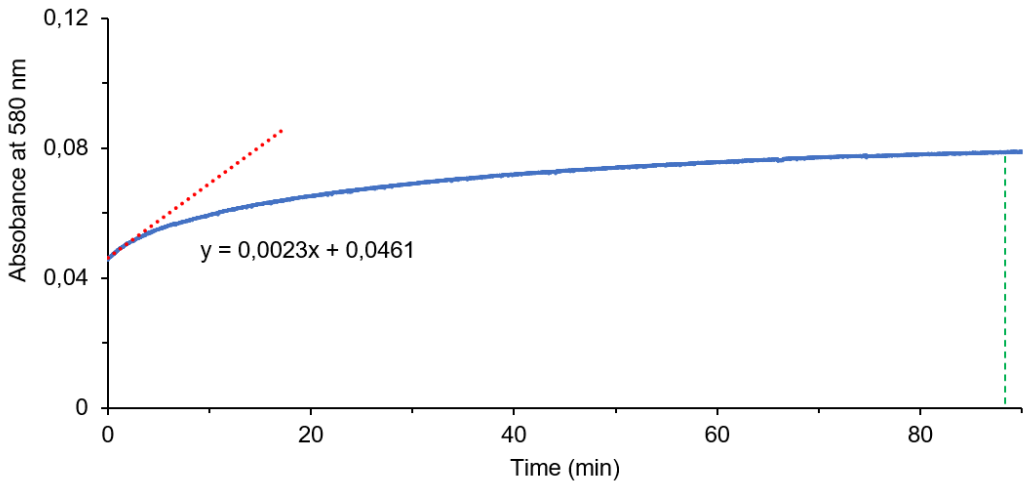

Figure 4.15: Evolution of the absorbance at 580 nm in time after 90 min of irradiation of the DASA-A2-D2 in toluene at 10^{-4} M

DASA-A3-D3

By irradiating the DASA-A3-D3 dissolved in chloroform at 614 nm, the photoswitching from the open to the closed form is observed (Figure 4.16).

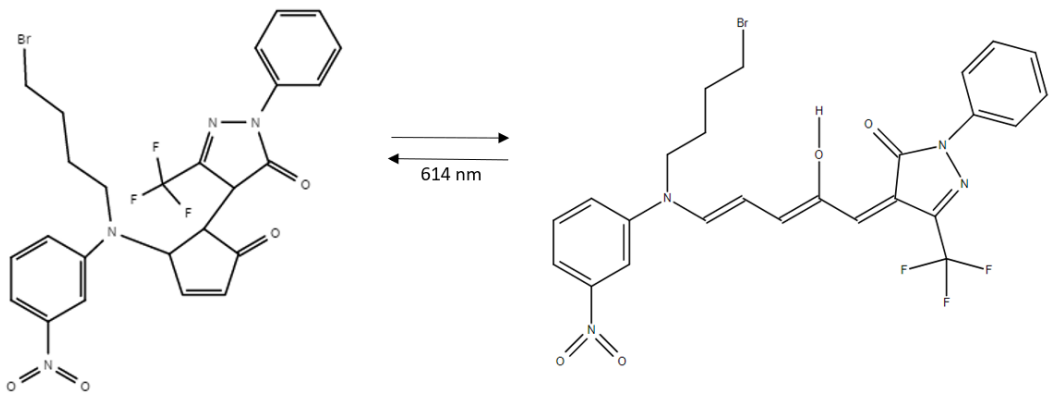

Figure 4.16: Photoisomerization from the close to open form of the DASA-A3-D3

Once again Figure 4.17 evidences the photochromic behaviour of the DASA-A3-D3. Starting from the irradiated compound at t= 0, Figure 4.17 shows that the initial absorbance at 614 nm is weak (around 0.04), and it is increasing in time until reaching almost 0.12 50 minutes after illumination.

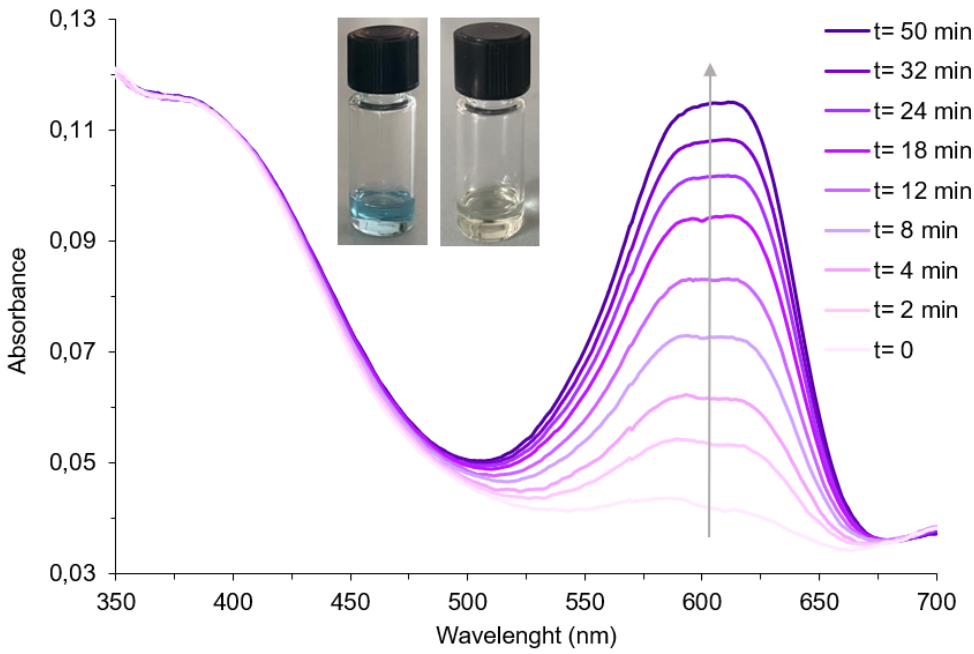

Figure 4.17: Absorption spectra of the DASA-A3-D3 in time in chloroform at 10^{-4} M after 30 min of irradiation. Inset: DASA-A3-D3 in chloroform before irradiation on the left and after irradiation on the right

Table 4.5 shows the in-time absorbance recovery:

	after 4 min	after 12 min	after 24 min	after 32 min	after 50 min
% of recovery	17	37	58	63	70

Table 4.5: % of absorbance recovery of the DASA-A3-D3 in chloroform at 10^{-4} M at different times

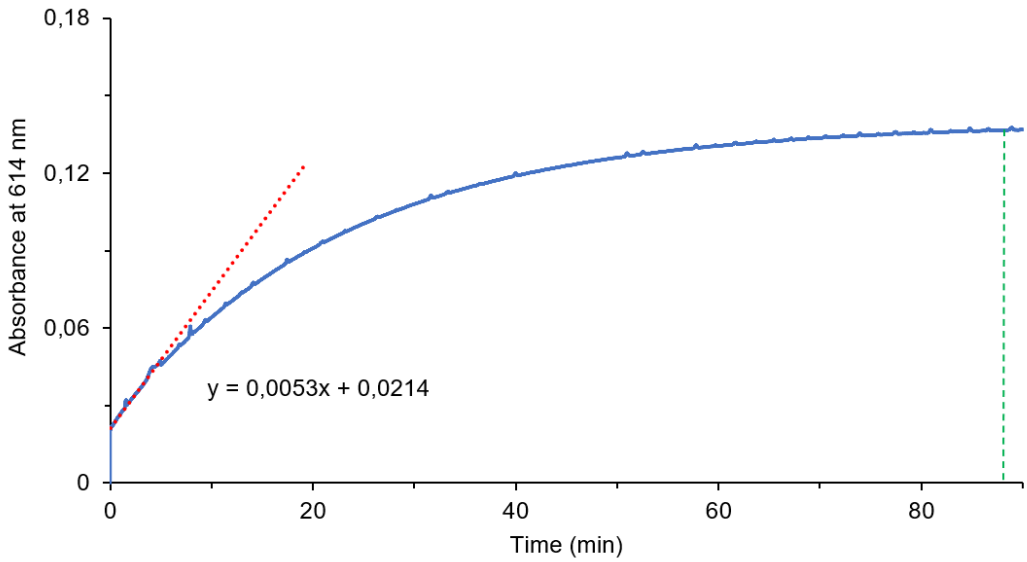

Figure 4.18: Evolution of the absorbance at 614 nm in time after 90 min of irradiation of the DASA-A3-D3 in chloroform at 10^{-4} M

Again, after 90 min irradiation of the DASA-A3-D3 in chloroform, and monitoring of the absorbance intensity at 614 nm in time, the Figure 4.18 has been plotted. The initial slope, the time to reach the plateau and the amount of recovered absorbance can be estimated as:

$$\begin{cases} \mu = 0.0053\ min^{-1} \\ \tau = 87\ min \\ \delta(\tau) = 115\% \end{cases} \tag{4.7}$$

The value of the recovered absorbance exceeds 100%. This leads us to think that in the absorption spectrum realized in the section 4.1, some molecules had already switched into the closed form due to the natural light entering the room.

DASA-A4-D2

Starting from the irradiated compound at t= 0, Figure 4.19 (zoomed on the interesting wavelength window) shows that the initial absorbance at 587 nm is weak (around 0.07), and is increasing in time until reaching almost 0.1 40 minutes after illumination. Due to the presence of remaining reactants in solution, the photochromic behaviour is less clear than with the other DASAs synthesized in this project, but is still visible.

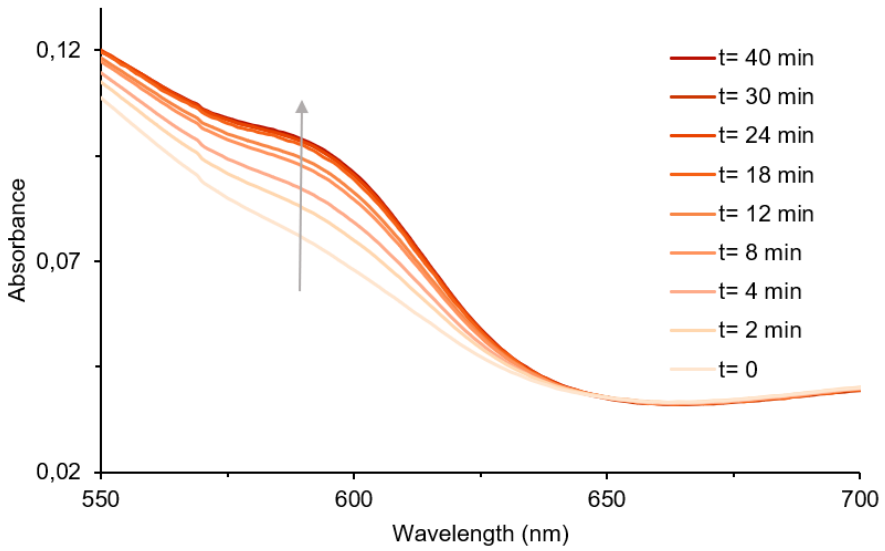

Figure 4.19: Absorption spectra of the DASA-A4-D2 in time in acetonitrile at 10^{-4} M after 30 min of irradiation

Table 4.6 shows the in-time absorbance recovery:

	after 2 min	after 12 min	after 24 min	after 30 min	after 40 min
% of recovery	7.8	18	23	23.5	24.4

Table 4.6: % of absorbance recovery of the DASA-A4-D2 in acetonitrile at 10^{-4} M at different times

Once again, the DASA-A4-D2 in acetonitrile has been irradiated for 90 minutes. The monitoring of the absorbance intensity at 587 nm in time led to the graph plotted on the Figure 4.20. The experiment has been stopped after 15 minutes. The initial slope has been estimated to:

$$\left\{\mu = 0.0036\ min^{-1}\right. \tag{4.8}$$

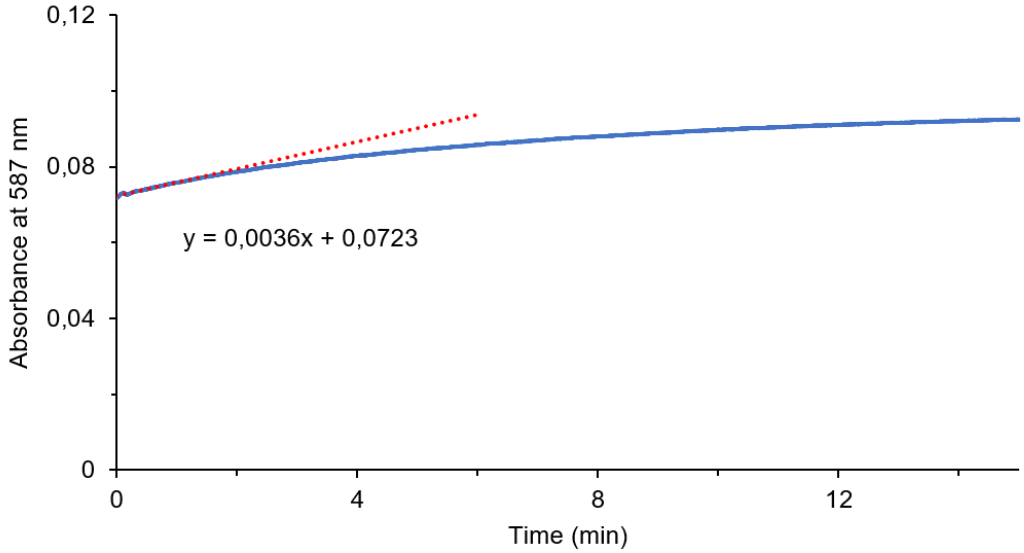

Figure 4.20: Evolution of the absorbance at 587 nm in time after 90 min of irradiation of the DASA-A4-D2 in acetonitrile at 10^{-4} M

DASA-A2-D2 with the polar head

By irradiating the DASA-A2-D2 with polar head dissolved in acetonitrile at 487 nm, the photoswitching from the open to the closed form should be observed (Figure 4.21).

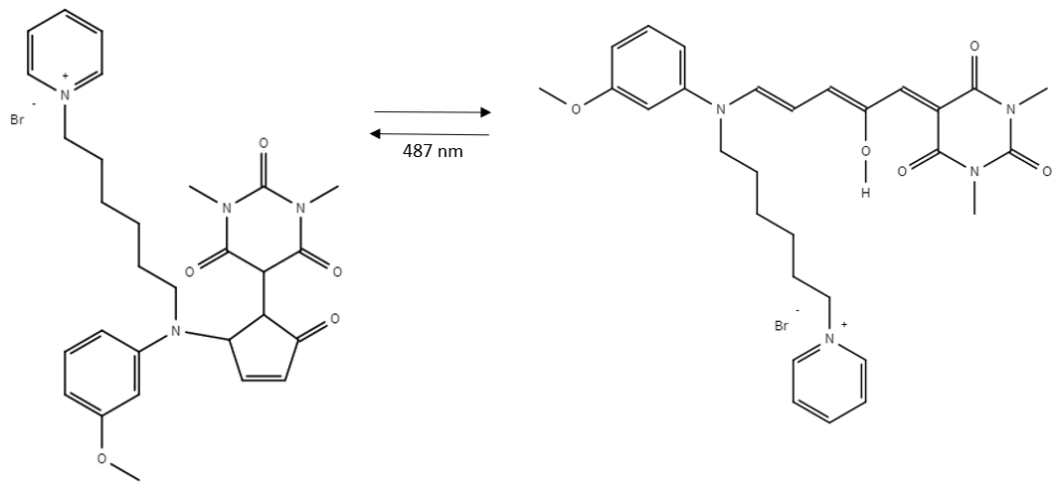

Figure 4.21: Photoisomerization from the close to open form of the DASA-A2-D2 with the polar head

Figure 4.22 shows the evolution in time of the absorption spectrum after having irradiated the compound for 30 minutes. In 45 minutes, no change is observed in the spectrum, leading to the following possible conclusions: either the DASA-A2-D2 with the polar head leads to a not photochromic structure, or the interaction with the solvent (DMSO) impedes the photoswitching, or the kinetics of the switching is very slow or hindered.

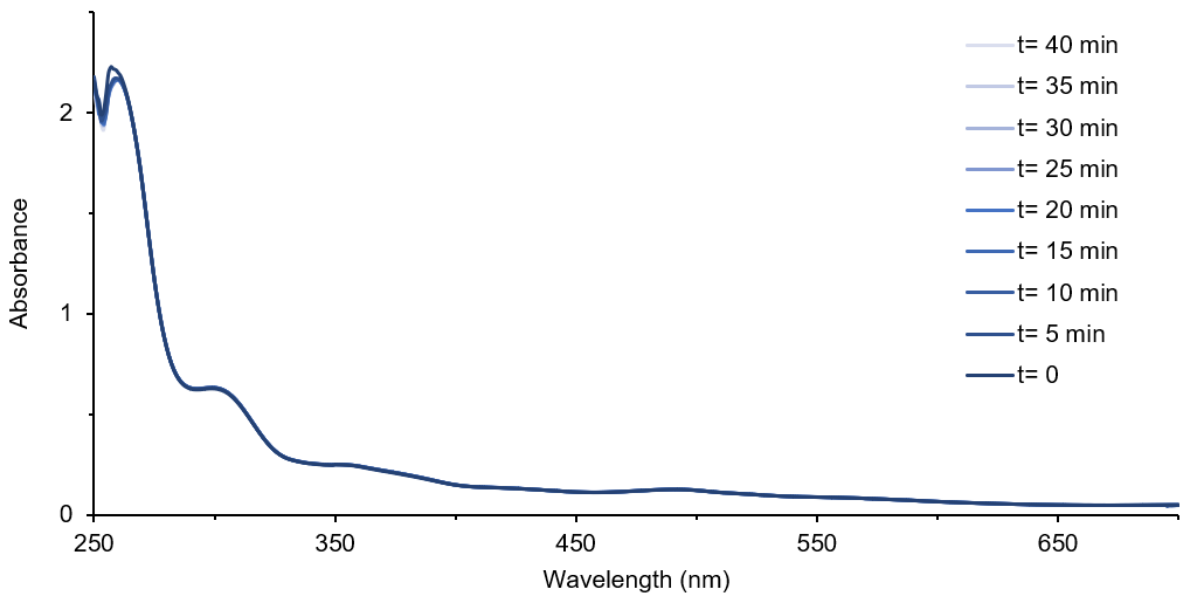

Figure 4.22: Absorption spectra of the DASA-A2-D2 with polar head in time in DMSO at 10^{-4} M after 30 min of irradiation

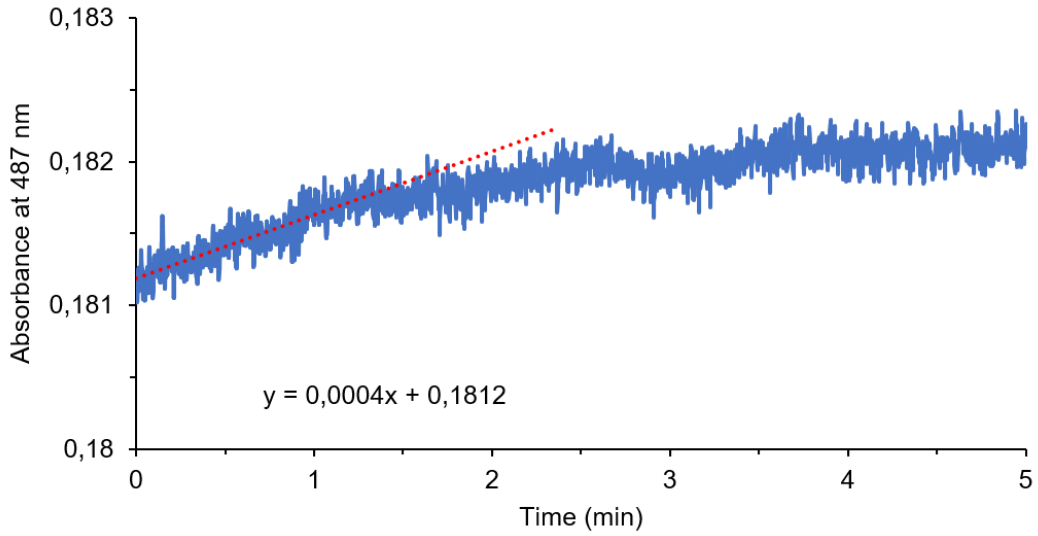

Figure 4.23: Evolution of the absorbance at 487 nm in time after 10 min of irradiation of the DASA-A2-D2 with polar head in acetonitrile at 10^{-4} M

Finally, a solution of DASA-A2-D2 with polar head in acetonitrile has been irradiated for 10 minutes. The monitoring of the absorbance intensity at 487 nm in time led to the graph plotted on Figure 4.23. The experiment has been stopped after 5 minutes.

$$\left\{\mu = 0.0004\ min^{-1}\right. \tag{4.9}$$

Even if a small increase in the absorbance is noticed, it is clear that the μ of the DASA-A2-D2 with polar head is very low compared to the previous DASAs analyzed (from one to two order of magnitude lower). The results obtained here confirm the idea according to which this DASA is not photochromic anymore, or at least photoswitches very slowly. The small increase in absorbance could also be due to some remaining reagent (DASA-A2-D2) that would not have reacted with the pyridine, therefore still displaying a photochromic behaviour.

DASA-A3-D3 with the polar head

By irradiating the DASA-A3-D3 with polar head dissolved in chloroform at 397 nm, the photoswitching from the open to the closed form should be observed (Figure 4.24).

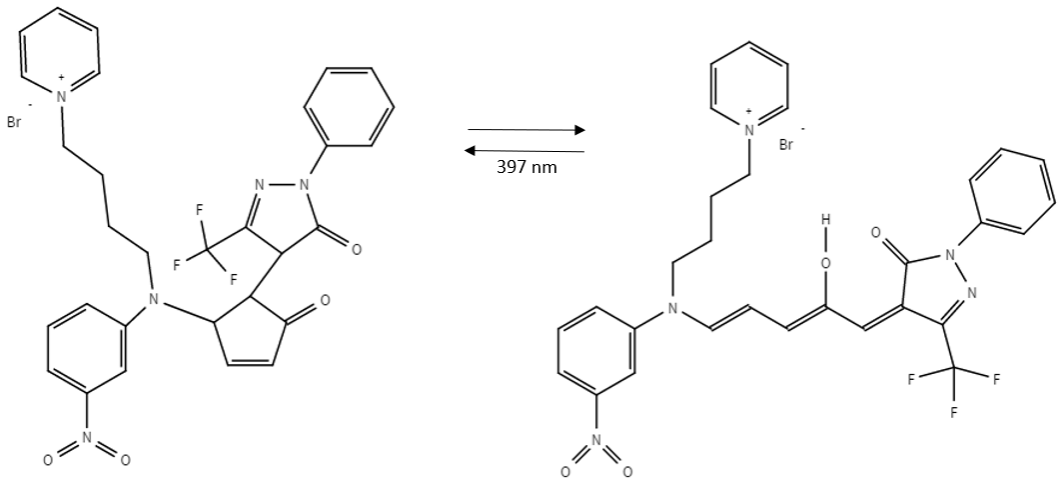

Figure 4.24: Photoisomerization from the close to open form of the DASA-A3-D3 with the polar head

Again, Figure 4.25 shows the evolution in time of the absorption spectrum after having irradiated the compound for 30 minutes. Compared to the absorption spectrum plotted on the Figure 4.6, it seems that the intensity of the absorbance at 397 nm has slightly decreased after the irradiation. However, in 45 minutes, no change is observed compared to the spectrum realized at t= 0, leading to the following possible conclusions: i) the switching has occurred but it has been irreversible, or ii) the DASA-A3-D3 with the polar head is not photochromic anymore and the loss in absorbance is explained by a remaining amount of non reacted DASA-A3-D3, or iii) the kinetics of the switching is very slow and in 45 minutes nothing can be observed.

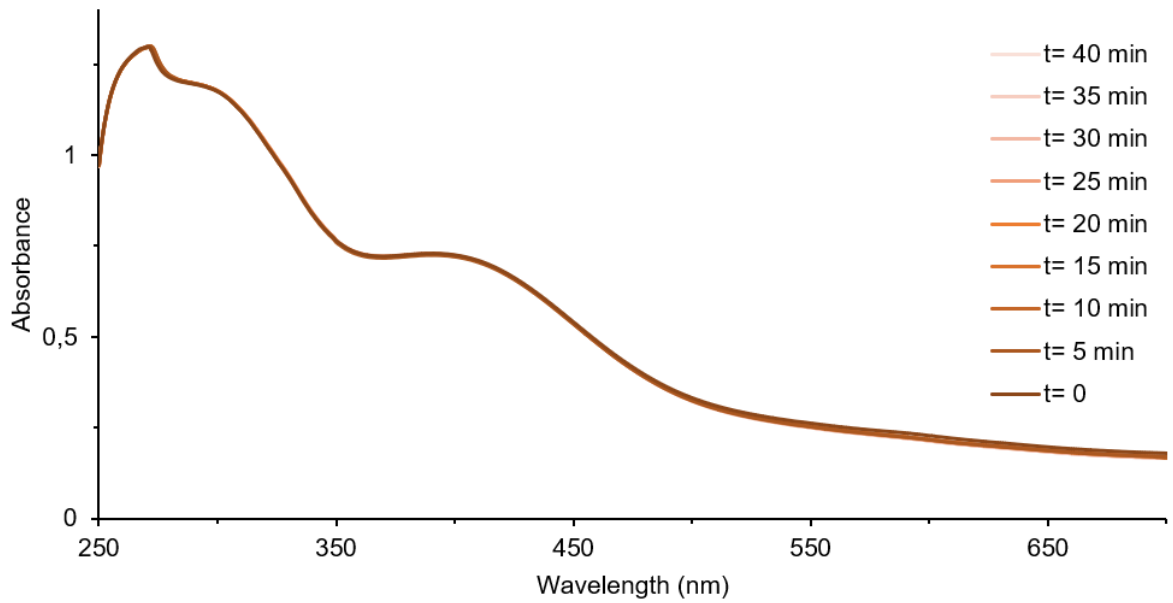

Figure 4.25: Absorption spectra of the DASA-A3-D3 with polar head in time in chloroform at 10^{-4} M after 30 min of irradiation

For this compound, as Figure 4.25 showed that the photochromic properties have been lost or severely degraded, and that the same has been confirmed by the kinetic experiment made on the DASA-A2-D2 with polar head (Figure 4.23), it did not seem relevant to realize a kinetic spectrum.

For the last two presented DASAs (A2-D2 with polar head, and A3-D3 with polar head) no recovery of the absorbance at all time was observed. This would either mean that the DASAs are able to switch but in an irreversible way (might be the case for the DASA-A3-D3 with polar head), or that they are not able to switch at all (DASA-A2-D2 with polar head). This behaviour might be explained by the presence of a counterion in the salts (pyridinium bromide complex), which might stabilize the zwitterionic isomer of the closed DASA, effectively preventing the thermal back-relaxation. This might be avoided by using a polar head with an inner salt, such as phosphocholine.

4.2.2. Emission/excitation spectra

Photoisomerization of the DASA-A1-D1 was studied also through emission spectra. The spectrofluorimeter can either provide:
-emission spectra: the compound is irradiated with one wavelength (excitation wavelength) and if it is emissive, the emitted light is recorded at a higher wavelength (the loss

in energy is due to non radiative relaxation phenomena).
-excitation spectra: by knowing the emission wavelength, irradiation of the compound with photons at a lower wavelength allows to find out which one will excite the emission.

Here, emission spectra have been registered, and the excitation wavelength has been taken equal to the absorption wavelength of the compound (range of light able to be absorbed and therefore to excite the electronic states), being 580 nm for the DASA-A1-D1. A measure of the intensity of emission has been carried out every 1 nm from 600 to 800 nm.

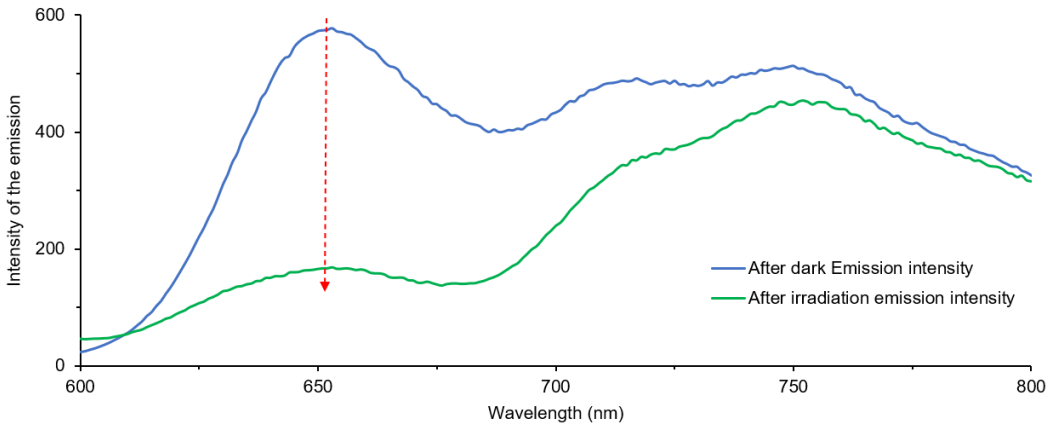

Figure 4.26: Emission spectra of the DASA-A1-D1 in chloroform at a concentration of 10^{-4} M in the dark in blue and after irradiation in green upon excitation at 580 nm

Figure 4.26 shows the emission spectrum of the DASA-A1-D1 in chloroform when excited with a light ray of 580 nm. In blue the emission spectrum recorded when the compound was left in the dark is shown. In green the emission spectrum recorded after irradiation of the compound with artificial light is shown. The first interesting thing is that the non-irradiated compound (absorption at 580 nm, violet-blue coloured) shows a quite intense emission around 650 nm, namely a reddish emitted light. The second thing to notice is the difference in the intensity of the emission at 650 nm when the compound has been submitted to light irradiation. The closed form of the DASA seems to be weakly emissive in the visible range.

Figures 4.27, 4.28 and 4.29 represent the evolution of the emission spectrum in time after irradiation of the DASA-A1-D1. Therefore, the change in emission properties during the reverse reaction was monitored, from the closed to the open isomer. The spectra have been recorded in chloroform and the excitation wavelength has been set at 580 nm. Several concentrations have been tested: 10^{-4} M in the Figure 4.27, 10^{-5} M in the Figure 4.28 and

10^{-6} M in the Figure 4.29.

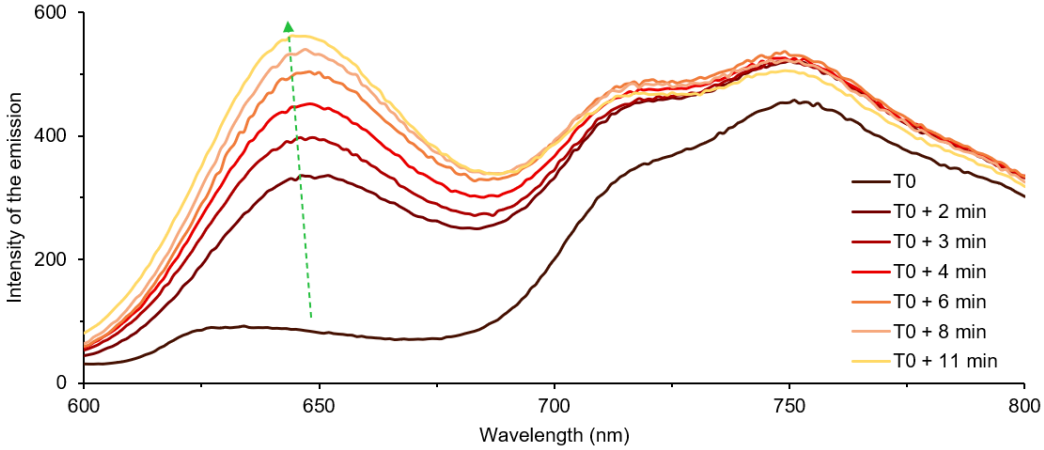

Figure 4.27: Emission properties in time after irradiation of the DASA-A1-D1 at a concentration of 10^{-4} M in chloroform and excitation at 580 nm

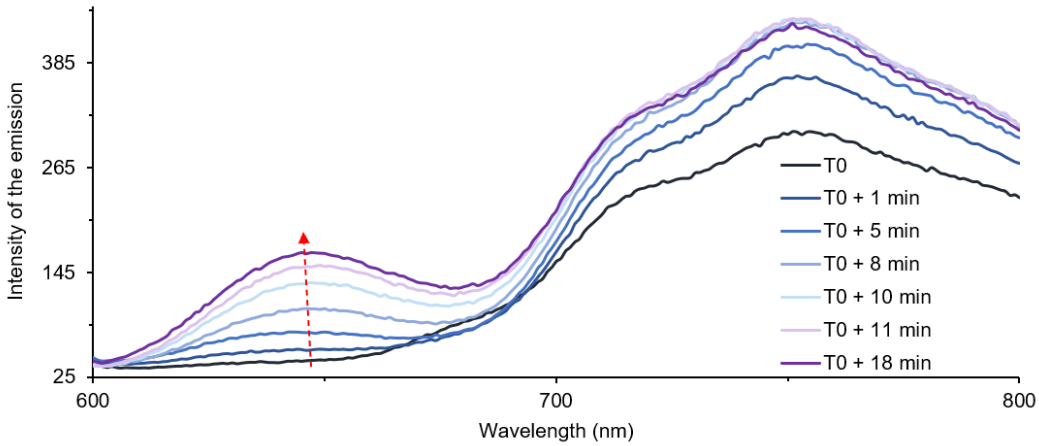

Figure 4.28: Emission properties in time after irradiation of the DASA-A1-D1 at a concentration of 10^{-5} M in chloroform and excitation at 580 nm

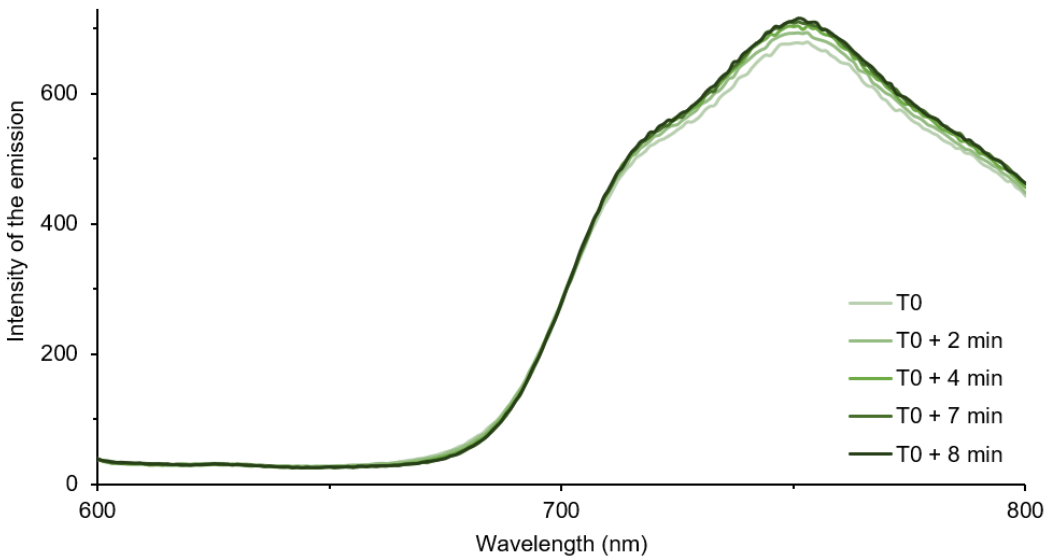

Figure 4.29: Emission properties in time after irradiation of the DASA-A1-D1 at a concentration of 10^{-6} M in chloroform and excitation at 580 nm

The more diluted the solution, the lower the intensity of the emission at 650 nm in the open form, while the emission band around 750 nm seems to maintain its intensity. The least concentrated solution behaves in a similar way as the closed isomer. Therefore, the emission band at 650 nm could be due to the aggregation in the open isomer. It would explain why this band disappears at low concentrations and after irradiation of the compound.

The presence of an emission band at wavelength different from that of cell autofluorescence, which is between 350 and 550 nm, is quite useful. In fact this might allow for a better visualization of the localization of the actuator in the cell, without the need for a fluorescent marker that might modify the properties of the compound.

4.3. Solvent effect

It must be noted that DASAs show great dependence of their photoswitching rates on the polarity of the solvent, with a more polar solvent promoting the open-to-close isomerization and an apolar medium the closed-to open one. For this reason, the most promising candidate in terms of photophysical and chemical features was characterized in different solvents.

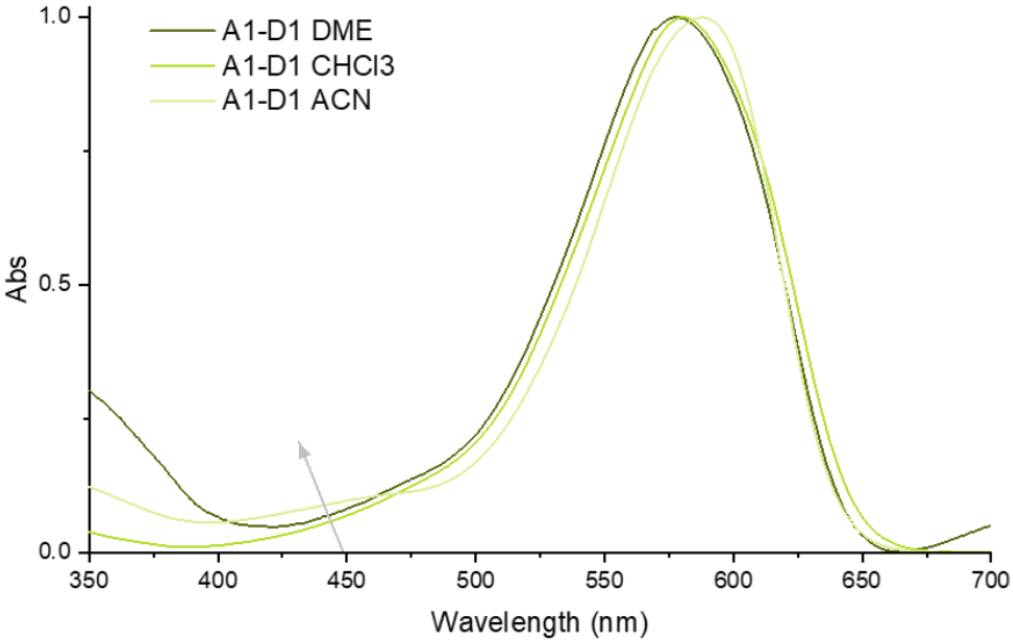

Figure 4.30: Absorption spectra of DASA-A1-D1 in dimethoxyethane, chloroform and acetonitrile in the dark

A redshift of the signal is visible for more polar solvents, albeit small, with the absorbance maximum going from 578 nm in dimethoxyethane to 587 nm in acetonitrile (Figure 4.30). Moreover, polar solvents promote a higher percentage of the closed isomer even in the dark.

The most dramatic effect, however, is in the kinetics, where the rate of switching from the open to the closed isomer is highly affected by the polarity, with an almost complete isomerization after one minute illumination in acetonitrile, while in chloroform only a small portion of the closed isomer is present (see Figure 4.31).

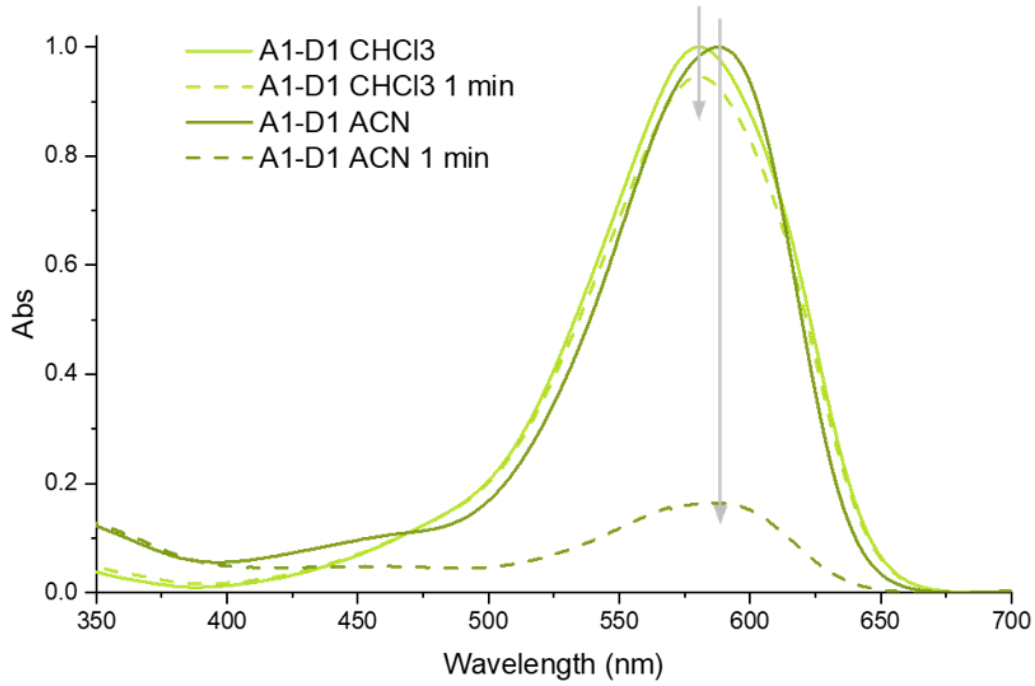

Figure 4.31: Absorption spectra of DASA-A1-D1 in chloroform and acetonitrile in the dark and after 1 minute irradiation

4.4. Stability and degradation of the DASAs

Fatigue and stability

A preliminary fatigue test has been performed on the DASA-A1-D1 in chloroform at 10^{-4} M with the UV/Vis spectrophotometer. We recall here that the maximum absorbance of this compound occurs at 580 nm. Several cycles of 40 min irradiation have been done, followed by a period of 1h in the dark. In order to perform a few number of cycles, the compound was not allowed to recover 90% of the initial intensity of the absorbance at 580 nm in the dark, as in the standard fatigue resistance experiment. Nevertheless, a qualitative observation of the phenomenon is still possible. The experiment consists in two phases: first of all, 40 minutes of irradiation was performed with absorption spectrum being collected every 10 minutes and absorbance values at 580 nm being extracted. Secondly, the compound was kept for 1h in the dark, during which a kinetic curve, similar to those plotted in the section 4.2.1, has been realized following the intensity of the absorbance at 580 nm (see Figure 4.32). During these 60 minutes, the measures have been performed every 0.4 second, and the spectral band width of the instrument has been set to 1 nm. The two phases have been eventually repeated over 5 cycles.

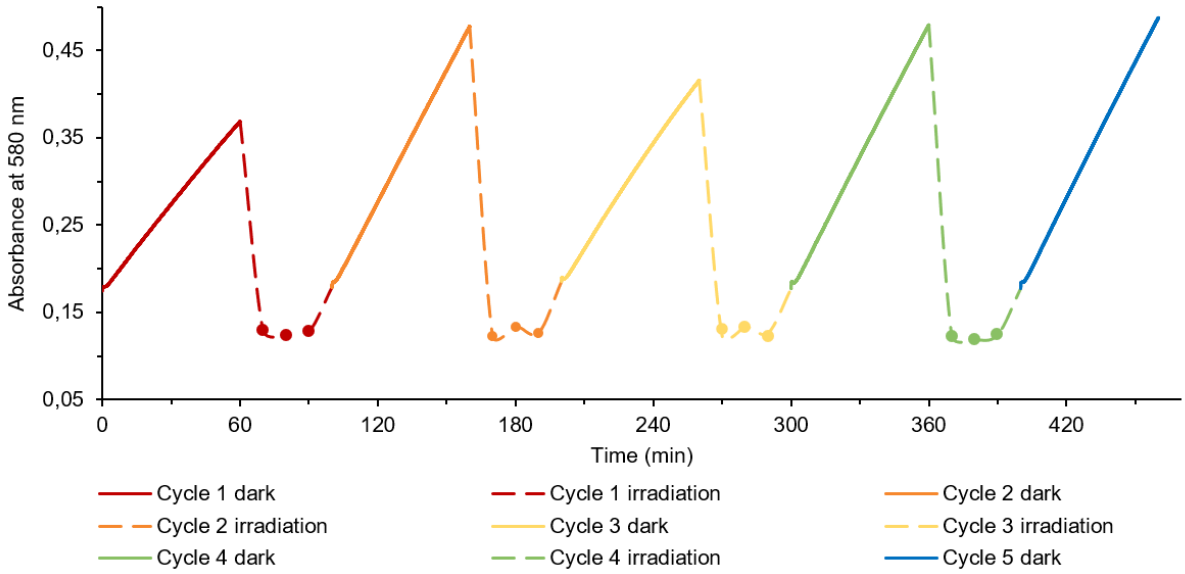

Figure 4.32: Evolution of the intensity of the absorption at 580 nm of the DASA-A1-D1 in chloroform at 10^{-4} M over several cycles of dark + irradiation

The plot demonstrates that during those five cycles, the compound shows rather consistent properties. During the irradiation, a minimal absorbance is quickly reached, around 0.12, with no dependence on the value of the absorbance at the end of the periods in the dark. Indeed, during those periods, the maximal absorbance that is reached changes with time, and appears to be lower for the first cycle than for the others. It is easily visible on the plot that the slope of the first curve is less steep than the other ones, as if the recovery was slower during the first cycle. This might be due to a change in temperature of the solution, which might have promoted a faster thermal relaxation. In the end, no degradation of the DASA-A1-D1 seems to have occurred during those 5 cycles.

Of course, more cycles, and especially longer ones, would be needed to make a more relevant comment on the fatigue behaviour of the compound.

Degradation

While recording all the previously described spectra, a tendency to degrade (or a loss in the reversibility of the switching) in some solvents has been observed. Numerous were the compounds which, after some irradiation cycles, or after a long time in solution, turned yellowish-orange. This might be due to a degradation of the DASAs towards their starting materials (furfural derivatives), which often appeared as red solids. A possible explanation for the poor stability of the DASAs could be the use of the hexafluoroisopropanol during the reaction pathway. It acts as the catalyst for the ring-opening reaction, this solvent can

also prove to be dangerous. It has been shown that too high concentrations (usually above 50 % in volume) of HFiP lead to an accelerated degradation of the product and of the starting material [36]. Even if, knowing this fact, the reactions have been thought in such a way that the amount of HFiP never exceeded 20% in volume, the DASAs synthesized in this project differ from those already synthesized in the literature and HFiP might be a source of degradation even at low concentrations. Another possibility, previously explained, is that the presence of a counterion promotes the formation of the photoacid product, which cannot react any further.

Spectra were collected with the UV-Vis spectrometer under the same conditions as the kinetic spectra realized in the section 4.2.1.

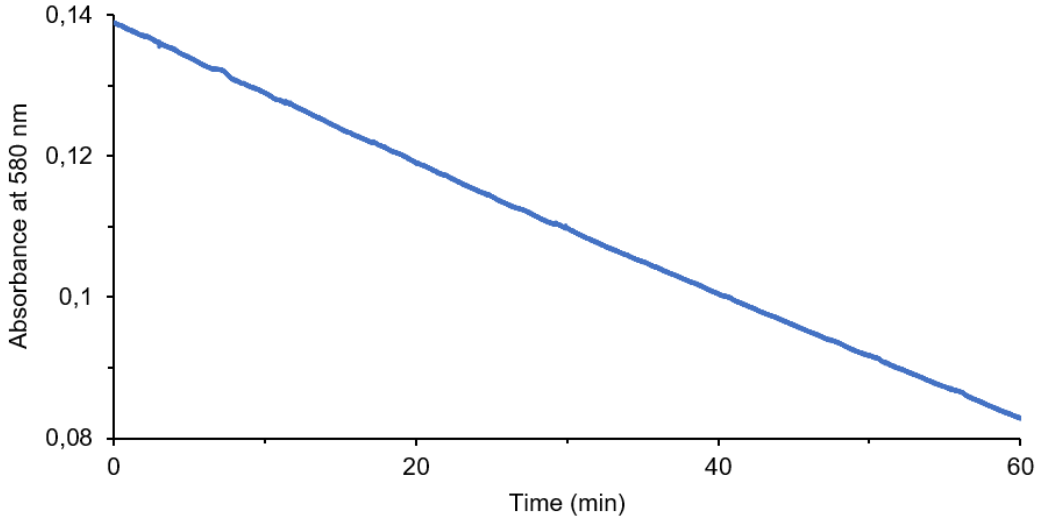

Figure 4.33: Evolution of the absorbance at the wavelength 580 nm in time after some irradiation cycles of the DASA-A1-D1 in chloroform

In the Figure 4.33 is plotted the evolution in time of the absorbance at 580 nm of the DASA-A1-D1 after some cycles of irradiation. A linear relationship between the decreasing absorbance and the time is observed. This phenomenon is called linear photodegradation upon irradiation and results from a low photochemical stability. Upon absorption of photons, the molecules in solution may degrade and a change in their optical (but not only) properties occurs.

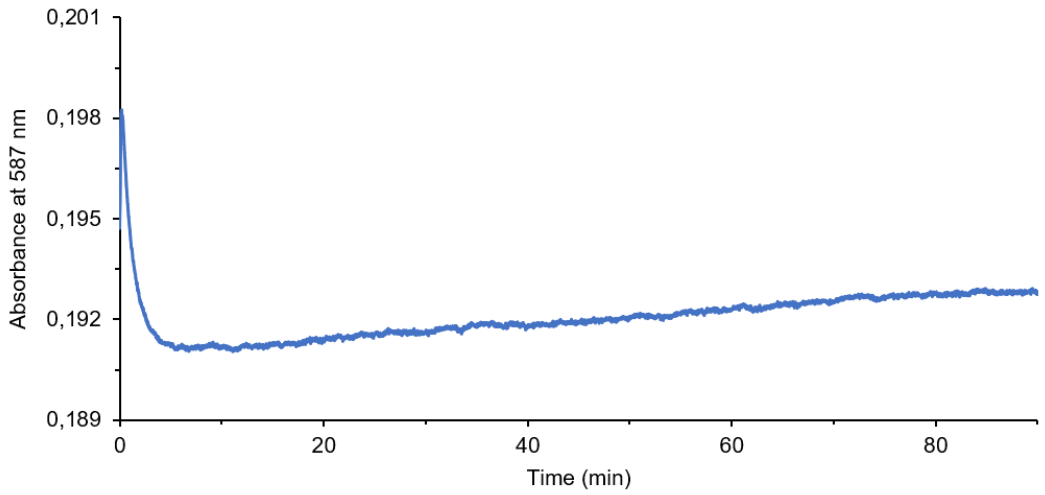

Figure 4.34: Evolution of the absorbance at 587 nm after 2 cycles of irradiation of the DASA-A4-D2 in acetonitrile

Figure 4.34 shows the evolution in time of the absorbance at 587 nm of the DASA-A4-D2 in acetonitrile after 2 cycles of irradiation. Several spectra, also on other compounds, have been found to show a similar trend. First of all an intense increase of the absorbance appears, as it is expected from photochromic DASAs after irradiation. Then, almost suddenly, an intense decrease of the absorbance is visible. This stage of the graph leads to think that a photodegradation has occurred. However, the subsequent slow increase in absorbance contradicts this idea. Further studies would be necessary to fully understand this phenomenon.

In order to rigorously measure the degradation of a compound (time to reach X% of degradation, or % of degradation observed after X cycles) the full monitoring of the intensity of absorbance upon cycles of irradiation (fatigue test) is necessary.

4.5. Results discussion

In the table presented below the main results of the previously described experiments are gathered.

			Absorption spectra			Kinetic experiments		
DASA	Solvent	Molar concentration (g/mol)	λ_{max} (nm)	% of abs. recovery at 10' and 20'		μ (min^{-1})	τ (min)	$\delta(\tau)$ (%)
DASA-A1-D1	CHCl3	10^{-4} and $5x10^{-6}$	580	2.2	4.4	0.0125	2	2.4
DASA-A1-D2	TOL	10^{-3}	585	92	117	0.0042		
DASA-A2-D2	TOL	10^{-4}	580	16.4	24.2	0.0023	88	24
DASA-A3-D3	CHCl3	10^{-4}	614	31	51	0.0053	87	115
DASA-A4-D2	ACN	10^{-4}	587	21.1	22.5	0.0036		
DASA-A2-D2 with polar head	DMSO	10^{-4}	487	0	0	0.0004		
DASA-A3-D3 with polar head	CHCl3	10^{-4}	397	0	0			

Table 4.7: Summary of the optical properties of the synthesized DASAs

The first parameter to be discussed is the position of the absorption maxima of the different DASAs. All the prepared compounds absorb light in or close to the therapeutic window. While four of the synthesized DASAs feature approximately the same absorption band between 580 and 587 nm, there is one DASA, A3-D3, presenting an absorption band more red shifted (614 nm). However, the introduction of the pyridinium-terminated alkyl chain results in a remarkable blue-shift, possibly after the isomerization to the photo-inactive zwitterionic form. The alkyl chain with the polar head might increase the distortions or stabilize the zwitterionic closed form through interactions between the

various ions, the latter being the more probable hypothesis. Therefore, the absorption bands observed for the DASAs with polar head would be related to their cyclic isomers.

Secondly, even if the molar concentrations and the solvents differ, some basic conclusions may be brought to the performed experiments. The DASA-A1-D1 at a very dilute concentration ($5x10^{-6}$ M) shows kinetic properties (μ and τ) quite different from the other DASAs, and appears to be the fastest DASA to photoswitch among those tested, featuring a photoisomerization rate close to the minute. However, as it is shown with its % of recovered absorbance at 10^{-4} M, and by the weak $\delta(\tau)$, this DASA shows a poor absorbance recovery at high concentration, which could be explained by the formation of aggregates impeding the complete recovery of the signal. All of the synthesized DASAs show a photoswitching kinetics faster than the ones published in the literature, albeit not yet quick enough for some biological applications, such as cell stimulation.

Moreover, it seems that when attaching the polar head, the photochromic behaviour is hindered. However, if, as previously explained, the back-relaxation is prevented by the presence of a counterion, this issue might not be one anymore inside the cellular membrane. Indeed the bromine counterion should not be able to penetrate inside the membrane, and therefore, even if adequate experiments on cells would have to be performed to confirm this hypothesis, the photoswitching of those compounds might still be effective for bio-optics purposes. Besides, this issue might also be overcome through the use of a different polar moiety. Lastly, the presence of an emission profile different from that of the cell autofluorescence proves useful for biological studies, as no further labelling would be required.

5 | Conclusion

In this thesis project, seven new DASAs have been designed in such a way that they could partition into a cell membrane and upon light irradiation, photoswitch into a second isomer featuring a different geometry and polarity. Different combinations of some donor and acceptor moieties have been tested in order to obtain a DASA with optimum properties. Their synthesis has followed a systemic reaction pathway, that proved itself to be efficient, and entered the green chemistry class. A great advantage of the reaction route chosen in this work is that starting from few chemicals (donors and acceptors), a large number of final products can be yielded thanks to the different allowed combinations. However, to make their synthesis even more eco-friendly, the use of greener solvents is to be thought of.

A photophysical characterization has been conducted on each synthesized DASA in order to study the optical and photochromic properties. The results of the photo-physical experiments have shown that the majority of the synthesized DASAs presented well red-shifted absorption spectra, and a kinetics still slow in comparison to biological events timescale, but faster than those reported in literature, and already acceptable for some bio-applications. The fastest DASA synthesized showed a photoswitching rate from the closed to the open isomer close to the minute, therefore not fast enough for the desired application. However, the study performed in this project has been done by continuous irradiation, while in order to establish the photoswitching rates, pump probe measures must still be performed in the future on the most promising candidates. Moreover, one of the synthesised DASA showed emissive properties, which could be very interesting to monitor its location inside the cells, avoiding a supplementary step in the reaction route to attach a fluorescent marker. The study has shown that the DASAs with the pyridinium as polar head showed a poor, or nonexistent, photochromism. However this issue might be overcome when the DASAs partition inside the cell membrane, leaving behind the counterion of the pyridinium, possibly responsible for the non-photochromic behaviour displayed by the compounds. As an alternative, a different polar head with no external counterion can be used instead of pyridinium bromide. Appropriate experiments should be conducted to draw deeper conclusions. Because of their many advantages, DASAs

might be very attractive for biological applications, and even if fast enough rates cannot be achieved for cell stimulation, several other uses might be developed such as photocages for drug delivery, platforms for controlled photorelease, or even as orthogonal wavelength selective systems when paired with other photoswitches.

From a critical point of view, some choices made for their synthesis are questionable. First of all, the use of hexafluoroisopropanol, being of great help and time-reducer for the synthesis of DASAs in the literature, might induce a fast degradation of the compounds. Finding another way to catalyse, or at least, to enable the ring-opening reaction, might be a future interesting problem to solve. Secondly, the choice to attach the alkyl chain with the polar head to the donor moiety of the DASA is also questionable. The acidic part being less involved in the 4-π-electrocyclization than the donor moiety, attaching the alkyl chain and the pyridine ring here might help decrease the steric hindrance close to the triene skeleton. An experiment to synthesize some acidic groups linked to the bromine chain has been performed but without great success.

In conclusion, even if the DASAs presented in this thesis project do not fully comply with the requirements for cell stimulation purposes, they possess numerous qualities that make them interesting candidates for several other applications where rapid photoswitching is not a mandatory feature. Besides, a panel of new red shifted DASAs has been established and a starting basis for their photo-physical characterization has been elaborated.

Bibliography

[1] J. K. Rad, Z. Balzade, and A. R. Mahdavian, "Spiropyran-based advanced photoswitchable materials: A fascinating pathway to the future stimuli-responsive devices," **2022**.

[2] J. Volaric, W. Szymanski, N. A. Simeth, and B. L. Feringa, "Molecular photoswitches in aqueous environments," **2021**.

[3] A. Prindle, J. Liu, M. Asally, S. Ly, J. Garcia-Ojalvo, and G. M. Süel, "Ion channels enable electrical communication in bacterial communities," **2015**.

[4] R. Bialecki, J. Valentin, and al., "Comprehensive toxicology," **2010**.

[5] Z. Shapira, N. Degani-Katzav, S. Yudovich, A. Grupi, and S. Weiss, "Optical probing of local membrane potential with fluorescent polystyrene beads," **2021**.

[6] A. Mourot, I. Tochitsky1, and R. H. Kramer, "Light at the end of the channel: optical manipulation of intrinsic neuronal excitability with chemical photoswitches," **2013**.

[7] Chegg, "Ion movement and gated channel." `https://www.chegg.com/learn/biology/anatomy-physiology-in-biology/ion-movement-and-gated-channel`.

[8] J. R. Hemmer, Z. A. Page, K. D. Clark, F. Stricker, N. D. Dolinski, C. J. Hawker, and J. R. de Alaniz, "Controlling dark equilibria and enhancing donoracceptor stenhouse adduct photoswitching properties through carbon acid design," **2018**.

[9] S. Helmy, F. A. Leibfarth, S. Oh, J. E. Poelma, C. J. Hawker, and J. R. de Alaniz, "Photoswitching using visible light: A new class of organic photochromic molecules," **2014**.

[10] M. M. Lerch, W. Szymanski, and B. L. Feringa, "The (photo)chemistry of stenhouse photoswitches: guiding principles and system design," **2018**.

[11] D. Arnold and W. Ware, "Photochemistry," **1974**.

[12] H. Bouas-Laurent and H. Durr, "Organic photochromism (iupac technical report)," **2001**.

[13] M. Irie, T. Fukaminato, K. Matsuda, and S. Kobatake, "Photochromism of diarylethene molecules and crystals: Memories, switches, and actuators," **2017**.

[14] D. Pousty, H. Mamane, V. Cohen-Yaniv, and J. R.Bolton, "Ultraviolet actinometry – determination of the incident photon flux and quantum yields for photochemical systems using low-pressure and ultraviolet light-emitting diode light sources," **2022**.

[15] A. Spangenberg, J. A. P. Perez, A. Patra, J. Piard, A. Brosseau, R. Métivier, and K. Nakatani, "Probing photochromic properties by correlation of uv-visible and infra-red absorption spectroscopy: a case study with cis-1,2-dicyano-1,2-bis(2,4,5-trimethyl-3-thienyl)ethene," **2010**.

[16] H. B. Laurent and H. Durr, "Photochromism: molecules and systems," **1990**.

[17] M. York and R. A. Evans, "Synthesis and properties of 1,3,3-trimethylspiro[indoline-2,30-naphtho[2,1-b][1,4]oxazin]-60-amine, a novel, red colouring photochromic spirooxazine," **2010**.

[18] K.-X. Wang, B.-W. Yin, P.-K. Jia, T.-S. Zhang, G. Cui, and B.-B. Xie, "Electronic structure calculations and nonadiabatic dynamics simulations on reversible photochromic mechanism of spirooxazine," **2022**.

[19] V. P. Rybalkin, S. Y. Pluzhnikova, L. L. Popova, Y. V. Revinskii, K. S. Tikhomirova, O. A. Komissarova, A. D. Dubonosov, V. A. Brenb, and V. I. Minkina, "A novel approach to fluorescent photochromic fulgides," **2016**.

[20] D. Lachmann, R. Lahmy, and B. König, "Fulgimides as light-activated tools in biological investigations," **2019**.

[21] Y. Jia, G. Jiang, S. Cui, and S. Pu, "Construction of reversible fluorescent switching systems with cdse quantum dots and photochromic diarylethenes," **2022**.

[22] M. L. DiFrancesco, F. Lodola, and E. Colombo, "Neuronal firing modulation by a membrane-targeted photoswitch," **2018**.

[23] Z. Li, D. Zhang, J. Weng, B. Chen, and H. Liu, "Synthesis and characterization of photochromic azobenzene cellulose ethers," **2013**.

[24] J. R. Thurston, M. P. Marshak, and al., "Encyclopedia of energy storage," **2022**.

[25] M. K. Katiyar, G. K. Dhakada, Shivani, S. Arora, S. Bhagat, T. Arora, and R. Kumar, "Synthetic strategies and pharmacological activities of chromene and its derivatives: An overview," **2022**.

[26] R. Fromm, R. Born, H. Dürr, J. Kannengießer, H. D. Breuer, P. Valat, and J. Kossanyi, "Spirodihydroazafluorenes: a new type of cis-fixed photochromic molecule with rigid region b showing extremely fast back reaction," **2000**.

[27] E. Chatir, M. Boggio-Pasqua, F. Loiseau, C. Philouze, G. Royal, and S. Cobo, "Synthesis of redox-active photochromic phenanthrene derivatives," **2022**.

[28] M. Hirai, T. Yuzawa, Y. Haramoto, and M. Nanasawa, "Synthesis and photochromic behavior of methylmethacrylate copolymers having anils as pendant," **2000**.

[29] Dorogan and Minkin, "Thermochromic and spectral properties of perimidinespirocyclohexadienones: A dft and ab initio studies," **2006**.

[30] H. Tahir and M. Saad, "Interface science and technology," **2011**.

[31] S. Ulrich, X. Wang, M. Rottmar, R. M. Rossi, B. J. Nelson, N. Bruns, R. Müller, K. Maniura-Weber, X.-H. Qin, and L. F. Boesel, "Nano 3d printed photochromic micro objects," **2021**.

[32] R. F. A. Gomes, J. A. S. Coelho, and C. A. M. Afonso, "Synthesis and applications of stenhouse salts and derivatives," **2018**.

[33] R. Castagn, D. P. Galyna Maleeva, and P. G. Carlo Matera, "A donor-acceptor stenhouse adduct displaying reversible photoswitching in water and neuronal activity," **2020**.

[34] B. F. Lui, N. T. Tierce, F. Tong, M. M. Sroda, H. Lu, J. R. de Alaniz, and C. J. Bardeen, "Unusual concentration dependence of the photoisomerization reaction in donor–acceptor stenhouse adducts," **2019**.

[35] M. M. Sroda, F. Stricker, J. A. Peterson, A. Bernal, and J. R. de Alaniz, "Donor–acceptor stenhouse adducts: Exploring the effects of ionic character," **2021**.

[36] M. Clerc, F. Stricker, S. Ulrich, M. Sroda, N. Bruns, L. F. Boesel, and J. R. de Alaniz, "Promoting the furan ring-opening reaction to access new donor–acceptor stenhouse adducts with hexafluoroisopropanol," **2021**.

[37] G. Noirbent, Y. Xu, A.-H. Bonardi, S. Duval, D. Gigmes, J. Lalevée, and F. Dumur, "New donor-acceptor stenhouse adducts as visible and near infrared light polymerization photoinitiators," **2020**.

[38] H. Zulfikri, M. A. J. Koenis, M. M. Lerch, M. D. Donato, W. Szymanski, C. Filippi, B. L. Feringa, and W. J. Buma, "Taming the complexity of donor acceptor stenhouse adducts: Infrared motion pictures of the complete switching pathway," **2019**.

[39] F. Sun, X. Xiong, A. Gao, Y. Duan, L. Mao, L. Gu, Z. Wang, C. He, X. Deng, Y. Zheng, and D. Wang, "Fast photochromism in solid: Microenvironment in metal-organic frameworks promotes the isomerization of donor-acceptor stenhouse adducts," **2022**.

[40] O. Rifaie-Graham, S. Ulrich, N. F. B. Galensowske, S. Balog, M. Chami, D. Rentsch, J. R. Hemmer, J. R. de Alaniz, L. F. Boesel, and N. Bruns, "Wavelength-selective light-responsive dasa-functionalized polymersome nanoreactors," **2018**.

[41] D. Zhong, Z. Cao, B. Wu, Q. Zhang, and G. Wang, "Polymer dots of dasa-functionalized polyethyleneimine: Synthesis, visible light/ph responsiveness, and their applications as chemosensors," **2017**.

[42] J. Alves, S. Wiedbrauk, D. Gräfe, S. L. Walden, J. P. Blinco, and C. Barner-Kowollik, "It's a trap: Thiol-michael chemistry on a dasa photoswitch," **2020**.

[43] B. P. Mason, M. Whittaker, J. Hemmer, S. Arora, A. Harper, S. Alnemrat, A. McEachen, S. Helmy, J. R. de Alaniz, and J. P. Hooper, "A temperature-mapping molecular sensor for polyurethane-based elastomers," **2016**.

[44] Y. J. Diaz, Z. A. Page, A. S. Knight, N. J. Treat, J. R. Hemmer, C. J. Hawker, and J. R. de Alaniz, "A versatile and highly selective colorimetric sensor for the detection of amines," **2017**.

[45] A. Balamurugan and H. il Lee, "A visible light responsive onoff polymeric photoswitch for the colorimetric detection of nerve agent mimics in solution and in the vapor phase," **2016**.

[46] S. Singh, K. Friedel, M. Himmerlich, Y. Lei, G. Schlingloff, and A. Schober, "Spatiotemporal photopatterning on polycarbonate surface through visible light responsive polymer bound dasa compounds," **2015**.

[47] X. Zhang, H. Zhao, D. Tian, H. Deng, and H. Li, "A photoresponsive wettability switch based on a dimethylamino calix[4]arene," **2014**.

[48] Y. Nicolas, F. Allama, and M. Lepeltier, "New synthetic routes towards soluble and dissymmetric triphenodioxazine dyes designed for dye-sensitized solar cells," **2014**.

[49] J. A. Peterson, F. Stricker, and J. R. de Alaniz, "Improving the kinetics and dark equilibrium of donor acceptor stenhouse adduct by triene backbone design," **2022**.

[50] A. Choudhary, "Synthesis, reactions and medicinal uses of pyridine and basicity of pyridine,"

[51] M. Asif, M. Imran, and A. Husain, "Approaches for chemical synthesis and diverse pharmacological significance of pyrazolone derivatives: A review," **2021**.

[52] J. N. Appaturi, R. J. Ramalingam, and H. A. Al-Lohedan, "Synthesis, characterization and catalytic activity of melamineimmobilized mcm-41 for condensation reactions," **2017**.

[53] M. Nayak, H. Batchu, and S. Batra, "Straightforward copper-catalyzed synthesis of pyrrolopyrazoles from halogenated pyrazolecarbaldehydes," **2012**.

[54] B. Chiranjeevi, E. N. Reddy, C. Madhi, N. J. Babu, and A. Krishnaiah, "A simple and catalyst free one pot access to the pyrazolone fused 2,8-dioxabicyclo[3.3.1]nonanes," **2014**.

[55] T. Ricardo, V. Carlos, S.-M. Amparo, M. M. Carmen, P. J. R., and B. Gonzalo, "Organocatalytic enantioselective 1,6-aza-michael addition of isoxazolin-5-ones to p-quinone methides," **2020**.

A | Appendix A: Chemical synthesis

A1

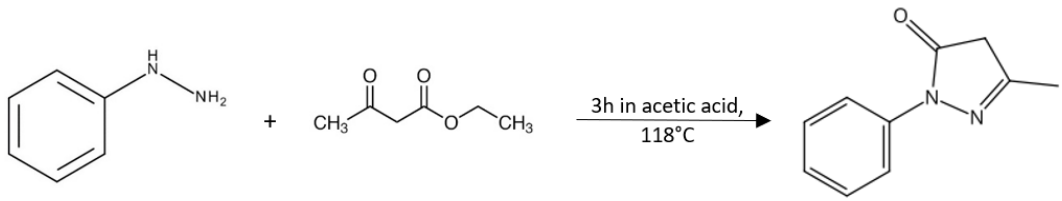

3-methyl-1-phenyl-2-pyrazolin-5-one (edaravone): Phenyl hydrazine (15 mmol) and ethyl acetoacetate (15 mmol) were mixed together in 7 mL of acetic acid and stirred at reflux for 3 h. The reaction mixture was evaporated by reduced pressure and the remaining product was extracted with water and dichloromethane (DCM). The organic layer was dried over anhydrous sodium sulphate and the solvent removed under under reduced pressure to obtain the final product as a yellowish solid [53]. ^{1}H-NMR (400 MHz, $CDCl_3$) δ 7.86 (dd, J = 8.7, 1.0 Hz, 2H), 7.42 – 7.36 (m, 2H), 7.18 (t, J = 7.4 Hz, 1H), 3.46 – 3.41 (m, 2H), 2.20 (s, 3H).

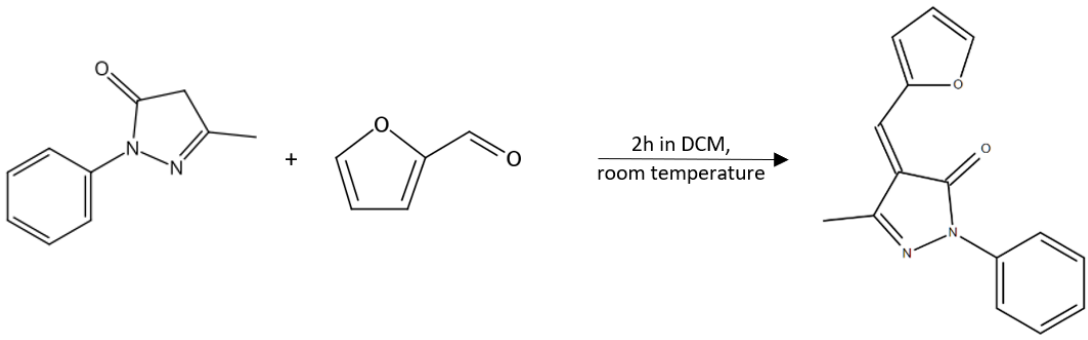

4-(2-Furanylmethylene)-2,4-dihydro-5-methyl-2-phenyl-3H-pyrazol-3-one: Furfural (12,2 mmol) and edaravone (5,7 mmol) were combined in 10 mL of dichloromethane and stirred for 12 hours at room temperature. Then the remaining solution was rinsed with water and methanol, and the organic phase was dried and put under reduced pressure

to remove the solvent. The pure product was obtained through column chromatography in ether petroleum : ethyl acetate as eluent in a ratio 10 : 1. The first spot was collected and the solvent evaporated under reduced pressure. A red powder was obtained [8]. ^{1}H-NMR (400 MHz, $CDCl_3$) δ 8.75 (d, J = 3.7 Hz, 1H), 7.98 – 7.94 (m, 2H), 7.75 (d, J = 1.2 Hz, 1H), 7.44 – 7.38 (m, 3H), 7.33 (s, 1H), 7.18 (s, 1H), 6.72 (dd, J = 3.7, 1.0 Hz, 1H), 2.33 (s, 3H).

A3

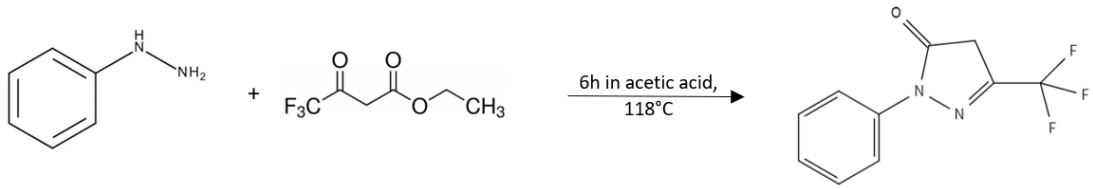

1-Phenyl-3-(trifluoromethyl)-5-pyrazolone: Ethyl 4,4,4-trifluoro-3-oxobutano-ate (30 mmol) and phenyl hydrazine (30 mmol) were mixed in acetic acid (18 mL) at reflux for 6h. The reaction mixture was allowed to cool to room temperature. A precipitate formed, was filtered out and the remaining solution was put under reduced pressure to remove the solvent. The remaining product was recovered as a solid and washed with water and hexane [54]. The product has been purified through a column chromatography in ether petroleum : ethyl acetate as eluent in a ratio 95 : 5 to collect the 3 first spots and in a ratio 60 : 40 to collect the last spot which was the expected product. ^{1}H-NMR (400 MHz, $CDCl_3$) δ 7.71 (dd, J = 8.6, 1.1 Hz, 2H), 7.43 (dd, J = 10.6, 5.0 Hz, 2H), 7.32 (dd, J = 10.6, 4.3 Hz, 1H), 5.81 (s, 1H), 3.71 (d, J = 1.2 Hz, 1H).

As the number of protons is quite low (7 protons), the result of the ^{1}H-NMR has been confirmed by a mass spectrum shown in Figure A.1. The peak at 229 m/z corresponds to the desired product (molar mass 228 g/mol).

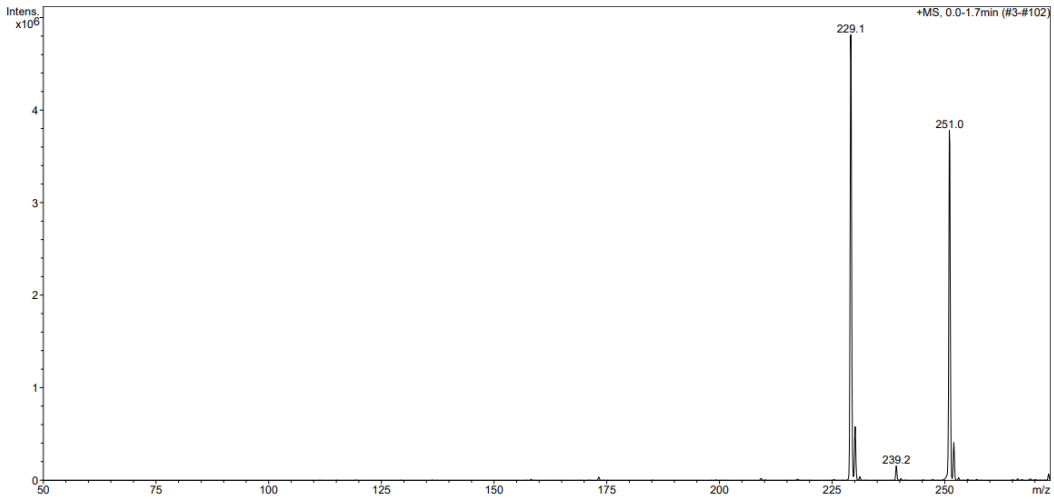

Figure A.1: Mass spectrum of the products of the reaction aiming to yield the precursor of A3

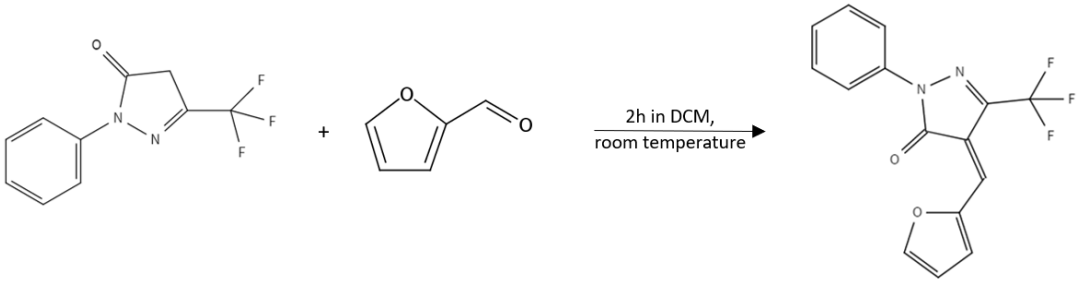

3H-Pyrazol-3-one, 4-(2-furanylmethylene)-2, 4-dihydro-2-phenyl-5-(trifluoromethyl): 1-Phenyl-3-(trifluoromethyl)-5-pyrazolone (8,7 mmol) and furfural (18,5 mmol) were mixed together in dichloromethane (20 mL) for 2h at room temperature. 60 mL of water were added to the reaction mixture and the solvent was evaporated under reduced pressure. A solid precipitated and was collected by filtration and rinsed with water [8]. The product has been purified through a column chromatography in hexane : diethyl ether as eluent in a ratio 2 : 1 and was found in the first spot. ^{1}H-NMR (400 MHz, $CDCl_3$) δ 8.92 (d, J = 3.9 Hz, 1H), 7.93 (d, J = 7.8 Hz, 2H), 7.88 (d, J = 1.5 Hz, 1H), 7.70 (s, 1H), 7.48 – 7.43 (m, 2H), 7.29 (s, 1H), 6.81 (d, J = 3.7 Hz, 1H).

A4

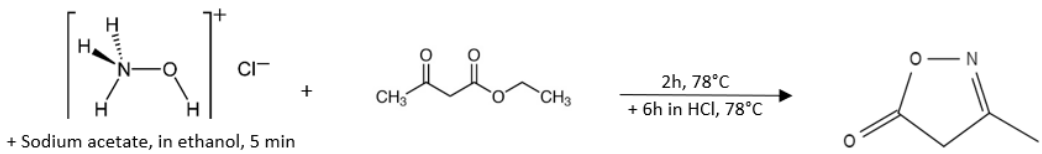

3-Methyl-5(4H)-isoxazolone: Sodium acetate (45 mmol) and hydrolyxamine hydrochloride (45 mmol) were dissolved in ethanol (60 mL) and the mix was stirred for 5 minutes. Then ethyl acetoacetate was added (30 mmol) and the mixture was heated until 78°C. When no more starting material was observed on a TLC, the reaction has been allowed to cool to room temperature. Aqueous chloridric acid ($HCl_{37\%}$) (5 µL per mmol of ethyl acetoacetate) was added and the reaction was heated back to 78°C for 4 to 6 hours. The solution was filtered and concentrated under reduced pressure. Purification of the product has been made through a column chromatography in ether petroleum : ethyl acetate as eluent in a ratio 6 : 4 [55]. ^{1}H-NMR (400 MHz, $CDCl_3$) δ 3.36 (d, J = 0.7 Hz, 2H), 2.07 (s, 3H).

As the number of protons is quite low (5 protons), the result of the ^{1}H-NMR has been confirmed by a mass spectrum shown in Figure A.2. The peak at 100 m/z corresponds to the desired product (molar mass 99 g/mol).

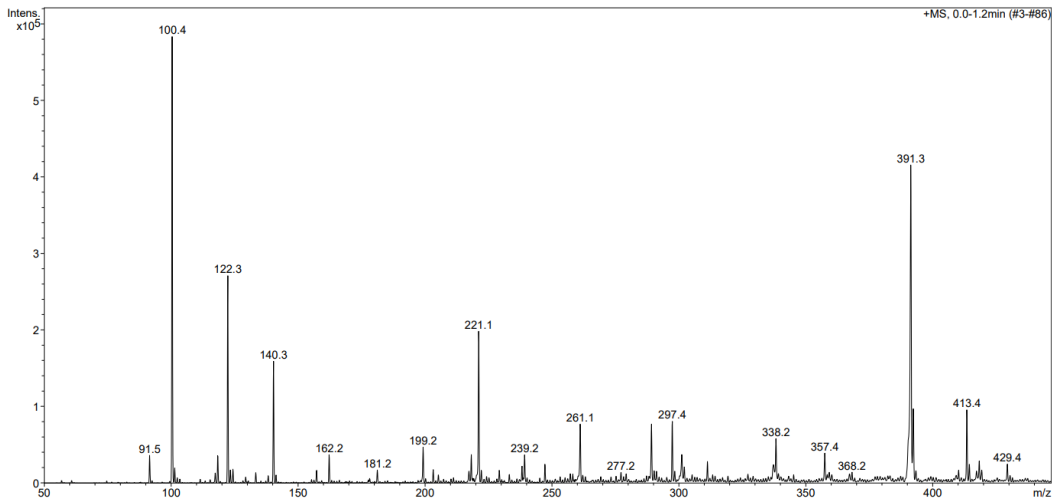

Figure A.2: Mass spectrum of the products of the reaction aiming to yield the precursor of A4

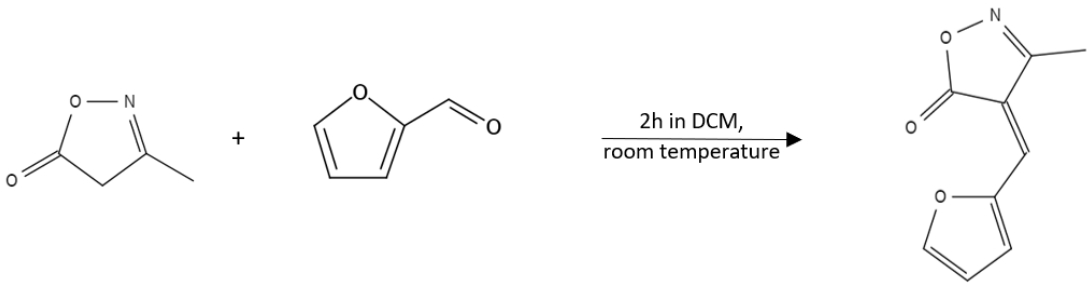

4-(2-Furanylmethylene)-3-methyl-5(4H)-isoxazolone: 3-Methyl-5(4H)- isoxazolone (11.7 mmol) and furfural (12.9 mmol) were mixed together in water (6 mL) for 2h at room

temperature. A yellow precipitate formed and was collected by filtration and rinsed with water. The product was dissolved in dichloromethane and washed with a saturated solution of sodium bicarbonate and then brine. The organic phase was separated and dried with magnesium sulfate. Finally the solvent was removed under reduced pressure and a yellow powder was recovered [8]. ^{1}H-NMR (400 MHz, $CDCl_3$) δ 8.58 (d, J = 3.8 Hz, 1H), 7.35 (s, 1H), 7.18 (d, J = 3.6 Hz, 1H), 6.71 (dd, J = 3.6, 1.8 Hz, 1H), 2.28 (s, 3H).

D2

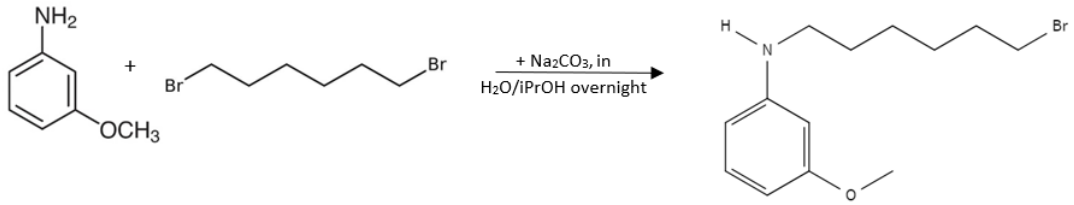

N-(6-Bromohexyl)-3-methoxybenzenamine: M-anisidine (30 mmol), dibromohexane (45 mmol) and sodium carbonate (30 mmol) were put together in a mix of water (15 mL) and propanol (15 mL) and stirred overnight at room temperature. The solvent was evaporated under reduced pressure and the remaining solution extracted with dichloromethane. The product was dried, and the dichloromethane evaporated. To take out the remaining dibromohexane, the solution was dissolved in acetonitrile (ACN) and subsequently washed a couple of times with hexane. The product was purified via column chromatography in dichloromethane : petroleum ether as eluent in a ratio of 9 : 1. The first spot was collected and the product was recovered after evaporation of the eluent as a yellowish viscous oil. ^{1}H-NMR (400 MHz, $CDCl_3$) δ 7.13 – 7.08 (m, 1H), 6.30 (ddd, J = 10.4, 8.1, 1.9 Hz, 2H), 6.23 (t, J = 2.2 Hz, 1H), 3.80 (s, 3H), 3.46 – 3.40 (m, 2H), 3.26 (dd, J = 10.5, 4.5 Hz, 1H), 3.14 (t, J = 7.1 Hz, 2H), 1.94 – 1.86 (m, 2H), 1.67 (dt, J = 14.4, 7.3 Hz, 2H), 1.54 – 1.42 (m, 4H).

To help understanding the results of the ^{1}H-NMR, a mass spectrum of the products obtained has been realized. The molar mass of D2 being equal to 286 g/mol, a peak at 286 m/z (+/- 1) is expected.

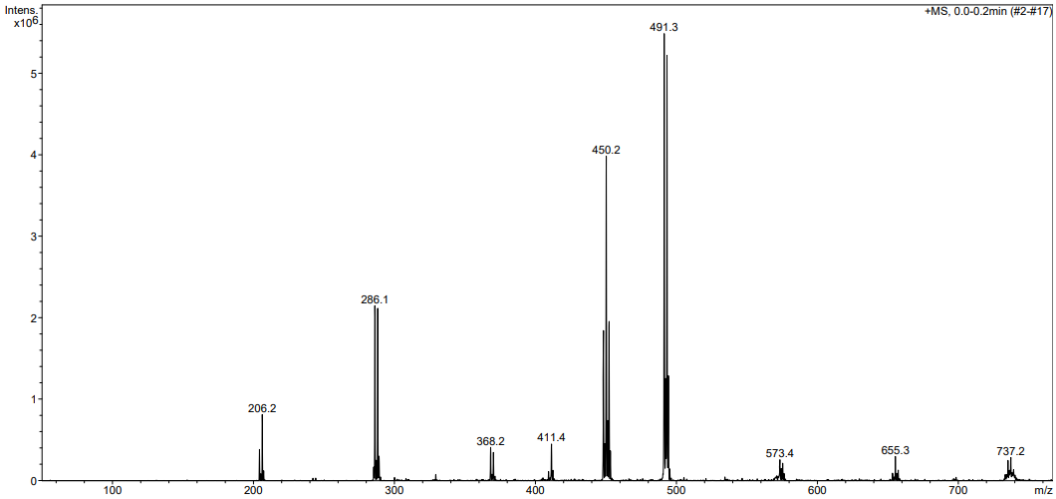

Figure A.3: Mass spectrum of the products of the reaction aiming to yield D2

From the mass spectrum (see Figure A.3), the desired product is present, although impure. Indeed, the peak at 450 m/z corresponds to the donor obtained featuring two hexylbromine chains attached to the nitrogen atom (tertiary amine yielded).

DASA-A1-D1

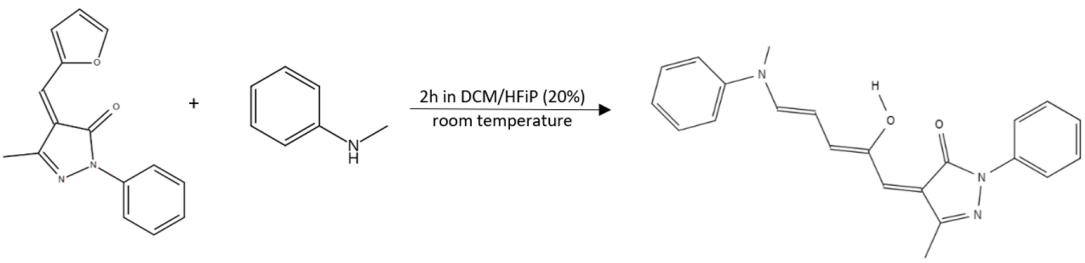

(Z)-4-((2Z,4E)-5-(N-methyl-benzeneamino)-2-hydroxypenta-2,4-dien-1-ylidene)-2-phenyl-5-(methyl)-pyrazol-3-one: 4-(2-Furanylmethylene)-2,4-dihydro-5-methyl-2-phenyl-3H-pyrazol-3-one (0.32 mmol) and N-methyl aniline (0.32 mmol) were dissolved in dichloromethane (0.8 mL) and hexafluoroisopropanol (HFiP) (0.2 mL) and the solution was stirred for 2h at room temperature. The solvent was removed under reduced pressure and the remaining solid triturated in diethyl ether (1 mL). After filtration the product was isolated as a grey-blue powder [36]. ^{1}H-NMR (400 MHz, CD_3CN) δ 7.80 (ddd, J = 12.0, 7.0, 1.3 Hz, 2H), 7.60 – 7.57 (m, 1H), 7.53 – 7.50 (m, 2H), 7.32 – 7.25 (m, 2H), 7.05 (t, J = 8.0 Hz, 2H), 7.00 – 6.96 (m, 1H), 6.72 (d, J = 8.1 Hz, 1H), 6.24 (dd, J = 5.9, 2.2 Hz, 1H), 5.52 (s, 1H), 3.33 (s, 1H), 3.20 (d, J = 3.5 Hz, 1H), 2.67 (s, 3H).

The ^{1}H-NMR spectrum is reported in acetonitrile, where the closed form is favoured, so

the reading of the spectrum is more easily made.

DASA-A1-D2

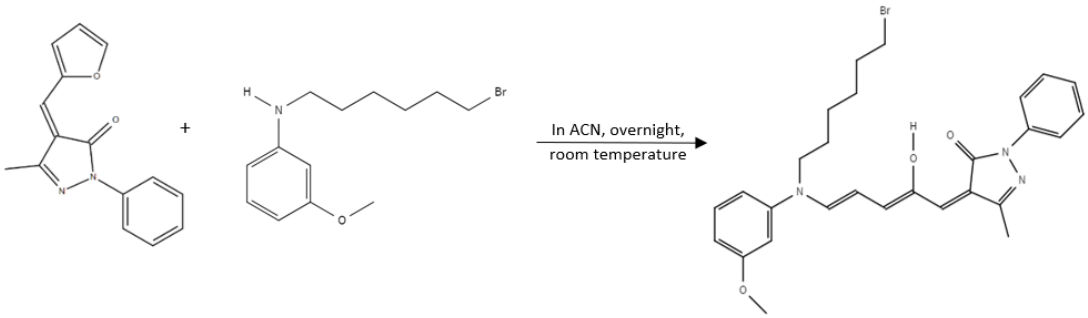

(Z)-4-((2Z,4E)-5-(N-(6-bromohexyl) -3-methoxybenzenamino)-2-hydroxy-penta-2,4-dien-1-ylidene)-2-phenyl-5-(methyl)-pyrazol-3-one: 4-(2-Furanyl-methylene) - 2,4-dihydro-5-methyl-2-phenyl-3H-pyrazol-3-one (0.32 mmol) and D2 (0.32 mmol) were dissolved in dichloromethane (0.8 mL) and hexafluoroisopropanol (0.2 mL) and the solution was stirred for 2h at room temperature. The solvent was removed under reduced pressure and the remaining solid triturated in diethyl ether (1 mL). After filtration the product was isolated as a dark blue powder [36]. ^{1}H-NMR (400 MHz, CD_3CN) δ 7.75 (d, J = 7.8 Hz, 2H), 7.43 (dd, J = 17.6, 9.9 Hz, 2H), 7.21 (s, 1H), 6.93 (d, J = 8.3 Hz, 0.4H), 6.88 (s, 0.4H), 6.32 (s, 0.5H), 6.17 – 6.07 (m, 2H), 4.90 (s, 0.3H), 3.70 – 3.66 (m, 2H), 3.55 – 3.51 (m, 3H), 2.97 (s, 1H), 2.68 (s, 1H), 2.26 (t, J = 28.8 Hz, 3H), 1.99 (d, J = 3.8 Hz, 0.4H), 1.84 – 1.77 (m, 3H), 1.41 (dd, J = 7.0, 3.5 Hz, 3H), 1.36 (s, 2H), 0.89 – 0.81 (m, 2H).

Seeing the results of the ^{1}H-NMR, the product afforded (DASA-A1-D2) is not pure, some reagents are still present so the proton's integration is not always exact. Some peaks (as example those corresponding to the pryazolone derivative in the aromatic part of the spectrum or those integrating for the bromohexyl chain) are more intense than those on the triene backbone around 6 ppm.

DASA-A2-D2

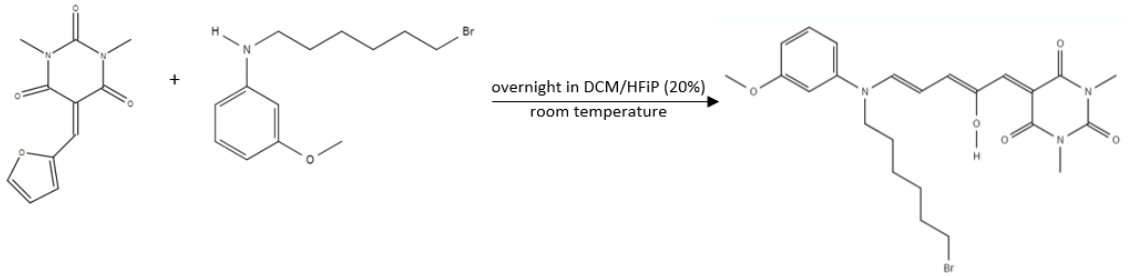

5-((2Z,4E)-5-(N-(6-bromohexyl) -3-methoxybenzenamino)-2-hydroxypenta-2,4-dien-1-ylidene)-1,3-dimethylpyrimidine-2,4,6-trione: The 5-(2-Furanyl methylene)-1,3-dimethyl-2,4,6-pyrimidine-trione (0.32 mmol) and D2 (0.32 mmol) were dissolved in dichloromethane (0.8 mL) and hexafluoroisopropanol (0.2 mL) and the solution was stirred overnight at room temperature. The solvent was removed under reduced pressure and the remaining solid triturated in diethyl ether (1 mL). To remove the diethyl ether, a bit of hexane was added, and the solvents were removed under reduced pressure to obtain a dark blue powder [36]. ^{1}H-NMR (400 MHz, CD_3CN) δ 8.16 (d, J = 6.1 Hz, 1H), 7.89 (t, J = 7.6 Hz, 1H), 6.97 – 6.93 (m, 1H), 6.15 (d, J = 8.3 Hz, 1H), 6.12 – 6.09 (m, 1H), 3.69 (d, J = 4.7 Hz, 1H), 3.66 (s, 2H), 3.52 (td, J = 6.6, 3.4 Hz, 3H), 3.10 (s, 1H), 2.98 – 2.94 (m, 2H), 2.08 (s, 2H), 1.91 (d, J = 6.2 Hz, 1H), 1.83 – 1.76 (m, 2H), 1.70 (s, 1H), 1.51 (dd, J = 13.9, 7.0 Hz, 3H), 1.42 – 1.37 (m, 3H), 1.30 (s, 2H), 1.24 – 1.10 (m, 2H).

Again, the ^{1}H-NMR spectrum is reported in acetonitrile, where the closed form is favoured, so the reading of the spectrum is more easily made. Moreover, to confirm that the expected product was present, a mass spectrum has been realized. A peak at 520 m/z (+/- 1) corresponding to the molar mass of the DASA-A2-D2 is expected.

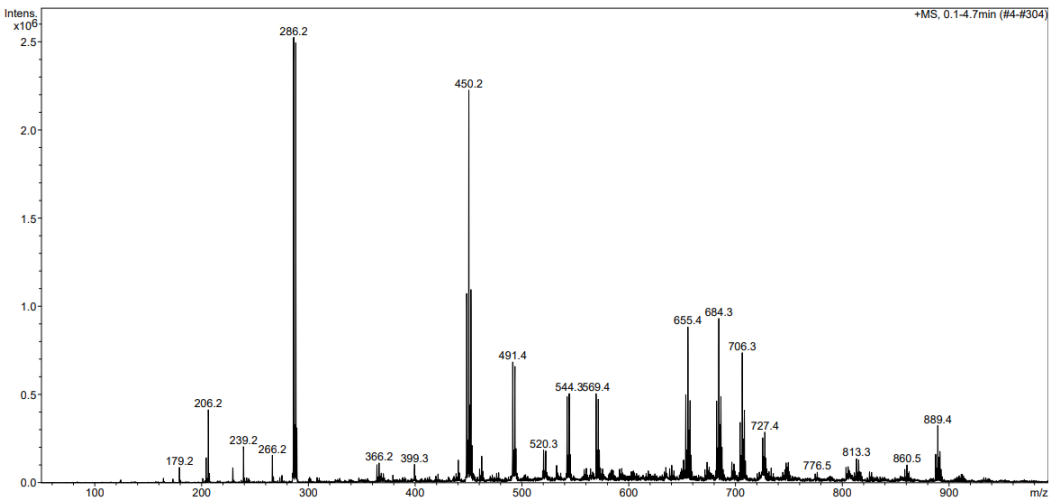

Figure A.4: Mass spectrum of the products of the reaction aiming to yield DASA-A2-D2

From the mass spectrum (see Figure A.4), the desired product is present, although this is not the only product yielded. Among others, the two peaks at 286 m/z and 450 m/z witness the residual amount of reagents (D2 and D2 with the two hexylbromine chains).

DASA-A3-D3

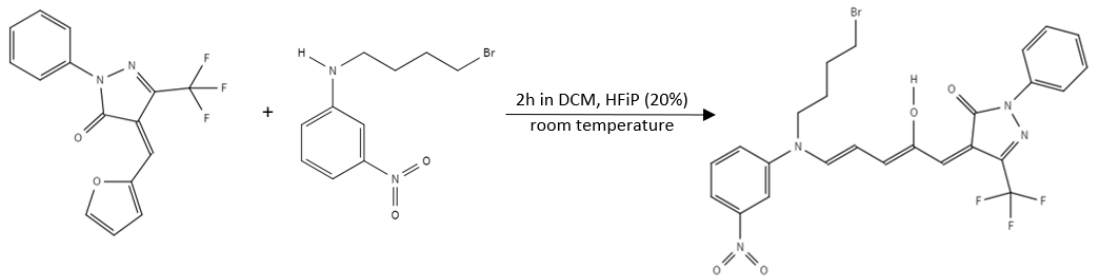

(Z)-4-((2Z,4E)-5-(N-(4-bromobutyl)-3- nitrobenzenamino)-2-hydroxypenta-2,4-dien-1-ylidene)-2-phenyl-5-(trifluoromethyl)-pyrazol-3-one: Pyrazol-3-one, 4-(2-furanylmethylene)- 2,4-dihydro-2-phenyl-5-(trifluoromethyl) (0.023 mmol) and N-(4-bromobutyl)-3-nitrobenzenamine (0.023 mmol) were dissolved in dichloromethane (80 µL) and hexafluoroisopropanol (HFiP) (20 µL) and the solution was stirred for 2h at room temperature. The solvent was removed under reduced pressure and the remaining solid triturated in diethyl ether. After filtration the product was isolated as a blue-green powder [36]. ^{1}H-NMR (400 MHz, CD_3CN) δ 8.49 (s, 1H), 7.41 (d, J = 10.9 Hz, 2H), 7.32 – 7.27 (m, 1H), 6.95 (d, J = 8.5 Hz, 1H), 4.54 – 4.49 (m, 2H), 3.12 (t, J = 6.9 Hz, 2H), 2.25 (d, J = 5.7 Hz, 1H), 1.99 (d, J = 7.2 Hz, 2H), 1.77 (d, J = 2.5 Hz, 1H), 1.61 (d, J = 7.0 Hz, 2H), 1.39 (s, 2H), 1.28 (s, 2H), 0.88 (d, J = 7.0 Hz, 2H).

DASA-A4-D2

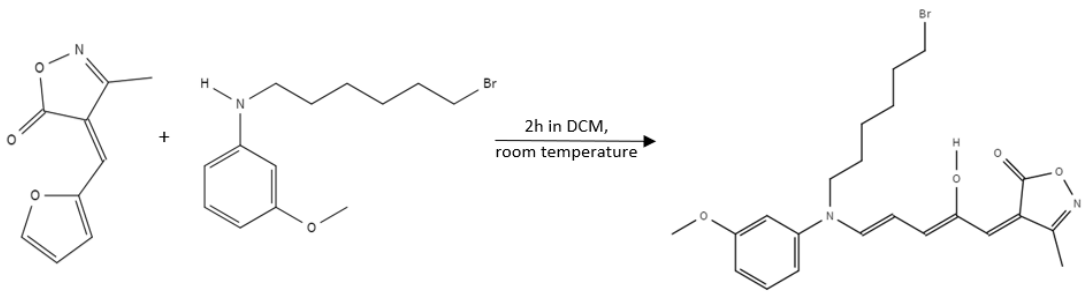

(Z)-4-((2Z,4E)-5-(N-(6-bromohexyl)-3- methoxybenzenamino)-2-hydroxypenta-2,4-dien-1-ylidene)-3-methylisoxazol5(4H)-one: 4-(2-Furanylmethylene) - 3-methyl-

5(4H)-isoxazolone (0.05 mmol) and N-(6-Bromohexyl)-3-methoxybenzenamine (0.05 mmol) were dissolved in dichloromethane (150 µL) and the solution was stirred for 5 minutes at room temperature. The solution immediately turned blue and the reaction was stopped here. The solvent was removed under reduced pressure and the remaining solid triturated in diethyl ether. After filtration the product was isolated as a violet-blue powder [8]. ^{1}H-NMR (400 MHz, CD_3CN) δ 7.00 – 6.94 (m, 1H), 6.22 (dd, J = 6.5, 4.6 Hz, 3H), 3.77 (d, J = 9.9 Hz, 1H), 3.70 (s, 3H), 3.67 (s, 0,4H), 3.28 (s, 0,2H), 3.11 – 3.04 (m, 0,5H), 2.24 (s, 1H), 1.81 (s, 0,4H), 1.79 – 1.76 (m, 1H), 1.60 (s, 2H), 1.43 (s, 1H), 1.27 (s, 0,7H).

Seeing the results of the ^{1}H-NMR spectrum, it is hard to tell if the product degraded in acetonitrile or if the product obtained is not the one desired. The mass spectrum below showed that the product obtained is not the expected one. More studies of the compound would have been needed to draw the exact molecule, but for quantity issues they could not be done.

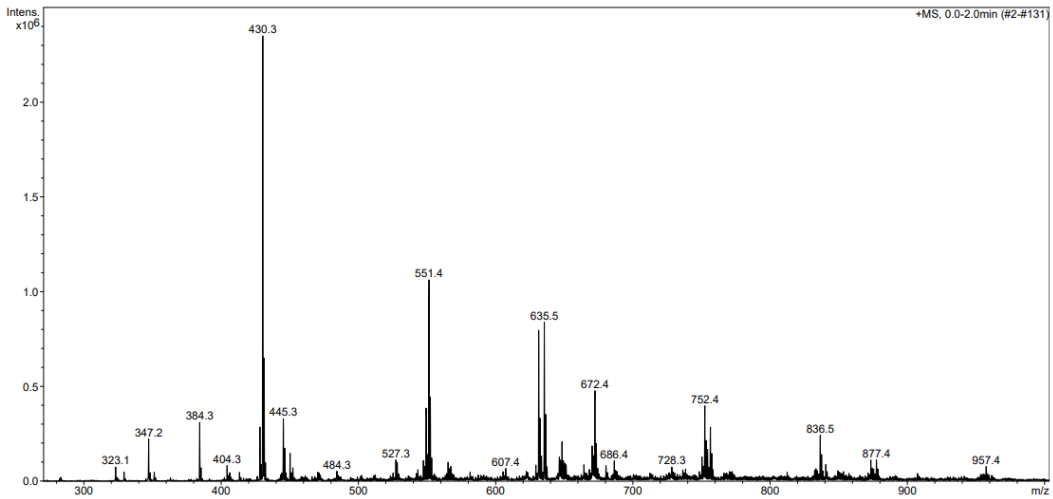

Figure A.5: Mass spectrum of the products of the reaction aiming to yield DASA-A4-D2

Attachment of the polar head on DASA-A2-D2

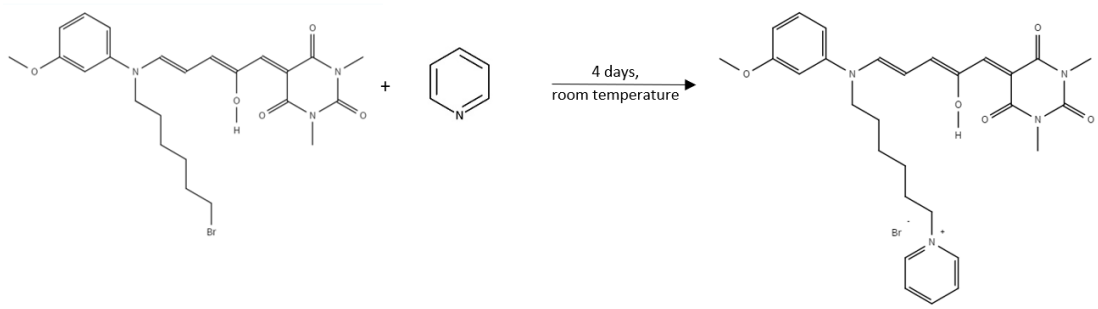

5-((2Z,4E)-5-(N-(6-pyridinium hexyl bromide (1:1))-3-methoxybenzenamino) -2-hydroxypenta-2,4-dien-1-ylidene)-1,3-dimethylpyrimidine-2,4,6-trione: 5-((2Z, 4E)-5-(N-(6-bromohexyl)-3-methoxybenzenamino)-2-hydroxypenta-2, 4-dien-1-ylidene)-1, 3-dimethylpyrimidine-2, 4, 6-trione (DASA-A2-D2) (0.037 mmol) and pyridine (0.037 mmol) were mixed at room temperature and the reaction was stirred for 4 days. The pyridine was removed under reduced pressure and the product was recovered as a dark red solid. ^{1}H-NMR (400 MHz, CD_3CN) δ 9.07 (d, J = 4.5 Hz, 1H), 8.62 (d, J = 4.5 Hz, 2H), 8.16 (d, J = 6.1 Hz, 1H), 7.89 (t, J = 7.6 Hz, 1H), 7.49 – 7.45 (m, 1H), 6.97 – 6.93 (m, 1H), 6.15 (d, J = 8.3 Hz, 1H), 6.12 – 6.09 (m, 1H), 4.62 – 4.55 (m, 1H), 3.69 (d, J = 4.7 Hz, 1H), 3.66 (s, 2H), 3.52 (td, J = 6.6, 3.4 Hz, 3H), 3.10 (s, 1H), 2.98 – 2.94 (m, 2H), 2.08 (s, 2H), 1.91 (d, J = 6.2 Hz, 1H), 1.83 – 1.76 (m, 2H), 1.70 (s, 1H), 1.51 (dd, J = 13.9, 7.0 Hz, 3H), 1.42 – 1.37 (m, 3H), 1.30 (s, 2H), 1.24 – 1.10 (m, 2H).

Attachment of the polar head on DASA-A3-D3

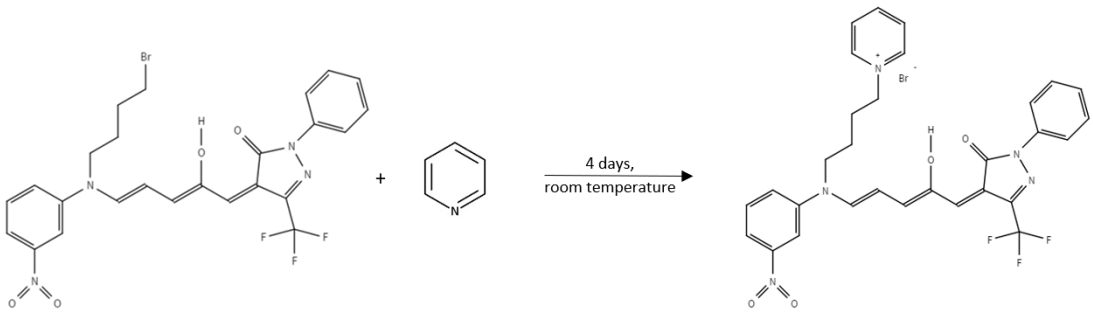

(Z)-4-((2Z,4E)-5-(N-(4-pyridinium butyl bromide (1:1))-3-nitrobenzenamino)-2-hydroxypenta-2,4-dien-1-ylidene)-2-phenyl-5-(trifluoromethyl)-pyrazol-3-one: (Z)-4-((2Z,4E) -5-(N-(4-bromobutyl) -3-nitrobenzenamino) -2- hydroxy-penta-2,4-dien-1-ylidene)-2-phenyl-5-(trifluoromethyl)-pyrazol-3-one (DASA-A3-D3) (0.02 mmol) and pyridine (0.02 mmol) were mixed at room temperature and the reaction was stirred for 4 days. The pyridine was removed under reduced pressure and the product was recovered as dark red solid. ^{1}H-NMR (400 MHz, CD_3CN) δ 8.68 (d, J = 5.0 Hz, 2H), 8.49 (s, 1H), 8.01 (s, 2H), 7.41 (d, J = 10.9 Hz, 2H), 7.35 (s, 1H), 7.32 – 7.27 (m, 1H), 6.95 (d, J = 8.5 Hz, 1H), 4.54 – 4.49 (m, 2H), 3.12 (t, J = 6.9 Hz, 2H), 2.25 (d, J = 5.7 Hz, 1H), 1.99 (d, J = 7.2 Hz, 2H), 1.77 (d, J = 2.5 Hz, 1H), 1.61 (d, J = 7.0 Hz, 2H), 1.39 (s, 2H), 1.28 (s, 2H), 0.88 (d, J = 7.0 Hz, 2H).

B | Appendix B: % of each isomer in solution computed with NMR spectra

In order to determine the approximate percentage of close and open form of the isomers in equilibrium in a specific solvent, the ^{1}H-NMR can reveal itself very useful. Some peaks are exclusive to one of the two forms, and their relative intensity (on a pure product) can give some hints to compute their relative amount. Based onto the work of James R. Hemmer et al. (2018), ^{1}H-NMR spectra of the DASA-A1-D1 have been realized in deuterated acetonitrile (Figure B.1) and chloroform (Figure B.2) [8]. The doublet at 7.8 ppm and the peaks at 6.25 ppm correspond to protons on the cyclopentenone ring; while the triplet at 6 ppm corresponds to one of the triene protons. By monitoring those peaks in the dark at the equilibrium, the relative amount of each isomer can be found.

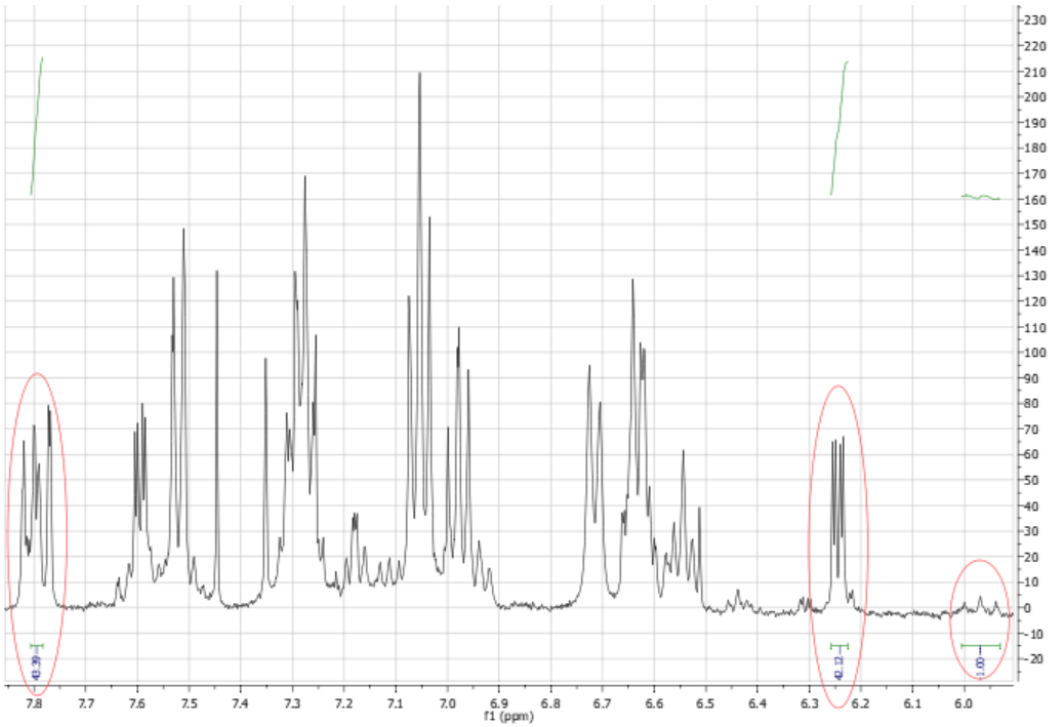

Figure B.1: Zoom on the relevant part of the ^{1}H-NMR spectrum of the DASA-A1-D1 in deuterated acetonitrile

In the figure B.1 the triplet at 6 ppm (open form) has been integrated as 1. The doublet at 6.25 ppm (close form) has been integrated as 42 and the peak at 7.8 ppm as 43. Therefore, in acetonitrile it is clear that the relative amount of the open isomer is negligible compared to the close one.

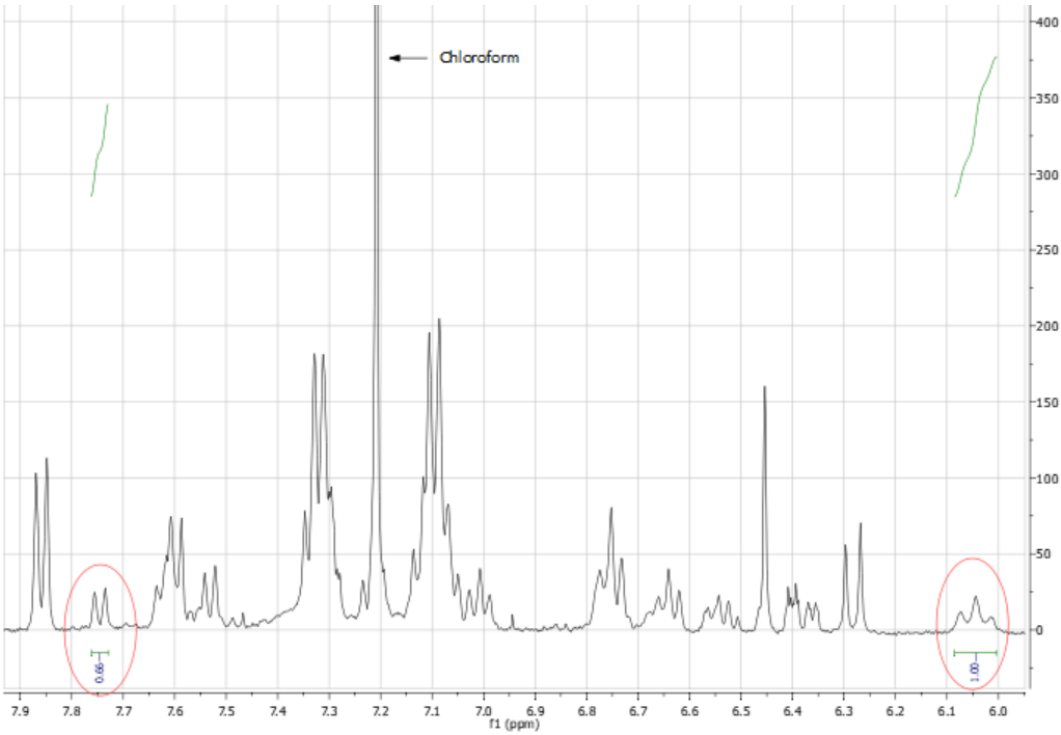

Figure B.2: Zoom on the relevant part of the ^{1}H-NMR spectrum of the DASA-A1-D1 in deuterated chloroform

In the figure B.2 the triplet at 6 ppm (open form) has been integrated as 1 and the doublet at 7.75 ppm (close form) as 0.66. Therefore, the relative fraction of each isomers are computed as:

$$\begin{cases} O_{\%} = \frac{1}{1+0.66} = 60\% \\ C_{\%} = \frac{0.66}{1+0.66} = 40\% \end{cases} \tag{B.1}$$

In conclusion, in acetonitrile the closed form seems to be favoured, while in chloroform a coexistence of both forms exist in equilibrium. This result is not surprising as acetonitrile is more polar than chloroform and should therefore favour the most polar form of the DASA in solution, which is indeed the closed one.

List of Figures

List of Tables

List of Symbols

Variable	Description	SI unit
$\boldsymbol{\lambda_{max}}$	absorption wavelength	nm
$\boldsymbol{O}\%$	percentage of the open form	%
$\boldsymbol{C}\%$	percentage of the closed form	%
$\boldsymbol{M}$	Molar concentration	g/mol
$\boldsymbol{\mu}$	initial slope of the kinetic curves	min^{-1}
$\boldsymbol{\tau}$	time to reach the plateau	min
$\boldsymbol{\delta}$	amount of recovered absorbance	/